2019

Neural Mechanisms that Control an Innate Foraging Behavior in Caenorhabditis Elegans

Alejandro Lopez-Cruz

NEURAL MECHANISMS THAT CONTROL AN INNATE FORAGING BEHAVIOR IN *CAENORHABDITIS ELEGANS*

A Thesis Presented to the Faculty of

The Rockefeller University

in Partial Fulfillment of the Requirements for

the degree of Doctor of Philosophy

by

Alejandro López-Cruz

June 2019

NEURAL MECHANISMS THAT CONTROL AN INNATE FORAGING BEHAVIOR IN *CAENORHABDITIS ELEGANS*

Alejandro López-Cruz, Ph.D.

The Rockefeller University 2019

The ability to efficiently locate food is critical for survival. Thus, animals modify their foraging patterns based on recent experience and current conditions to increase their likelihood of finding food. One highly conserved foraging strategy is local search, an intensive exploration over several minutes of the region where food resources were last encountered. As time since the last food encounter passes, animals transition to global search strategies to explore distant areas. The local-to-global search foraging pattern has been observed in fish, reptiles, insects, birds, and mammals, yet few studies ask how an animal's brain generates this ancient behavior. Here, I ask this question in the nematode *Caenorhabditis elegans.* In Chapter 1, I characterize the behavior in wildtype animals and find that local search is a food memory that is regulated by food history and by internal satiety states. In addition, I describe the behavior in individual animals and find that although the behavior is reliable at a population level, there is large variability between individuals. In Chapter 2, I conduct a candidate genetic screen to first find a gene important for local search, and then define a circuit for local search behavior. The circuit consists of two parallel

multimodal circuit modules that control local search. In each module, chemosensory or mechanosensory glutamatergic neurons that detect food-related cues trigger local search by inhibiting separate integrating neurons through a metabotropic glutamate receptor, MGL-1. The chemosensory and mechanosensory modules are separate and redundant, as glutamate release from either can drive the full behavior. In addition, the ability of the sensory modules to control local search is gated by the internal nutritional state of the animal. In Chapter 3, I characterize neuronal activity within the chemosensory module. Spontaneous activity patterns in the chemosensory module encode information about the time since the last food encounter and correlate with the foraging behavior. Glutamate acts within the module to shape activity patterns at various time scales. Taken together, these experiments reveal a circuit configuration that allows for the robust control of an innate adaptive behavior.

ACKNOWLEDGMENTS

Graduate school has been an incredibly rewarding experience. I am thankful to have had the opportunity to work in a fun, stimulating environment that has allowed me to grow personally and professionally. First, I want to thank my mentor, Dr. Cori Bargmann. The first time I met Cori I was immediately inspired by her insight, ideas, and her enthusiasm for science. Her excitement for scientific discovery reminds me constantly of why I went into research. Cori is an extremely nice person and has been a very supportive mentor. She has helped me design experiments, taught me about scientific writing, and provided comfort in tough times, while simultaneously challenging me to grow as a scientist. I have also enjoyed and learned a lot during our casual weekend conversations related to science, medicine, and everyday life. In the lab, she fosters an amazing work environment full of curious and intelligent students and postdocs. I'm grateful to have had the opportunity to work with her.

I also want to thank my Faculty Advisory Committee, Dr. Daniel Kronauer, Dr. Vanessa Ruta, and Dr. Songhai Shi. I worked with Songhai as an undergraduate in what was my first ever research experience in biology. It has been a great opportunity to continue to interact with him as a graduate student. Vanessa and Daniel have been very supportive and provided valuable guidance at key moments during my project. Also, many thanks to Dr. Benjamin de Bivort from Harvard University for serving as my external committee member.

I am indebted to former and current members of the Bargmann lab. Steven Flavell, a former postodoc in the lab was instrumental in my early years as a graduate student. He provided day-to-day guidance on experimental design and was encouraging in rough times, even after he had left the lab. I still aspire to design experiments as elegantly as Steve does. Navin Pokala is the most generous and collaborative person I worked with. I miss his genuine personality and contagious energy. Josh Greene and Xin Jin, two former graduate students in the lab, introduced me to molecular biology, and made me feel welcome in my first year in the lab. Sagi Levy and Andrew Gordus helped me with quantitative problems and coding, Aylesse Sordillo collaborated with me in a crucial part of this project, and Patrick McGrath analyzed sequencing data and found a gene mutation central to this work. I am also grateful to the support staff in the lab: Hernan Jaramillo, Manoush Ardzivian and Priscilla Kong. They take good care of us and are also so much fun to be around.

I have a great group of friends both inside and outside the lab. Elias Scheer, Aylesse Sordillo, May Dobosiewicz, Phil Kidd, Javier Marquina, and Du Cheng are my close friends in the lab; they make coming to work every day so much fun. I've travelled with many of them and have enjoyed numerous karaoke nights in Koreatown. Outside the lab, my friends from childhood (who now live in NYC), Nelson, Ednaliz, Dennis, Karla, Vero and Eduardo, and friends from NYC, Kevin, Luca, Michael, and Andy have made these years in New York unforgettable.

My father Gustavo, my mother Astrid, and my sister Laura have been incredibly supportive and loving. They inspire me to try to be the best that I can be. Finally, I want to thank my partner, Jessica Jimenez. Her support, love, and energy have made the past years in New York some of the happiest of my life.

TABLE OF CONTENTS

LIST OF FIGURES

LIST OF TABLES

CHAPTER 1:

Introduction

An animal's life consists of a series of behaviors that occur over varying time scales. Selecting and executing the right behaviors at the right time is essential for animal survival and fitness (Dall et al., 2005; McFarland, 1977). Thus, the nervous systems of animals must use information about their external environment, internal states, and previous experience to generate appropriate adaptive behaviors. One the most important behaviors that animals engage in is foraging, the set of processes by which an animal acquires food (Kramer, 2001; Pyke et al., 1977). Animals have developed behavioral strategies for efficiently finding and consuming food, many of which are conserved across species. However, little is known about the neural basis of foraging behaviors. The focus of my thesis is to understand the neural mechanisms of one foraging behavior, local search, in the nematode *Caenorhabditis elegans*.

In this Chapter, I will first introduce foraging by presenting various behavioral decisions that foraging animals make and discuss them in the context of foraging theory. I then focus on one of these behaviors, the search aspect of foraging, specifically on local search behavior. Finally, I discuss *C. elegans* as a model to study the neural basis of local search.

Foraging theory and empirical evidence

Foraging consists of a set of behaviors each associated with decisions that foraging animals must make. At any given time, an animal can decide to continue to do what it is doing, to do it in a different way, or to engage in a new

foraging activity. Understanding the rules that govern the decisions of foraging animals has been the goal of foraging theory over the last several decades (Pyke et al., 1977; Schoener, 1987). Foraging theory attempts to formulate 'decision rules' that describe the optimal behavioral strategy that an animal should adopt given a set of 'constraints' such as resource distribution, environmental information, and energetic costs (Kramer, 2001). A key assumption of foraging theory is that natural selection has favored the development of optimal foraging strategies in animals. Though this is not necessarily true (Pierce and Ollason, 1987), the value of foraging theory is that it makes predictions of the external and internal factors that animals may use to make behavioral decisions. Coupled with empirical observation of foraging behaviors, it provides a framework to formulate hypotheses of how the nervous systems of animals encode these adaptive behaviors.

There are many behavioral decisions encountered by foraging animals, and these vary depending on the type of animal, the habitat, and the feeding patterns. Yet, three foraging decisions are generally observed across species: (i) food choice- deciding whether or not to eat prey, (ii) exploitation vs. exploration- deciding whether to continue exploiting a food resource or to find a new one, and (iii) search strategy- deciding what search patterns to use when searching for food (Bartumeus and Catalan, 2009; Kramer, 2001; Pyke et al., 1977). Foraging theory has formulated decision rules for each of these behaviors. In each case animals must integrate external and internal information to generate behavioral decisions.

Food choice. When animals encounter a food source they must decide whether to eat it. Multiple factors contribute do this decision. One factor that has been well studied is the prey size, or the range of prey sizes that an animal should consume (Elner and Hughes, 1978; Meire and Ervynck, 1986; Richardson and Nicolaas, 1986). While larger prey provide more energy, they may also require more energy to process; thus only prey within a certain size range provide optimal nutrition. This decision is exemplified by the oystercatcher *Haemotopus astralegus*. This bird feeds on mussels of various sizes which it cracks open by hammering a hole through the shell (Meire and Ervynck, 1986). Larger mussels have thicker shells and thus require more energy to crack, while smaller mussels provide less energy when consumed, but are easier to crack. An elaborate foraging model predicted that when an oystercatcher finds a mussel, it should only eat it if it is between 30 mm and 45 mm long. In agreement with the model, experimental evidence showed that oystercatchers discard most oysters that are not within this range (Meire and Ervynck, 1986).

A second study provides further evidence that birds have evolved behaviors that increase their feeding efficiency (Richardson and Nicolaas, 1986). The common crow, *Corvus caurinus,* forages for clams of various sizes, and breaks them by flying and dropping them against a rock. In this case, the probability that the clam breaks is independent of its size. As predicted by a foraging model, the crows select clams above a certain threshold (28.5 mm), instead of within a range, as there are no diminishing returns for larger clams (Richardson and Nicolaas, 1986). These results suggest that animals represent

features of the external food world (such as prey size) to generate an adaptive behavior, such as food choice.

Exploitation vs. exploration. Another behavioral decision animals often face is deciding between exploiting an existing food resource and exploring other areas. This decision is described by the Marginal Value Theorem, which says that the optimal time for animals to leave a resource patch is when the average energy intake within the patch falls below the average energy intake in the environment as a whole (Charnov, 1976). This model makes two basic predictions: (i) that animals will spend more time in food patches of higher quality, and (ii) the greater the distance between different patches, the more time an animal will spend in a current patch (since a greater patch distance requires spending energy moving between patches, and thus makes average energy intake in the environment smaller). Experimental evidence supports this decision rule, at least qualitatively. It was shown that armadillos and guinea pigs, among many animals, spend more time in areas containing good resources than poor ones (Cassini et al., 1990), and that birds spend more time in a patch if the distance between patches is experimentally increased (Cowie, 1977). Animals thus use information about the current environmental conditions and integrate that with some expectation or previous experience of the environment to execute a behavior.

Searching. When trying to find new resources, animals must employ search strategies that maximize their chance of locating food. Search strategies are theoretically formulated by considering that animal locomotion is intermittent; it consists of discrete forward movements that are separated by pauses or turns

(Kramer and McLaughlin, 2001). The optimal search strategy employed by an animal depends on the amount of information that it has about its environment (Bartumeus et al., 2016; Bartumeus and Catalan, 2009). When an animal has recently encountered food, then it has information of where food resources may be located, so the most efficient search strategy is one in which the duration of forward movements follows a normal distribution, resembling Brownian motion (Grünbaum, 1998; Hills et al., 2013; Humphries et al., 2010; Kareiva and Odell, 1987). In this strategy, animals interrupt forward movement with turns relatively frequently, allowing them to perform an intensive exploration near the area where food resources where last encountered, a behavioral strategy termed local search. As time passes, if animals cannot find food, the optimal strategy is to transition to an extensive exploration pattern where turns are less frequent, a behavioral strategy termed global search. The optimal extensive search pattern may be a Levy walk (Viswanathan et al., 1999), a movement pattern in which the duration of forward runs come from a heavy tailed probability distribution. This type of search pattern is theoretically predicted to increase the chance of locating random food sources (Sims et al., 2008; Viswanathan et al., 1999). Thus, animals should initially perform an intensive search where they recently encountered food, and then transition to a global search as time passes.

The intensive to extensive search pattern has been described by ecologists for decades in species ranging from insects to humans (Bell, 1985; Benedix, 1993; Dias et al., 2009; Eifler et al., 2012; Gray et al., 2005; Hills et al., 2013; Lihoreau et al., 2016; Nakamuta, 1985; Papastamatiou et al., 2012;

Wakabayashi et al., 2004; Weimerskirch et al., 2007). This behavior has been recorded and analyzed in the nematode *C. elegans. C elegans* locomotion consists of forward runs interrupted by turns (reorientations) that are undirected. Turns fall into different categories based on the locomotor sequences. One type of turn, Omegas, interrupts forward movement at times drawn from a stretched exponential, which leads to a basal extensive search. Superimposed on this, another type of turn, pirouettes, occurs more frequently early after a food encounter. This combination of turns leads to an intensive search that transitions over time to a basal extensive search. Computer simulations showed that this strategy improves the efficiency of locating food sources (Salvador et al., 2014). Like other foraging behaviors, searching requires integrating previous experience (recent food encounter) with current internal and external conditions. Indeed, theoretical models of intensive-to-extensive foraging pattern include both external and internal factors to generate the behavior (Calhoun et al., 2014; Grünbaum, 1998; Grünbaum, 2000; Kareiva and Odell, 1987).

Local search behavior in various species

Local search behavior following a food encounter has been described in many animal species. The household fly, *Musca domestica* and the fruit fly, *Drosophila melagnoster,* execute local search after ingestion of a sucrose drop by increasing their turning rate and decreasing their speed for a few minutes (Bell et al., 1985; White et al., 1984). Manta rays will display local searching in areas

where they encounter high plankton density (Papastamatiou et al., 2012). Similarly, local search has been observed in birds, reptiles and mammals after encountering food (Eifler et al., 2012; Hills et al., 2013; Paiva Vitor et al., 2010). In each case, the animals execute a time limited exploration of an area were food resources where last encountered, using a set of motor program such as turns, slowing, and looping, that last several minutes. If animals fail to find food, then transition to global search strategies in which they explore larger areas and perform fewer turns.

Though local search has been mostly described as a food search, it has also been observed as a strategy to find other types of resources. For example, male insects perform local search after encountering a mate (Schal et al., 1983) and zebrafish perform an intensive exploration after encountering a region with light (Horstick et al., 2017). Thus, local search may be a general strategy that animals use to find essential resources.

What are the neuronal circuits that generate local search?

Although the motor programs employed during local search vary greatly between different species --swimming, crawling, flying, walking -- the underlying behavioral state consisting of a sustained period of intensive searching after food encounter is highly conserved. Understanding the molecular and circuit mechanisms underlying this searching state may provide insight into the basis of ancient conserved behaviors.

Two features of local search hint at circuit elements that may be required for this search behavior:

1. The role of sensory features in local search. Animals execute local search not only after a direct encounter with resources, but also after encounters with only the sensory cues associated with resources. For example, the ladybird beetle *Cocinella Septempuncta bruckii*, which eats aphids, will execute local search after contact with an agar block covered in aphid fluid (Nakamuta, 1985) and *Drosophila* will execute local search after stimulation of pharyngeal gustatory neurons that detect sugar (Murata et al., 2017). Similarly, the German cockroach, *Blatella germanica*, will execute local search after stimulation with sex pheromone (Schal et al., 1983) and zebrafish will execute local search in response to changing levels of light (Horstick et al., 2017). The observation that sensory features alone can trigger local search, suggests that local search involves a neuronal representation of food-related (or more generally, resource-related) sensory features.

2. Local search represents a short-term food memory. A second observation is that search behavior is persistent and outlasts its sensory trigger, likely representing a short-term memory. Typically, local search will last for several minutes after the food encounter. In addition, local search is modulated by features of food history. For example, lizards modulate the duration of local search based on prey identity; they perform longer local search after encountering termites than flies or rice (Eifler et al., 2012). Likewise, *Drosophila* will perform a longer and more intense local search if given more concentrated

and larger sugar droplets (Bell, 1985). These features suggest that local search results from an internally generated short-term food memory.

While the external sensory triggers and dynamics of local search have been extensively characterized, the neuronal circuits that represent the external sensory environment and the sites that hold the short-term food memory are not fully understood. Here, we addressed this question in the nematode *Caenorhabditis elegans*.

***C. elegans* as a model to study foraging behavior**

The compact nervous system of *C. elegans*, which consists of exactly 302 neurons, presents an ideal system to study the neural circuits that generate foraging behaviors. *C. elegans* is a free-living nematode that lives in rotting vegetable material and feeds on bacterial food (Brenner, 1974). Bacteria is a complex sensory stimulus, and *C. elegans* can detect a variety of sensory aspects related to bacterial food using different types of neurons (Bargmann, 2006). The olfactory neurons AWA and AWC directly detect attractive volatile bacterial odors such as butanone and diacetyl. The ASE sensory neurons detect salt and water-soluble attractants, whereas the ASK neurons detect amino acids. URX, AQR, PQR, and BAG neurons detect the gasses oxygen and carbon dioxide, which are associated with bacterial metabolism (Bargmann, 2006). Multiple mechanosensory neurons detect textures associated with food including the dopaminergic CEP, ADE, and PDE neurons, the light touch sensing ALM,

AVM, PLM, and PVM neurons, and the multidendritic FLP and PVD neurons (Albeg et al., 2011; Park et al., 2008; Sawin et al., 2000; Yemini et al., 2013). The full repertoire of synaptic connections between these sensory neurons and the rest of the nervous system have been mapped by serial-sectioned electron microscopy (White et al., 1986), making this an excellent system for defining neuronal circuits related to foraging.

Foraging behaviors in *C. elegans*

Dwelling and roaming. While on bacterial food, *C. elegans* alternates between two foraging behavioral states; an exploitation state called dwelling and an exploration state called roaming. Dwelling animals have a low speed and turn frequently, remaining in a small area, whereas roaming animals have a high speed and rarely turn, exploring the food environment (Ben Arous et al., 2009). Animals spontaneously alternate between these states and the frequency of each state is controlled by features of the food environment. Animals on lower quality food will spend more time roaming and vice versa, suggesting that these foraging behaviors reflect an evaluation of the external environment (Ben Arous et al., 2009; Fujiwara et al., 2002; Shtonda and Avery, 2006). The neural circuits and molecules that generate these long lasting behavioral states in *C. elegans* have been mapped (Flavell et al., 2013).

Dwelling is generated by serotonin release from NSM and HSN neurons, which silences target neurons expressing *mod-1*, a serotonin-gated chloride

channel. Roaming is generated by release of pigment dispersing factor 1 (*pdf-1*) from PVP and other neurons, which leads to increased cAMP signaling in target neurons expressing *pdfr-1*. The serotonin and *pdf-1* circuits are mostly non-overlapping neuromodulatory circuits that drive opposing behavioral states. Interestingly, the partners in the neuromodulatory circuit (neurons that make serotonin or *pdf-1* and neurons that receive them) have no traditional synaptic connections between them in the *C. elegans* wiring diagram (White et al., 1986). In addition, these circuits are not organized in a traditional sensory-to-motor hierarchy; the serotonin sources NSM and HSN are both motor neurons, whereas some of the neurons that express the serotonin receptor *mod-1* are sensory neurons. Thus, the circuits that generate these foraging states are orthogonal to the traditional fast synaptic circuits and have a different organization (Flavell et al., 2013).

Animals on food transition spontaneously between roaming and dwelling. The start of dwelling is associated with an increase in NSM activity that last about 60 seconds but can predict the dwelling state for the next several minutes. Consistent with this observation, stimulating NSM triggers persistent dwelling even after the stimulation has stopped, suggesting that serotonin from NSM initiates and also extends the dwelling state (Flavell et al., 2013). Serotonin has also been implicated in other behavioral components of exploitation. For example, animals on better food increase their feeding bursts, an effect mediated by serotonin release from NSM and downstream serotonin receptors, *ser-2* and *ser-4* (Lee et al., 2017). Thus, serotonin may coordinate multiple aspects of a

foraging exploitation state (like dwelling and feeding) by signaling through different receptors.

Roaming is initiated and extended by *pdf-1* action on *pdfr-1*-expressing neurons. Though the roaming state results in high food exploration in foraging animals, *pdf-1*-mediated roaming may represent a more general arousal state. For example, arousal from the resting lethargus behavior associated with molting is mediated by PDF-1 release, which enhances mechanosensation in peripheral touch neurons. Additionally, the neuropeptide receptor *npr-1* promotes the lethargus state by inhibiting PDF-1 release (Choi et al., 2013).

Leaving behavior. A second foraging behavior that has been well characterized is the decision to leave a bacterial food lawn. Animals on food will spontaneously exit the food to explore other areas. This behavior is also regulated by features of the food environment. Animal will rarely leave high quality concentrated food, but will more frequently leave lawns of poor quality or lawns with a high density of animals (Gloria-Soria and Azevedo, 2008; Shtonda and Avery, 2006). Neuronally, leaving behavior is controlled by catecholamines that act on sensory neurons (Bendesky et al., 2011). Also, *npr-1* inhibits leaving, consistent with its general suppression of arousal and related behaviors.

Local search behavior in *C. elegans*

Upon removal from food, *C. elegans* executes a stereotypical local search behavior in which it explores a small area by executing many random, undirected

reversals and turns (reorientations) for about fifteen minutes. If it fails to find food, it transitions to a global search in which it explores larger areas by suppressing reorientations and executing long forward runs (Ahmadi and Roy, 2016; Calhoun et al., 2014; Gray et al., 2005; Hills et al., 2004; Salvador et al., 2014; Wakabayashi et al., 2004). Several studies have identified neurons and genes that may be important for this behavior (Fig. 1.1).

Ablation studies have identified a set of sensory neurons and interneurons that affect the spontaneous reorientations of local search (Fig. 1.1) (Gray et al., 2005; Wakabayashi et al., 2004). The glutamatergic sensory neurons AWC and ASK promote reorientations, as ablating them leads to decreased reorientations after food removal. Conversely, the sensory neuron ASI, which releases TGF-β among other peptides, normally inhibits reorientations, as ablating it leads to an increased reorientation frequency off food. These sensory neurons synapse onto four downstream interneurons that also affect reorientations; AIB, AIZ, AIY and AIA. AIB, and to a lesser extent AIZ, normally promote reorientations, whereas AIY and AIA normally inhibit reorientations. These ablation experiments also suggest that the sensory neurons act by interacting with these downstream interneurons; for example, AWC is thought to act by inhibiting AIY, as ablating both AWC and AIY is indistinguishable from ablating AIY alone. Later imaging experiments (described below) confirmed the interaction between these neurons. The interneurons ultimately synapse onto downstream command motor neurons that generate reorientations (Fig. 1.1).

Several of the neurons implicated in local search respond to changes in food or bacterial-related odors. In general, neurons that promote reorientations show an OFF-response to food (they are activated by the removal of food), whereas neurons that inhibit reorientations show an ON-response (they are activated by the addition of food and are silent in the absence of food). AWC and ASK are OFF-response neurons. AWC is normally silent in the presence of food or food-related odors. Upon removal of bacterial conditioned media or odor, AWC reliably shows a transient increase in calcium activity that lasts about 20 seconds, with a gradual return to baseline (Chalasani et al., 2007). Similarly, ASK shows a reliable increase in calcium levels upon food removal with a return to baseline in about 60 seconds (Calhoun et al., 2015; Wakabayashi et al., 2009). For both neurons, the magnitude and duration of the response are dependent on the food concentration, with more concentrated food leading to larger responses (Calhoun et al., 2015; Chalasani et al., 2007). Conversely, the sensory neuron ASI is ON-responding; it has a low baseline in the absence of food and shows an increase in calcium upon food addition (Calhoun et al., 2015).

The responses of some of the sensory neurons have been shown to be propagated to the downstream interneurons. Upon food removal, AWC activates AIB by releasing glutamate onto the AMPA receptor, *glr-1*, a glutamate-gated cation channel. The responses in AIB are longer than those in AWC and appear to be associated with a persistent activity pattern in multiple neurons that is sustained for the length of a reversal. Conversely, AWC inhibits AIY by releasing glutamate onto the glutamate-gated anion channel, *glc-3.* Unlike in AWC, the

responses to food removal in downstream interneurons, especially in AIB, are probabilistic and modified by internal network states (Gordus et al., 2015). The prevailing model is that upon food removal, AWC activates AIB which promotes reorientations, and simultaneously silences AIY to permit reorientations. Consistent with this model, animals lacking glutamate, *glr-1*, or *glc-3*, perform fewer reorientations off food (Chalasani et al., 2007; Hills et al., 2004).

The relationship between other sensory neurons and interneurons has not been as extensively examined. Nevertheless, ASK is glutamatergic and has connections to AIY and AIB, so a similar glutamate-dependent relationship may exist (White et al., 1986). In addition, it is likely ASK and AWC inhibit AIA, as AIA shows ON-responses like AIY (activated by food odor and silent in the absence of odor) (Larsch et al., 2015). In summary, ablation and imaging studies have identified sets of mutually antagonistic sensory neurons and interneurons that either promote reorientations or inhibit reorientations by signaling through glutamate gated ion channels (Fig. 1.1).

In addition to glutamate, dopamine has been implicated in local search behavior in *C. elegans* (Hills et al., 2004). In one study, animals lacking dopamine or the dopaminergic neurons CEP and PDE failed to perform local search after food removal, a phenotype that was rescued by adding exogenous dopamine to the assay plate. The rescue with exogenous dopamine was dependent on glutamate and on the glutamate receptors *glr-1* and *glr-2*, suggesting that dopamine functions in the same pathway as glutamate to modulate local search. The role of dopamine, however, is dependent on assay

conditions. Dopamine plays a role when animals are transferred from food plates to assay plates that differ in mechanical properties, pH, and cholesterol content, features that dopaminergic neurons may be able to detect (Hills et al., 2004). Assays that transfer animals from NGM plates with food to identical NGM plates without food did not find a role for dopamine (Gray et al., 2005). Thus, the circuits and molecules recruited for local search may be dependent on the set of sensory changes that animals experience upon food removal.

Like other foraging behaviors, local search in *C. elegans* is regulated by features of the food environment. The intensity (reorientation rate) of local search after food removal is dependent on the size of the bacterial lawns that animals experienced. Animals removed from larger lawns perform more local search than animals removed from smaller lawns (Calhoun et al., 2015); the difference occurs because animals in smaller patches experience the lawn edge more frequently and detect more variability. The effect is mediated by the sensory neurons ASK and ASI and a downstream dopamine-dependent circuit (Calhoun et al., 2015).

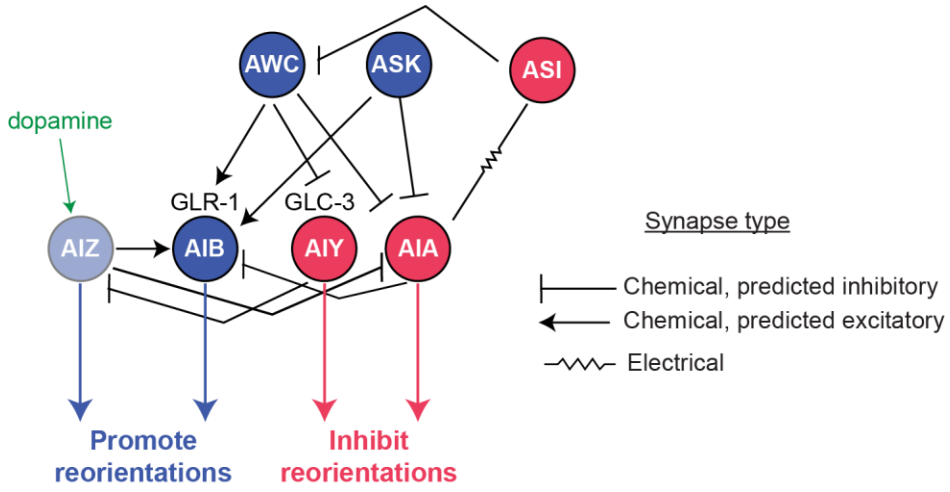

Figure 1.1. Neurons previously implicated in local search.

Previous work has identified neurons involved in reorientations off food. Neurons in blue promote reorientations and are activated by food removal. Neurons in pink inhibit reorientations and are active in the presence of food and inactive in the absence of food. AIZ promotes reorientations but its activity in response to food removal has not been carefully examined, though it is active during reversals. The nature of the connection (excitatory or inhibitory) is predicted based on the neuron's function. Dopamine has been predicted to regulate plasticity of local search by acting in AIZ (shows in green).

Goals of this work

In summary, previous studies have identified neurons and molecules important for acute reorientations during local search. Nevertheless, a circuit mechanism for the local search foraging state is not fully defined, and several important questions remain. How do animals represent the food environment? Food is a complex environment with multiple sensory features, and *C. elegans* has tens of sensory neurons that can detect various aspects of food. Previous studies have identified only chemosensory neurons that are important for local search reorientations. However, what is the contribution of different types of sensory neurons, especially ones associated with other sensory modalities? Do they act additively, redundantly, or synergistically? More generally, how are the circuits for local search organized to generate a minute-long behavior?

Many of the genes that have been identified to be important for local search are ion channels that signal over sub-second timescales, whereas local search occurs over minutes. Similarly, the neuronal responses to food removal that have been characterized occur over seconds (Calhoun et al., 2015; Chalasani et al., 2007; Wakabayashi et al., 2009). The minutes long-term activity patterns that match local search have not been described. What is the relationship between acute sensory signals and the longer-term dynamics of the local search state? The goal of my thesis was to address these questions.

CHAPTER 2:

Local search foraging behavior in *C. elegans*

INTRODUCTION

Most behaviors in *C. elegans* are assessed by looking at its locomotion. *C. elegans* propagates itself by crawling on its side and bending its body in the dorsoventral direction, leading to forward undulatory locomotion. Occasionally, animals interrupt their forward movement with reorientations. During a reorientation, an animal executes a pause, or a reversal followed by a shallow turn (Upsilon) or sharp turn (Omega), and then resumes motion in a new direction (Gjorgjieva et al., 2014). Reorientations fall into various subtypes based on the presence or absence of a reversal and the angle of the turn (shallow Upsilon vs. sharp Omega), and different subtypes are used during different behaviors.

Fast behaviors in *C. elegans*, such as escape responses to noxious stimuli, often consist of a single deterministic reorientation in which an animal reverses, turns, and moves away from the aversive stimulus (Culotti and Russell, 1978; Hilliard et al., 2004). More complex behaviors such as chemotaxis, aerotaxis, and foraging consist of sequences of reorientations that are organized over longer time scales (de Bono and Maricq, 2005). In these more complex behaviors, the frequency of reorientations is modulated temporally or spatially to produce a desired behavioral outcome. For example, during chemotaxis to an odor, animals increase their reorientation frequency when they are moving away from the odor and decrease it when they are approaching it. This spatial modulation of reorientations, called a biased random walk, allows animals to

efficiently turn and navigate towards odor sources and eventually find them (Larsch et al., 2015; Pierce-Shimomura et al., 1999) .

When *C. elegans* are removed from food, they exhibit a stereotypical foraging pattern in which they modulate their reorientation frequency over time. Immediately after food removal, *C. elegans* executes frequent random, undirected reorientations for about fifteen minutes (local search), which causes the animals to explore a relatively small area. If they fail to find food, animals transition to a global search in which they explore larger areas by decreasing their reorientation frequency and executing long forward runs (Ahmadi and Roy, 2016; Calhoun et al., 2014; Gray et al., 2005; Hills et al., 2004; Salvador et al., 2014; Wakabayashi et al., 2004). This behavioral sequence allows animal to modify their behavior based on recent experience and current conditions to increase their likelihood of finding food.

In this Chapter, we first characterized several features of this foraging behavior in wildtype animals. By recording animals on large plates and tracking their behavior automatically, we were able (i) look at different reorientation subtypes to uncover two categories, (ii) track 1,000+ single animals continuously to characterize the behavior in individuals. In addition, we examined the role of food history and satiety states in controlling local search behavior.

RESULTS

Local search behavior in wildtype *C. elegans*

We studied local search behavior by transferring young adult hermaphrodite animals from a standard bacterial food lawn to a large agar plate without food (~80 cm^2), where we filmed and quantified their behavior continuously for 45 min (Fig. 2.1A). While on the bacterial food lawn, animals showed limited exploration, expressed as a low mean squared displacement (MSD) in Fig. 2.1B. Upon removal from food, animals initially explored a relatively small area by performing many reorientations (Fig. 2.1B-C, local search), then gradually transitioned to exploring a larger area by performing fewer reorientations over time (Fig. 2.1B-C, global search). This foraging sequence is not an effect of the transfer (Zhao et al., 2003) as animals removed from a plate without food do not show the high reorientation state of local search (Fig. 2.1C).

C. elegans can perform a variety of reorientations using different locomotor sequences (Fig. 2.2). To ask if all reorientations are dependent on the time since food removal, we looked at the frequency of different reorientation subtypes over time. We found that reorientations fell into two categories: those that start with a reversal were time-dependent (elevated during local search, Fig 2.2A-C), whereas those resulting from turning during forward movement were time-independent (similar frequencies during local and global search, Fig. 2.2D-E). Here, we focused on the time-dependent reorientations that drive local search behavior (Fig. 2.1C).

Figure 2.1. Off-food foraging in the population of wildtype animals.

(A) Schematic of off-food foraging assay. Animals were transferred from a homogeneous bacterial food lawn to a large plate (80 cm^2) without food, where their behavior was filmed for 45 min. The behavior varies from day to day, so all experiments were compared to control animals recorded simultaneously in an adjacent behavioral chamber.

(B) Average mean squared displacement per minute on food and after food removal (n=413)

(C) Thick line: off-food foraging showing mean reorientations in 2-min time windows after food removal. The first two minutes are not plotted as these are affected by transfer (Zhao et al., 2003). Thin line: similar animals transferred after 45 min on a plate without food (n=413)

Figure 2.1

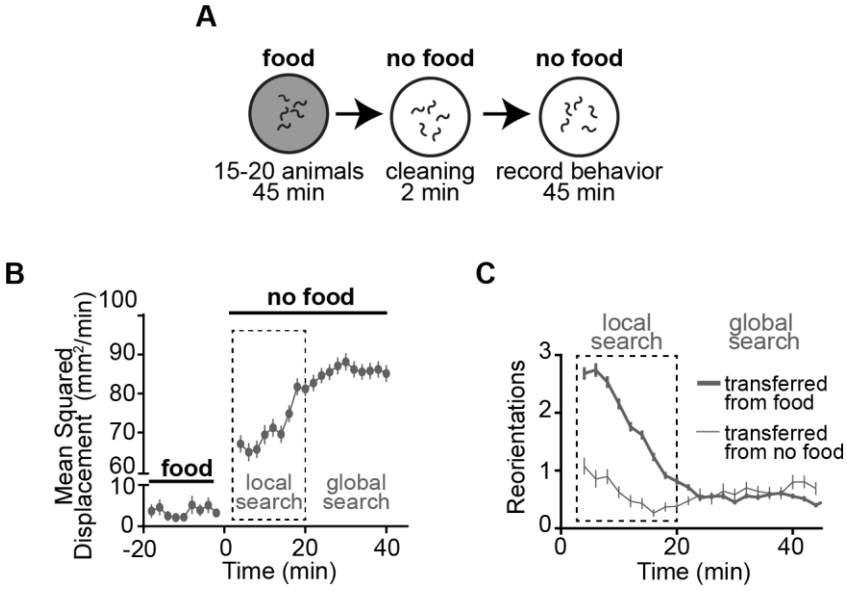
A
food
no food
no food
15-20 animals
45 min
cleaning
2 min
record behavior
45 min
B
Mean Squared Displacement (mm²/min)
100
90
80
70
60
10
0
food
no food
local search
global search
-20
0
20
40
Time (min)
C
local search
global search
Reorientations
3
2
1
0
transferred from food
transferred from no food
0
20
40
Time (min)

Figure 2.2. Reorientation behaviors fall into time-dependent and time-independent categories.

(A-C) Reorientations whose frequency is dependent on the time since food removal. All include an initial reversal. (A) Reversal + deep bend (Omega). (B) Reversal only. (C) Reversal + shallow bend (Upsilon).

(D-E) Reorientations whose frequency is not dependent on time since food removal. (D) Pause + Upsilon. (E) Pause + Omega. Data also includes animals that show an abrupt Upsilon or Omega during forward movement, without a pause.

Figure 2.2

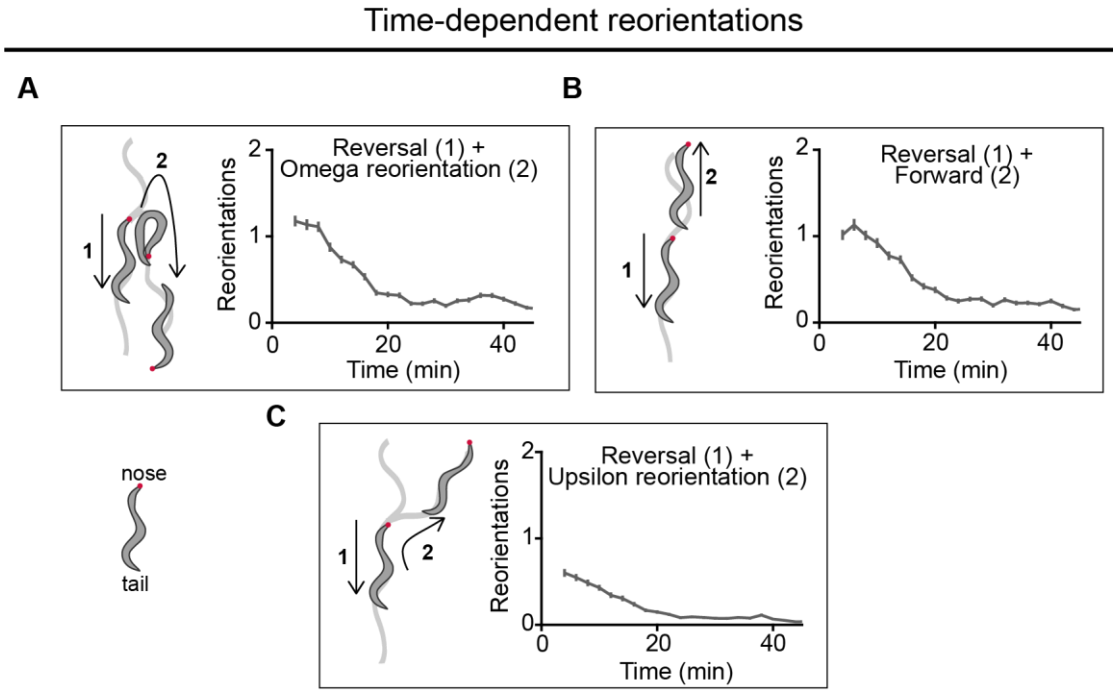
Time-dependent reorientations
A
B
Reversal (1) +
Omega reorientation (2)
Reversal (1) +
Forward (2)
Reorientations
Time (min)
C
nose
tail
Reversal (1) +
Upsilon reorientation (2)
Time-independent reorientations
D
E
Pause (1) +
Upsilon reorientation (2)
Pause (1) +
Omega reorientation (2)

Reorientation dynamics in individual animals

The transition from local to global search is gradual at a population level (Fig. 2.1C) but has been suggested to be either graded or abrupt at an individual level (Calhoun et al., 2014; Klein et al., 2017). To further characterize the transition sharpness in individual animals, we looked at the reorientation dynamics of 1,631 animals whose behavior we were able to track continuously for 45 min after food removal. We plotted the cumulative sum of time-dependent reorientations over time after food removal and searched for abrupt transitions in reorientation frequency (Fig. 2.3A-B). We found that 50.7% of animals best fit a single abrupt transition corresponding to the end of local search (Fig. 2.3A-C), whereas 49% exhibited multiple transitions or no clear transition (Fig. 2.3A-B). Thus, different dynamics probably exist within the population. Indeed, both dynamic patterns (abrupt transition vs. no transition) were observed in different animals on the same plate.

We also found high variability in the foraging behavior between animals. For animals that showed a single abrupt transition, the timing of the transition (the duration of local search) ranged from 3 min to 26 min after removal from food (Fig. 2.3C). This range partly explains the gradual decrease in reorientations of the population (Fig. 2.1C). In addition, there was substantial variability in the absolute number of reorientations in individual animals, both during local and global search (Fig. 2.3D). Despite this variability, 93% of the animals performed more reorientations at early times after food removal (Fig. 2.3E), indicating that local search is a robust behavioral response to a recent food encounter.

Figure 2.3. Reorientation dynamics in individual animals

(A-C) Off-food reorientation dynamics for 1,631 individual animals from 198 different experiments collected over two years. (A) Examples of individual animals. Normalized cumulative sum of reorientations after food removal for 36 individual animals. Each circle represents a reorientation. Top 18 panels best fit a single abrupt behavioral transition (marked with blue line) recognized as a change in the slope of the cumulative sum; bottom 18 panels did not. Each individual animal was analyzed by: (1) using the MATLAB function *findchangepts* to find a potential transition time. This function divides each trace into two regions that minimize the sum of the residual squared error of each region from a local linear regression, and then (2) visually inspecting the potential transition time to determine if it corresponded to a single transition. (B) Percentage of animals that performed abrupt transitions vs. non-abrupt transitions based on the method described above (n = 1,631). (C) Cumulative distribution of transition times for animals that showed a single abrupt transition (n=827). The abrupt transition time corresponds to the end of local search.

(D) Total number of reorientations of individual animals during the entire 45 min off food, during the first 20 min (local search), and during the last 20 min (global search). There is high variability in the reorientation rates of individual animals (n=1,631). Data presented as mean ± s.d.

(E) $\log_2$ (number of reorientations in first 20 minutes / number of reorientations in last 20 min) for each individual animal. 93.3% of animals perform more reorientations early than late after food removal (1,521/1,631; gray dots), suggesting that local search is a robust response to a recent food encounter. 6.7% of animals perform the same number or fewer reorientations early than late after food removal (84/1,631; red dots).

Figure 2.3

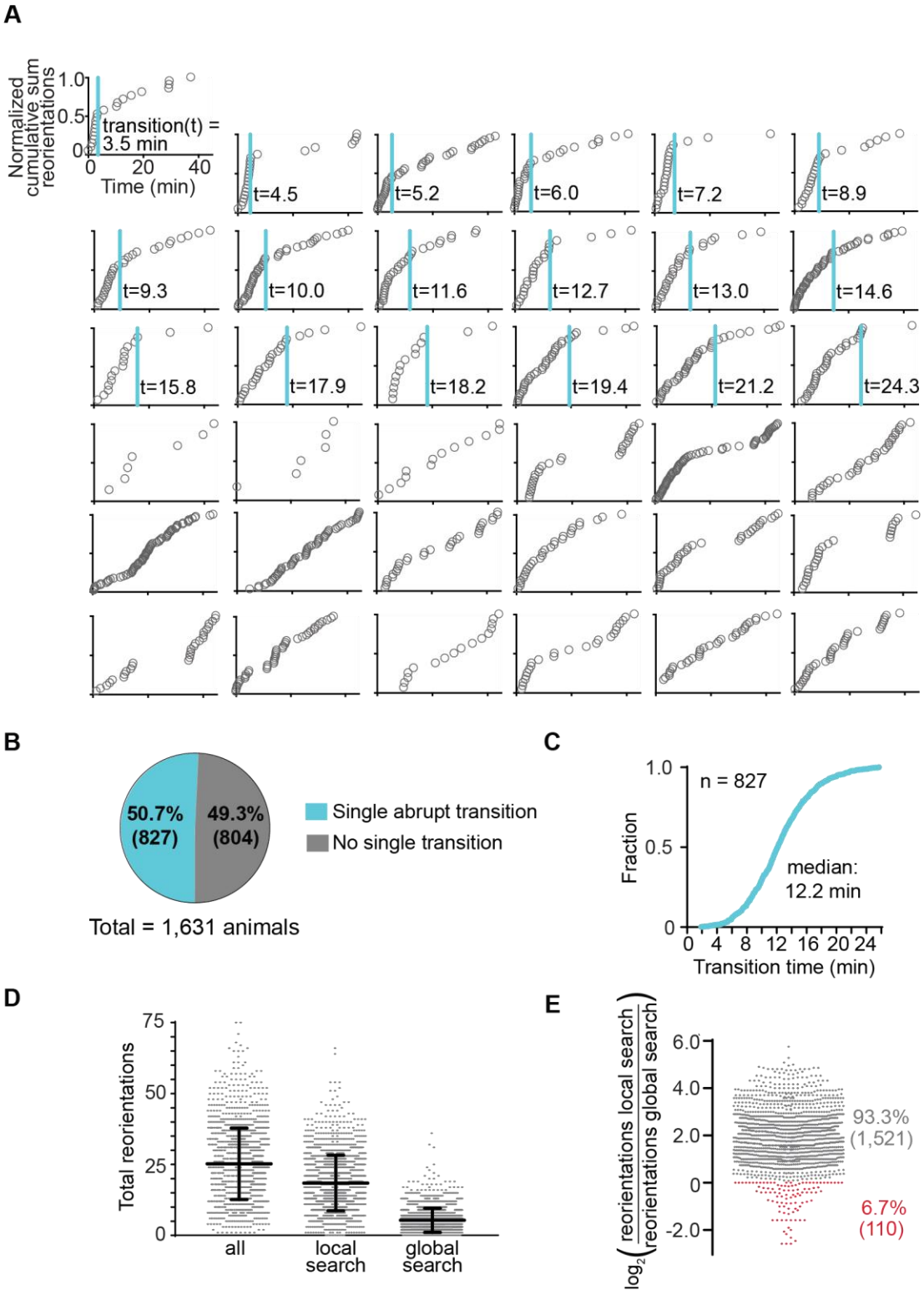
A
Normalized cumulative sum reorientations
1.0
0.5
0
transition(t) = 3.5 min
0
20
40
Time (min)
t=4.5
t=5.2
t=6.0
t=7.2
t=8.9
t=9.3
t=10.0
t=11.6
t=12.7
t=13.0
t=14.6
t=15.8
t=17.9
t=18.2
t=19.4
t=21.2
t=24.3
B
50.7% (827)
49.3% (804)
Single abrupt transition
No single transition
Total = 1,631 animals
C
1.0
0.5
0
Fraction
n = 827
median: 12.2 min
0 4 8 12 16 20 24
Transition time (min)
D
75
50
25
0
Total reorientations
all
local search
global search
E
6.0
4.0
2.0
0
-2.0
log2(reorientations local search / reorientations global search)
93.3% (1,521)
6.7% (110)

Local search behavior is modulated by food history

If local search represents a short-term memory of recent food experience, it should be modulated by features of the food history. To test this prediction, we varied the food concentration that animals experienced prior to food removal (Fig. 2.4A). We placed animals on bacterial lawns of different concentrations, and then removed them and examined their local and global search behaviors. Animals that had been in dilute food performed fewer time-dependent reorientations during local search than animals that had been in concentrated food (Fig. 2.4B). Reorientations during global search were unchanged by initial food conditions. This result and others (Calhoun et al., 2015), suggest that local search is a memory state that is actively generated and modulated in response to food removal, and that it transitions or decays over time to a memoryless, default global search state (Salvador et al., 2014). This pattern is also observed in arthropods, who modulate local search based on resource history (Bell, 1985)

Consistent with our previous observation, we found that the levels of time-independent reorientations were not affected by the food history. Animals removed from different food concentrations showed similar level of time-independent reorientations at all times off-food (Fig. 2.4C). This supports the view that foraging is a combination of ‘memory’ related time-dependent behaviors and basal time-independent behaviors (Salvador et al., 2014). For all subsequent experiments, we quantified only time-dependent reorientations, as these are the ones related to local search behavior.

In a complimentary set of experiments exploring the role of food history on off-food foraging, we asked if food re-exposure could 'reset' local search in animals that had already transitioned to global search. To address this, we removed animals from a standard bacterial food lawn, and recorded their behavior for 45 min, as previously described. We then re-exposed these same animals to food for various amounts of time and examined off food-foraging again for 45 min (Fig. 2.5A). The goal was to ask how long animals needed to be re-exposed to food to re-trigger local search.

We found that animals that were re-exposed to food for 0 min or 5 min did not show any local search behavior upon food removal (Fig. 2.5B-C), suggesting that a quick sensory re-exposure cannot trigger local search. Animals re-exposed to food for 15 min showed some local search, but lower in intensity and shorter in duration (Fig. 2.5D). Animals re-exposed to food for 30 min or 45 min displayed a full local search, indistinguishable from the previous food removal (Fig. 2.5 E-F). Finally, animals re-exposed to food for 60 min showed local search that was higher in intensity than the previous one (Fig. 2.5G). Together, these results suggest that animals use information not only about food quality (concentration, Fig. 2.4), but also about the duration of food history to modulate subsequent local search behavior.

Figure 2.4. Effect of food concentration on local search behavior

(A) Experimental scheme for food concentration experiments. Animals were placed on bacterial food lawns of different concentration for 45 min, and subsequently removed to a plate without food where their behavior was recorded for 45 min. The 1x concentration is a bacterial culture of OD of 0.5 (see Experimental Procedures)

(B-C) Effect of food concentration on subsequent off-food foraging. Animals were removed from either a standard OD=0.5 bacterial lawn (n=103), a lawn diluted 10-fold (n=114), or a lawn diluted 100-fold (n=100), and their subsequent off-food behavior was recorded (B) Time-dependent reorientations and (C) Time-independent reorientations over time after food removal.

All data are presented as mean ± s.e.m. ***$p < 0.001$ by Wilcoxon rank sum test with Bonferroni correction.

Figure 2.4

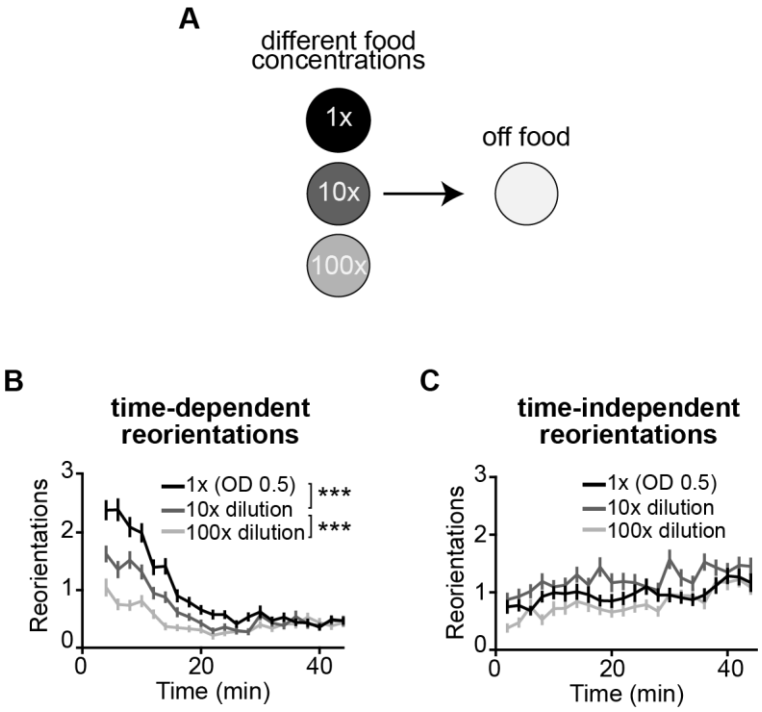
A
different food concentrations
1x
10x
100x
off food
B
time-dependent reorientations
1x (OD 0.5)
10x dilution
100x dilution
***
***
Reorientations
Time (min)
C
time-independent reorientations
1x (OD 0.5)
10x dilution
100x dilution
Reorientations
Time (min)

Figure 2.5. Effect of food re-exposure duration on subsequent local search behavior

(A) Experimental scheme for food re-exposure experiments. Animals were placed on a standard food lawn for 45 min and subsequently transferred to a plate without food where their behavior was recorded for 45 min (off food 1, gray lines in B-G). The same animals were then transferred back to a standard food lawn for varying amounts of time, and then removed to a plate without food, where their behavior was recorded again for 45 min (off food 2, pink lines in B-G, the time animals spent on food is indicated on plot).

(B-G) Effect of food re-exposure duration on subsequent off-food foraging. Local search behavior after food re-exposure for 0 min (animals transferred straight to another off-food plate, n=71), 5 min (n=60), 15 min (n=55), 30 min (n=55), 45 min (n=71), and 60 min (n=59). Comparison are between the first (gray) and second (pink) food removal in the same animals.

All data are presented as mean ± s.e.m. p-values calculated using Wilcoxon rank sum test with Bonferroni correction, *p<0.05 ***p < 0.001

Figure 2.5

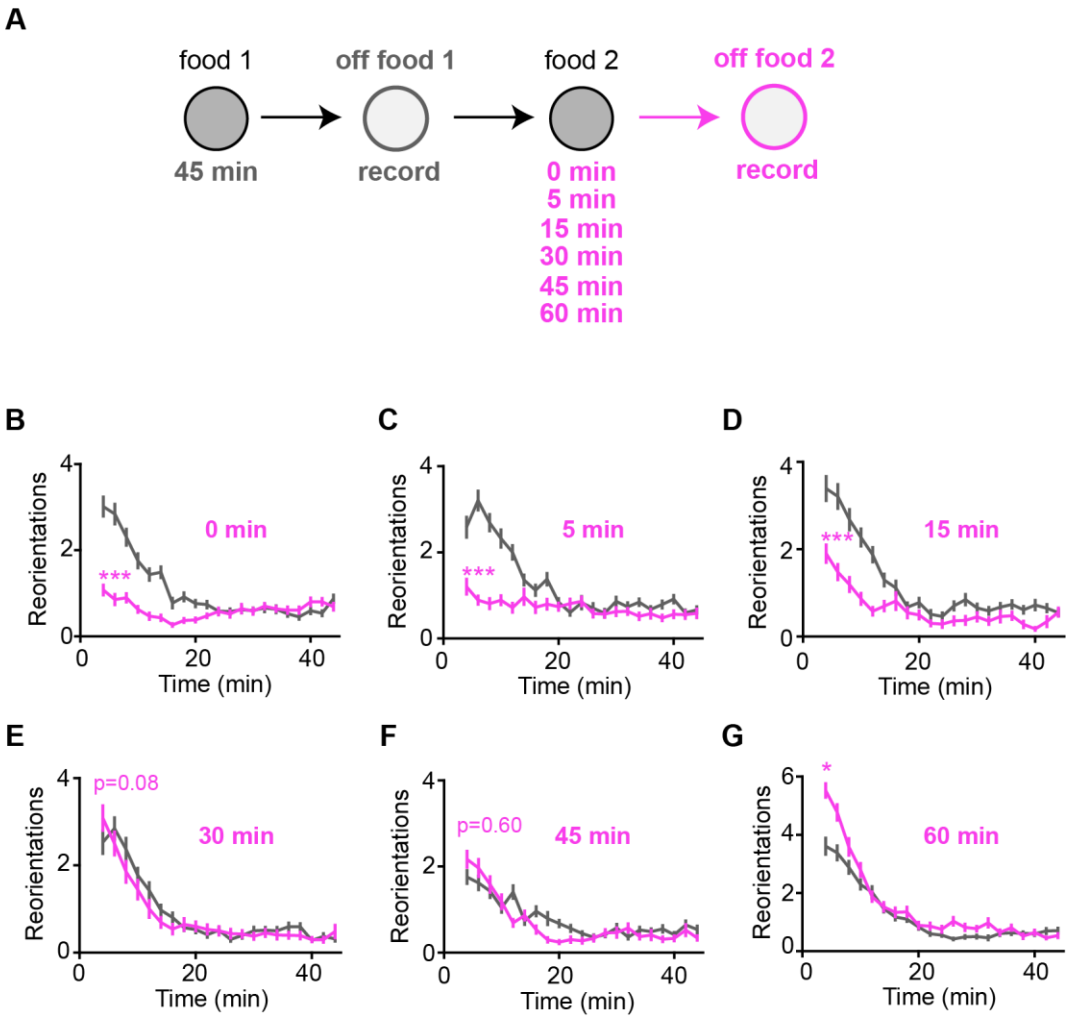
A
food 1
off food 1
food 2
off food 2
45 min
record
0 min
5 min
15 min
30 min
45 min
60 min
record
B
C
D
E
F
G
Reorientations
Time (min)
0 min
5 min
15 min
30 min
45 min
60 min
***
p=0.08
p=0.60
*

Role of satiety state in local search behavior

Previous work in insects has described the role of internal state in modulating local search behavior (Bell, 1985; Murata et al., 2017). All the experiments described thus far were conducted in well-fed animals. To understand how internal satiety state affects local search behavior, we used an optogenetic tool to inhibit feeding while animals were on food. We expressed the red-shifted channelrhodopsin variant ReaChR (Lin et al., 2013) in pharyngeal muscle, and used light to depolarize and paralyze the pharynx. Compared to control animals, these animals should have similar sensory experiences upon food removal but different satiety levels. We then removed these animals from food to assess local and global search behavior.

Inhibiting feeding for 10 min or 20 min prior to removal from food had little effect on the foraging sequence (Fig. 2.6A-B). This result suggests that the transition from local to global search that normally happens within 20 minutes is not driven by a direct input from the pharynx or by the time since feeding. On the other hand, inhibiting feeding for 45 min greatly reduced local search (Fig. 2.6C). Similarly, wildtype animals did not perform local search after 45 minutes on inedible aztreonam-treated bacteria (Gruninger et al., 2008) (Fig. 2.6D). Together, these results suggest that the transition from local to global search does not follow a metabolic clock of time since feeding, but that satiety, on a longer time scale, modifies local search behavior.

In the next two chapters, we identify and characterize a sensory circuit that controls local search. In each chapter, we ask if the satiety state interacts with the sensory circuits that control local search.

Figure 2.6. Role of satiety state in local search behavior

(A-C) Off-food foraging after feeding inhibition for various times prior to food removal. Pharyngeal pumping was inhibited by delivering light to retinal-treated animals expressing the red-shifted channelrhodopsin, ReaChR, in the pharynx. Control animals expressed ReaChR and were treated with light, but not retinal. (A) Off-food foraging after 10 min of feeding inhibition prior to food removal (control, n=37; 10 min, n=61). (B) Off-food foraging after 20 min of feeding inhibition prior to food removal (control, n=36; 20 min, n=31). (C) Off-food foraging after 45 min of feeding inhibition prior to food removal (control, n=75; 45 min, n=78).

(D) Off-food foraging after 45 min on inedible aztreonam-treated bacteria. Control were animals on regular bacteria (control, n=98; inedible bacteria, n=96).

All data presented as mean ± s.e.m. All p-values calculated using Wilcoxon rank sum test with Bonferroni correction. ***$p < 0.001$.

Figure 2.6

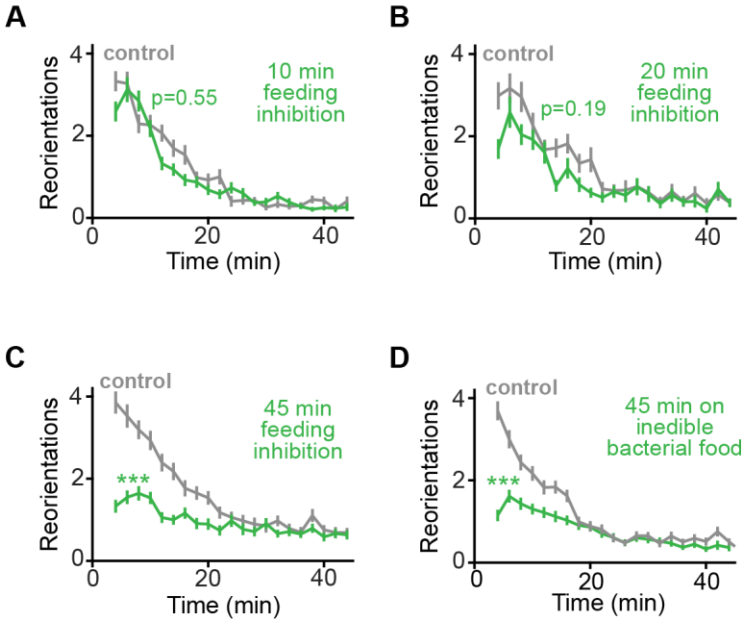
A
control
10 min
feeding
inhibition
p=0.55
Reorientations
Time (min)
B
control
20 min
feeding
inhibition
p=0.19
Reorientations
Time (min)
C
control
45 min
feeding
inhibition
***
Reorientations
Time (min)
D
control
45 min on
inedible
bacterial food
***
Reorientations
Time (min)

DISCUSSION

Reorientations in foraging and in other behaviors in *C. elegans*

When removed from food, *C. elegans* executes a stereotypical local-to-global search foraging pattern by modulating the frequency of reorientations over time. We found that reorientations during this behavior fall into two categories: time-dependent and time-independent. Time-dependent reorientations have memory-like features; they are dependent on the time since food removal and are modulated by food history (Fig. 2.2A-C, Fig. 2.4B). Time-independent reorientations are 'memoryless' as they have a basal frequency that is not modulated by food history (Fig. 2.2D-E, Fig. 2.4C). This is consistent with the idea that the most effective foraging strategy when there is no explicit information about the location of resources combines memory components with basal searching components (Salvador et al., 2014).

Interestingly, both types of reorientations share similar locomotor components- the Upsilon and Omega turns- which suggests that they may be generated by overlapping neural mechanisms. Yet, we found genes that selectively regulate the frequency of time-independent reorientations, without affecting time-dependent reorientations (the cholecystokinin receptor, *ckr*-2, Fig. 2.7A-B, we found this mutant while conducting the genetic screen described in the next Chapter). In addition, the metabotropic glutamate receptor, MGL-1, described in the next Chapter, affects only time-dependent reorientations. Throughout this work, we were unable to find any manipulation or mutation that

affects both types of reorientations. Thus, though these two types of reorientations may overlap as acute motor programs, their frequencies are likely to be regulated by different molecular and cellular mechanisms.

All reorientations during local search are spontaneous, occurring in the absence of obvious external stimuli. The same types of reorientations are observed in sensory-evoked behaviors like chemotaxis. However, during chemotaxis there is no functional distinction between reorientation subtypes; during chemotaxis both 'time-dependent' and 'time-independent' reorientations are modulated spatially based on the animal's orientation (going towards or away from an odor) (unpublished results from the lab) (Pierce-Shimomura et al., 1999). In fact, 'time-independent' reorientations may contribute to the weathervane chemotaxis strategy, one of two key behavioral mechanisms, whereas 'time-dependent reorientations' contribute to the pirouette chemotaxis strategy (Iino and Yoshida, 2009). Thus, when there is explicit information about the location of resources (like the odor during chemotaxis), search strategies may not need to incorporate a basal behavioral component.

Foraging behavior in individual animals

Foraging strategies are conserved and stereotyped at a population level. Individual animals, however, show large variability in various aspects of the foraging behavior. First, only about half of the animals showed an abrupt behavioral transition from local to global search (Fig. 2.3A-B). Previous studies

had reported that either all animals showed an abrupt behavioral transition (Calhoun et al., 2014), or that no animals showed abrupt transitions (Klein et al., 2017). By looking at many animals, we showed that both types of dynamics exist within the population, even on animals on the same plate. Second, there was a wide range in the duration of local search (for animals that showed an abrupt transition, Fig. 2.3C). This behavioral heterogeneity has been described previously in insects (flies and cockroaches), where individual animals show variability in the 'giving up time', the duration of intensive searching after a resource encounter (Bell, 1985; Schal et al., 1983). Thus, variability may be a general feature of local search behavior. Third, animals show a large variation in the absolute number of reorientations after food removal, despite consistently doing more reorientations early than late after food removal. This suggests that there is considerable variability in the mechanisms that control the baseline number of reorientations, but less in the mechanisms that control the relative number of reorientations early vs. late after food removal.

During our experiments, we did not precisely control environmental conditions such as temperature and humidity, which might be sources of variability. However, animals on the same plate showed large differences in their search patterns, suggesting that there may be internally generated sources of variability. Indeed, studies in *C. elegans* under controlled environmental conditions have identified behavioral differences between animals that cannot be attributed to external sources (Stern et al., 2017).

Local search is a short-term memory of the recent food encounter

Several features of food history affect subsequent local search behavior. Here, we found that the intensity of local search depends on the previous food concentration (Fig. 2.4B). Additionally, re-triggering local search after animals have transitioned to global search is deponent on the time of food re-exposure (Fig. 2.5). Other studies in *C. elegans* found that the size of the bacterial lawn affects the intensity of local search, with larger lawns leading to more local search after food removal (Calhoun et al., 2015). Studies in other species have described similar effects. Flies given more concentrated sugar perform more local search following ingestion (Bell, 1985; Murata et al., 2017). Lizards modify their local search based on features of the prey encountered, such as the type of prey and its size (Eifler et al., 2012). In all cases, local search is modulated by the features of the recent food encounter, and thus represents a short-term food memory.

In the next Chapter, we set out to find the circuits and molecules that generate this highly conserved local search behavior.

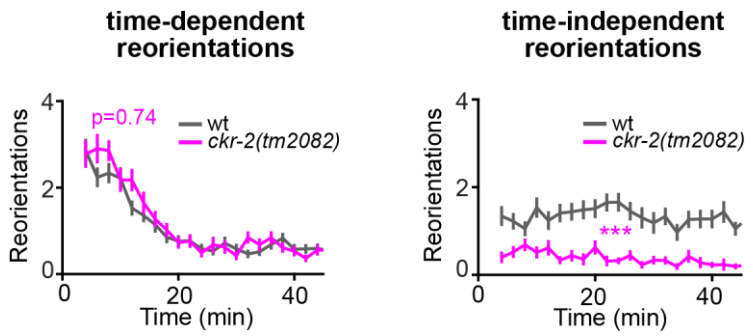

Figure 2.7. Reorientation subtypes in cholecystokinin receptor, *ckr-2,* mutants

(left) Time-dependent and (right) time-independent reorientations over time after food removal in *ckr-2* mutants (wt, n=49; *ckr-2*, n= 42).

All data presented as mean ± s.e.m. p-values calculated using Wilcoxon rank sum test with Bonferroni correction ***$p < 0.001$.

CHAPTER 3:

A neural circuit for local search behavior

INTRODUCTION

Previous studies in *C. elegans* have identified several neurons important for reorientations during foraging in the absence of food (Gray et al., 2005; Wakabayashi et al., 2004). Chemosensory neurons that directly detect food metabolites are necessary to generate off-food reorientations, as animals lacking sensory cilia act as if they were still on food (Gray et al., 2005). Among chemosensory neurons, AWC and ASK appear to be the most important, as ablating these neurons leads to a large decrease in reorientations off-food (Gray et al., 2005; Wakabayashi et al., 2004). These sensory neurons are predicted to contribute to acute off-food reorientations by releasing glutamate that activates glutamate-gated ion channels, such as *glr-1,* on downstream interneurons, such as AIB (Fig. 1.1) (Chalasani et al., 2007; Gray et al., 2005; Hills et al., 2004; Wakabayashi et al., 2004).

These studies, however, did not distinguish between circuits that are important to generate acute reorientations and circuits that contribute specifically to generating the high reorientation state of local search. For example, many of the genes and neurons identified to be important for local search are also important for the fast reorientations seen in escape behaviors (Maricq et al., 1995; Pokala et al., 2014). In addition, the ion channels identified in previous studies open and close over sub-second timescales, whereas local search occurs over minutes. The relationship between acute sensory signals and the longer-term dynamics of the local search state is not known.

Here, we conduct a candidate genetic screen to find genes that preferentially affect the local search behavioral state. We identify a G protein-coupled glutamate receptor, MGL-1, as a transducer of sensory information into a sustained circuit state. We show that parallel chemosensory and mechanosensory modules have redundant capability to generate the local search behavioral state by inhibiting separate downstream integrating neurons through MGL-1. Our findings reveal a circuit organization that allows for the robust execution of a conserved adaptive behavior.

RESULTS

A candidate genetic screen for local search behavior

To gain insight into the neuronal circuit mechanisms that generate local search behavior, we tested 42 candidate mutant strains lacking individual ionotropic and metabotropic neurotransmitter receptors by filming their behavior and comparing their reorientation rates to matched controls. For each mutant strain, we calculated the average fold-change in reorientations relative to wildtype during local search (2-20 min) (Fig. 3.1A, Table 3.1) and global search (30-45 min) (Table 3.1). We focused on mutants that had stronger defects during local search. Of the 42 mutant strains tested, two notable categories emerged: a set of ionotropic acetylcholine receptor mutants (*lgc-46, acc-4, acr-12*, Fig.3.1B, Table 3.1), and the mutant strain CX17083 (Fig. 3.1C, Table 3.1).

Mutants lacking the inhibitory acetylcholine receptors *lgc-46* and *acc-4* showed diminished local search (Fig. 3.1B), whereas mutants in the excitatory acetylcholine receptor *acr-12* showed augmented local search behavior (Fig. 3.1B). These results suggest an involvement of acetylcholine in controlling reorientation probabilities during local search. *lgc-46* and *acc-4* have been hypothesized to form heteromeric channels and are both expressed broadly in cholinergic neurons (Pereira et al., 2015; Takayanagi-Kiya et al., 2016). However, we were unable to rescue *lgc-46* in specific subset of neurons (cholinergic motor neurons, sets of interneurons) to uncover a circuit mechanism, and therefore did not study the cholinergic mutants further.

Figure 3.1. Candidate genetic screen for local search behavior

(A) Local search (2-20 min) reorientation rates normalized to wildtype controls for 42 mutant strains. Data show the fold change in reorientations during local search for each mutant strain, presented as the $\log_2$ of mutant/wildtype reorientation ratio. Mutants bolded and marked with the p-value asterisks met two criteria: (i) showed a statistically significant fold change during local search of at least 1.5 (abs($\log_2$(ratio))>0.58), and (ii) local search was affected more than global search. For detailed results and explanations, see Table S1.

(B) Off-food foraging in mutants for the inhibitory acetylcholine receptors, *lgc-46* and *acc-4*, and for the excitatory acetylcholine receptor, *acr-12*. ($wt_{lgc\text{-}46,acc\text{-}4}$, n=55; *lgc-46,* n=51; *acc-4*, n=55; $wt_{acr\text{-}12}$, n=56; *acr-12*, n=61). All three genes encode ligand-gated ion channels that are broadly expressed in interneurons and cholinergic motor neurons. Presented as mean ± s.e.m. ***p < 0.001 by Wilcoxon rank sum test.

(C) Off-food foraging for mutant strain CX17083 [*npr-9(tm1652);mgl-1(ky1060)*] (wt, n =56; CX17083, n=62). Presented as mean ± s.e.m. ***p < 0.001 by Wilcoxon rank sum test.

Figure 3.1

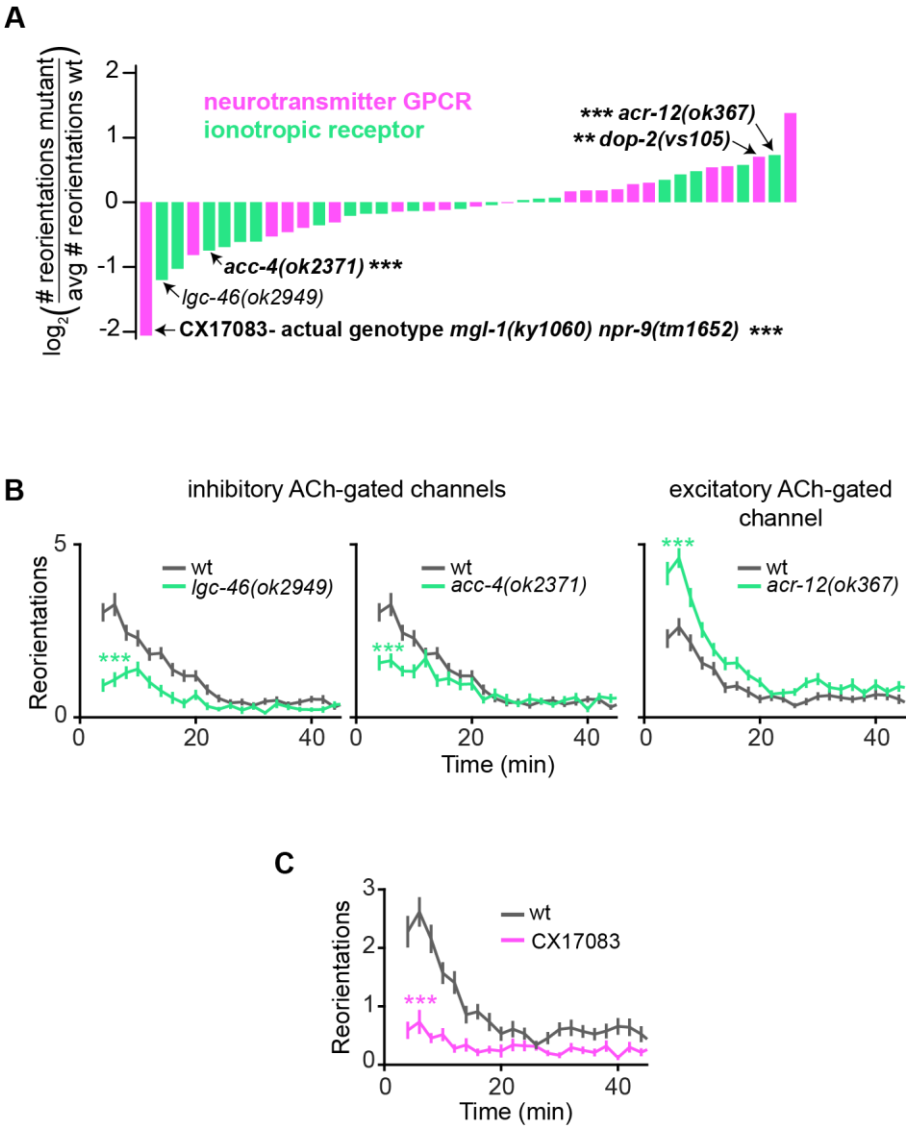
A
log2(# reorientations mutant / avg # reorientations wt)
2
1
0
-1
-2
neurotransmitter GPCR
ionotropic receptor
*** acr-12(ok367)
** dop-2(vs105)
acc-4(ok2371) ***
lgc-46(ok2949)
CX17083- actual genotype mgl-1(ky1060) npr-9(tm1652) ***
B
inhibitory ACh-gated channels
excitatory ACh-gated channel
Reorientations
5
0
wt
lgc-46(ok2949)
***
wt
acc-4(ok2371)
***
***
wt
acr-12(ok367)
0
20
40
Time (min)
C
Reorientations
3
2
1
0
wt
CX17083
***
0
20
40
Time (min)

Table 3.1. Results for candidate genetic screen.

Strain name, genotype, number of times backcrossed to wildtype animals, and screen results. Since each mutant strain was matched to different control animals, we defined a ratio for each mutant strain by counting the number of reorientations of each mutant animal during the local search (2-20 min) or global search (30-45) time window and dividing it by the average number of reorientations of matched wildtype animals. Table shows mean ratio ± SEM for each mutant strain. In parentheses, bolded, are the $\log_2$ values for the ratio, which are plotted in Figure 2.

To analyze the screen results, we selected mutants that met two criteria: (1) the mutant was statistically different from wildtype during local search by at least 1.5-fold change ($abs(\log_2(ratio)) > 0.58$). Mutants that met this first criteria have their p-value result (asterisks) indicated in the 'local search' column, (2) local search was affected more than global search, which we assessed by comparing the two ratios. Strains meeting both criteria are indicated in the right column and marked with their local search p-value result (asterisks) in Figure 2.

p-values were calculated using Wilcoxon rank sum test with Bonferroni correction.

* $p<0.05$ ** $p < 0.01$ *** $p < 0.001$. Statistics were conducted by comparing the number of reorientations of mutant animals to matched controls during local search (see Methods).

Table 3.1

STRAIN	GENOTYPE	BACKCROSSED TO WILDTYPE	LOCAL SEARCH (2-20 MIN)	GLOBAL SEARCH (30-45 MIN)	LARGER LOCAL SEARCH DEFECT?
CX17083	*mgl-1(ky1060) npr-9(tm1652) X*	6x	0.24 ± 0.04 **(-2.06)*****	0.41 ± 0.06 **(-1.28)**	**YES**
CX12722	*lgc-46(ok2949)*	4x	0.44 ± 0.07 **(-1.20)*****	0.55 ± 0.11 **(-0.85)**	no
KP4	*glr-1(n2461)*	4x	0.49 ± 0.06 **(-1.03)*****	0.42 ± 0.06 **(-1.25)**	no
CX12797	*mgl-2(tm355)*	4x	0.57 ± 0.06 **(-0.81)****	0.68 ± 0.16 **(-0.55)**	no
CX12724	*acc-4(ok2371)*	4x	0.60 ± 0.06 **(-0.75)*****	1.09 ± 0.12 **(0.13)**	**YES**
CX12723	*gab-1(tm3577)*	4x	0.62 ± 0.07 **(-0.69)***	0.87 ± 0.15 **(-0.19)**	no
CX12720	*glr-2(tm669)*	4x	0.65 ± 0.07 **(-0.61)***	0.76 ± 0.10 **(-0.40)**	no
CX16989	*lgc-48(gk964294)*	3x	0.66 ± 0.05 **(-0.61)***	0.61 ± 0.08 **(-0.70)**	no
CX16990	*npr-35(ok3258)*	3x	0.69 ± 0.06 **(-0.53)**	0.80 ± 0.10 **(-0.32)**	
CX16986	*gar-2(ok520)*	3x	0.73 ± 0.07 **(-0.46)**	1.04 ± 0.14 **(0.05)**	
CX13890	*npr-4(tm1782)*	4x	0.76 ± 0.06 **(-0.39)**	1.15 ± 0.12 **(0.20)**	
VW4509	*nmr-1(ak4)*	12x	0.78 ± 0.07 **(-0.35)**	0.78 ± 0.11 **(-0.35)**	
CX16403	*seb-3(gk382193)*	6x	0.86 ± 0.07 **(-0.31)**	0.71 ± 0.08 **(-0.50)**	
VM1846	*glr-3(ak57)*	?	0.87 ± 0.05 **(-0.21)**	0.81 ± 0.12 **(-0.31)**	
NC293	*acr-5(ok180)*	4x	0.88 ± 0.06 **(-0.18)**	1.02 ± 0.09 **(0.02)**	
CX13755	*avr-14(ad1305)*	3x	0.89 ± 0.10 **(-0.17)**	1.39 ± 0.15 **(0.47)**	
CX14394	*npr-5(ok1583)*	5x	0.90 ± 0.07 **(-0.14)**	1.22 ± 0.16 **(0.30)**	
CX16985	*glc-3(ok321)*	3x	0.91 ± 0.08 **(-0.13)**	0.71 ± 0.08 **(-0.50)**	
CX15563	*ador-1(gk744003)*	3x	0.91 ± 0.06 **(-0.13)**	1.30 ± 0.19 **(0.38)**	
MT1222	*egl-6(n592)*	1x	0.92 ± 0.09 **(-0.12)**	0.58 ± 0.08 **(-0.77)**	
CX13889	*lgc-52(tm4596)*	5x	0.93 ± 0.08 **(-0.10)**	1.23 ± 0.14 **(0.30)**	
CX16983	*gar-1(ok755)*	2x	0.96 ± 0.07 **(-0.06)**	0.90 ± 0.10 **(-0.15)**	
CX16988	*acc-2(ok2216)*	3x	0.97 ± 0.05 **(-0.04)**	1.15 ± 0.08 **(0.20)**	
CX8579	*npr-11(ok594)*	4x	0.99 ± 0.09 **(-0.01)**	0.87 ± 0.13 **(-0.20)**	
CX14904	*glr-6(tm2729)*	4x	1.02 ± 0.10 **(0.03)**	1.43 ± 0.16 **(0.51)**	
CX16982	*lgc-54(tm3448)*	3x	1.04 ± 0.08 **(0.05)**	0.91 ± 0.11 **(-0.14)**	
CX12721	*acc-1 (tm3268)*	4x	1.05 ± 0.07 **(0.07)**	1.92 ± 0.18 **(0.94)**	
CX16402	*npr-14(ok2375)*	4x	1.12 ± 0.10 **(0.17)**	0.93 ± 0.12 **(-0.10)**	
CX15961	*ckr-2(tm2082)*	4x	1.14 ± 0.08 **(0.18)**	1.04 ± 0.12 **(0.06)**	
LX636	*dop-1(vs101)*	4x	1.14 ± 0.08 **(0.18)**	0.89 ± 0.10 **(-0.16)**	
CX11751	*dop-4(ok1321)*	4x	1.15 ± 0.09 **(0.20)**	0.99 ± 0.11 **(-0.02)**	
BZ873	*dop-3(ok295)*	6x	1.22 ± 0.08 **(0.28)**	1.06 ± 0.10 **(0.08)**	
CX15899	*gbb-1 (tm1406)*	7x	1.23 ± 0.12 **(0.30)**	1.15 ± 0.11 **(0.20)**	
CX15901	*lgc-38 (gk177664)*	5x	1.27 ± 0.11 **(0.35)**	1.00 ± 0.16 **(0.00)**	
CX15900	*lgc-37 (tm0864)*	5x	1.35 ± 0.08 **(0.43)**	0.92 ± 0.08 **(-0.12)**	
CX11500	*lgc-53(tm2735)*	5x	1.39 ± 0.10 **(0.48)**	1.17 ± 0.11 **(0.23)**	
CX14102	*ntr-1(tm2765)*	6x	1.46 ± 0.10 **(0.54)**	1.33 ± 0.11 **(0.41)**	
CX13156	*mgl-3 (tm1766)*	3x	1.47 ± 0.10 **(0.56)**	1.04 ± 0.12 **(0.06)**	
CX16987	*lgc-47(ok2963)*	2x	1.49 ± 0.10 **(0.58)**	1.65 ± 0.13 **(0.72)**	
LX702	*dop-2(vs105)*	4x	1.62 ± 0.12 **(0.70)****	1.31 ± 0.13 **(0.39)**	**YES**
VC188	*acr-12(ok367)*	1x	1.66 ± 0.09 **(0.73)*****	1.40 ± 0.14 **(0.48)**	**YES**
CX14295	*pdfr-1(ok3425)*	5x	2.60 ± 0.08 **(1.38)*****	2.44 ± 0.17 **(1.29)**	NO

The metabotropic glutamate receptor, *mgl-1*, is necessary for local search

The strain CX17083 was profoundly defective in local search, with milder defects in reorientation rates during global search (Fig. 3.1C, Table 3.1). We originally selected this strain based on its annotated *npr-9(tm1552)* mutation (Bendena et al., 2008), but were unable to rescue its local search defect by rescuing functional *npr-9* expression with a transgene (Fig. 3.2A). To ask if *npr-9* was responsible for the phenotype in CX17083, we made a new loss-of-function *npr-9* mutant strain using CRISPR/Cas9. This strain, *npr-9(ky1030)*, did not recapitulate the phenotype in CX17083 (Fig. 3.2B), suggesting that a background mutation caused the observed phenotype of CX17083.

To identify the unmapped background mutation, we sequenced strain CX17083 and found a large deletion, predicted to be loss-of-function, within *mgl-1,* a G-protein coupled inhibitory metabotropic glutamate receptor (Fig. 3.2C) (Dillon et al., 2006). Restoring *mgl-1* expression by injecting a *mgl-1* transgene into CX17083 rescued the mutant behavior (Fig. 3.2D), and a new CRISPR-generated *mgl-1(ky1037)* mutant allele recapitulated the CX17083 phenotype (Fig. 3.2E), confirming that *mgl-1* is the causative mutation affecting local search. Our results indicate that *mgl-1* is necessary to generate local search. *mgl-1* has been implicated in food-related physiological responses (Greer et al., 2008; Kang and Avery, 2009a, b), pharyngeal pumping (Dillon et al., 2015), and foraging (Ahmadi and Roy, 2016), making it a good entry point to circuit mechanisms related to food-related behaviors.

Figure 3.2. The metabotropic glutamate receptor, *mgl-1*, is necessary for local search

(A) Off-food foraging defect in CX17083 (pink) is not rescued by a fosmid containing an *npr-9* genomic fragment (blue) (CX17083, n=51; *npr-9* fosmid, n=29).

(B) Off-food foraging of the new CRISPR/Cas9 generated *npr-9(ky1030)* mutant does not recapitulate the phenotype in CX17083 (compare to A).

(C) *mgl-1* deletion in CX17083, identified by whole genome sequencing. Deletion spans three exons and is predicted to truncate transmembrane domains in all *mgl-1* isoforms.

(D) Foraging defect in CX17083 (pink) is rescued by a PCR product encompassing the *mgl-1* genomic region (blue) (CX17083, n=87; *mgl-1* PCR rescue, n=88).

(E) Off-food foraging for CRISPR-generated *mgl-1(ky1037)* (wt, n=61; *mgl-1(ky1037)*, n=41).

All data presented as mean ± s.e.m. p-values calculated using Wilcoxon rank sum test with Bonferroni correction ***$p < 0.001$.

Figure 3.2

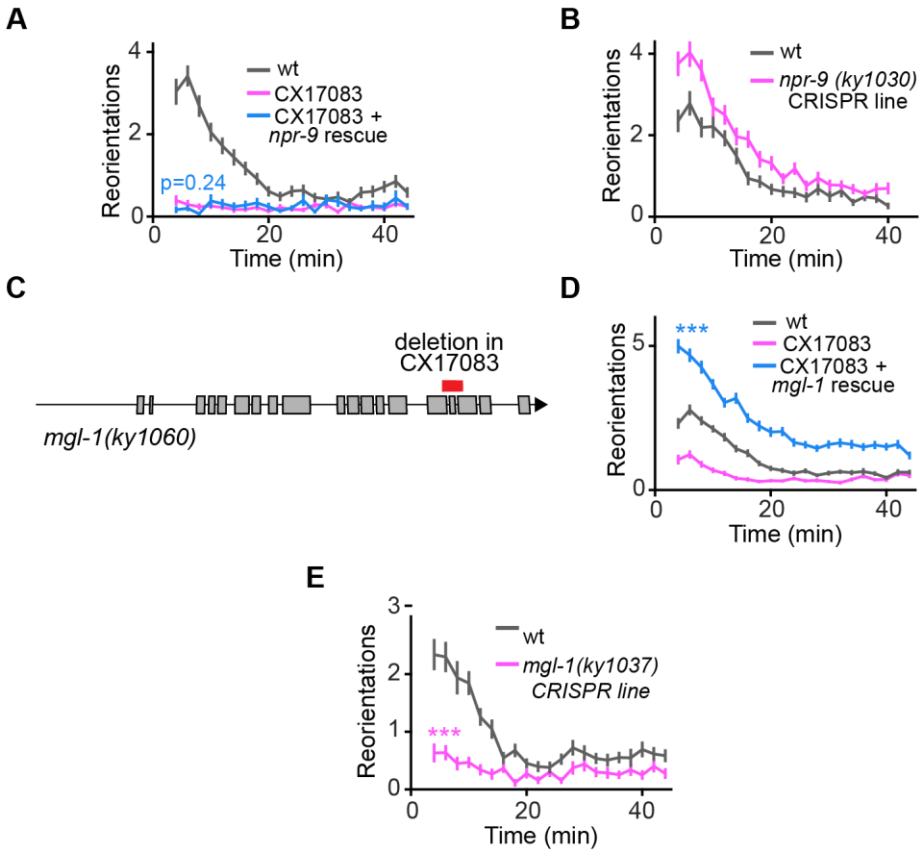
A
Reorientations
wt
CX17083
CX17083 +
npr-9 rescue
p=0.24
Time (min)
B
Reorientations
wt
npr-9 (ky1030)
CRISPR line
Time (min)
C
deletion in
CX17083
mgl-1(ky1060)
D
Reorientations
***
wt
CX17083
CX17083 +
mgl-1 rescue
Time (min)
E
Reorientations
***
wt
mgl-1(ky1037)
CRISPR line
Time (min)

mgl-1 inhibits AIA and ADE to generate local search

To identify the circuits where *mgl-1* acts to generate local search, we rescued *mgl-1* in subsets of its endogenous expression pattern using an intersectional transgene approach (Fig. 3.3A). A transgene containing an inverted, inactive floxed *mgl-1* genomic fragment was activated in a subset of cells by a second transgene expressing Cre recombinase under cell-specific promoters. Successful expression was confirmed by GFP (Fig. 3.3A). To validate this approach, we activated the *mgl-1* fragment in all neurons; this rescued the *mgl-1* local search defect (Fig. 3.3B) and showed broad *mgl-1* GFP expression.

To narrow down the sites of *mgl-1* action, we activated the *mgl-1* fragment in a smaller subset of cells using a *mod-1::nCre* transgene (Fig. 3.3C), including the sensory neurons ASI, Il1, and ADE, the interneuron AIA, and the motor neurons RMD. This pattern of activation rescued local search (Fig. 3.3C). To further narrow down the sites of *mgl-1* action, we activated the *mgl-1* fragment in each of these neuronal classes individually. Activating *mgl-1* in AIA and ADE or both neurons (Fig. 3.3D), but not in RMD, IL1, ASI, or NSM (Fig. 3.3E), was sufficient for rescue. In control experiments, transgenes with nonsense mutations in the *mgl-1* coding region failed to rescue local search (Fig. 3.3F-G), suggesting that rescue is due to functional *mgl-1* expression in AIA and ADE.

mgl-1 had been previously reported to be expressed in AIA, but not in ADE. The expanded expression we observe is likely due to the use of a genomic fragment that includes all introns, and is supported by single cell transcriptomics (Cao et al., 2017).

Figure 3.3 *mgl-1* expression in AIA and ADE is sufficient to generate local search.

(A) *mgl-1* rescue in subsets of its endogenous expression pattern using an intersectional transgene approach. Schematic depicts Cre-Lox transgene and its activation. Successful activation is confirmed by GFP, which is expressed with *mgl-1* in a bicistronic transcript.

(B) Rescue of *mgl-1* by reconstituting inverted transgene in all neurons using pan-neuronal Cre (*tag-168::nCre*). Animals that only express the inverted transgene are labelled 'no Cre' (no Cre, n=72; pan neuronal Cre, n=69).

(C) Activating the *mgl-1* inverted transgene in AIA, ADE, RMD, IL1, ASI and NSM using *mod-1::nCre* rescues local search behavior (no Cre, n= 72; *mod-1::nCre* rescue, n=80).

(D) Rescue of *mgl-1* by expression in AIA, ADE or both neurons (no Cre, n= 46; AIA rescue, n=50; ADE rescue, n=32; AIA+ADE rescue, n=48).

(E) Minimal rescue by expression of *mgl-1* in RMD, IL1, ASI or NSM. (no Cre_{RMD}, n= 72; RMD rescue, n=76; no Cre_{IL1}, n= 68; IL1 rescue, n=82; no Cre_{ASI}, n= 78; ASI rescue, n=89; no Cre_{NSM}, n= 72; NSM rescue, n=69). ASI and NSM rescue are statistically different from 'no Cre' but the magnitude of rescue is very small, so it may not be biologically meaningful.

(F) Control Cre-Lox *mgl-1* transgene, which when inverted has two adjacent nonsense mutations.

(G) Reconstituting nonsense *mgl-1* transgene in AIA and ADE does not rescue local search. Animals that only express the inverted nonsense transgene are labelled 'no Cre' (no Cre, n=66; AIA+ADE nonsense rescue, n=62).

All data presented as mean ± s.e.m. p-values calculated using Wilcoxon rank sum test with Bonferroni correction. *p<0.05 **p < 0.01 ***p < 0.001.

Figure 3.3

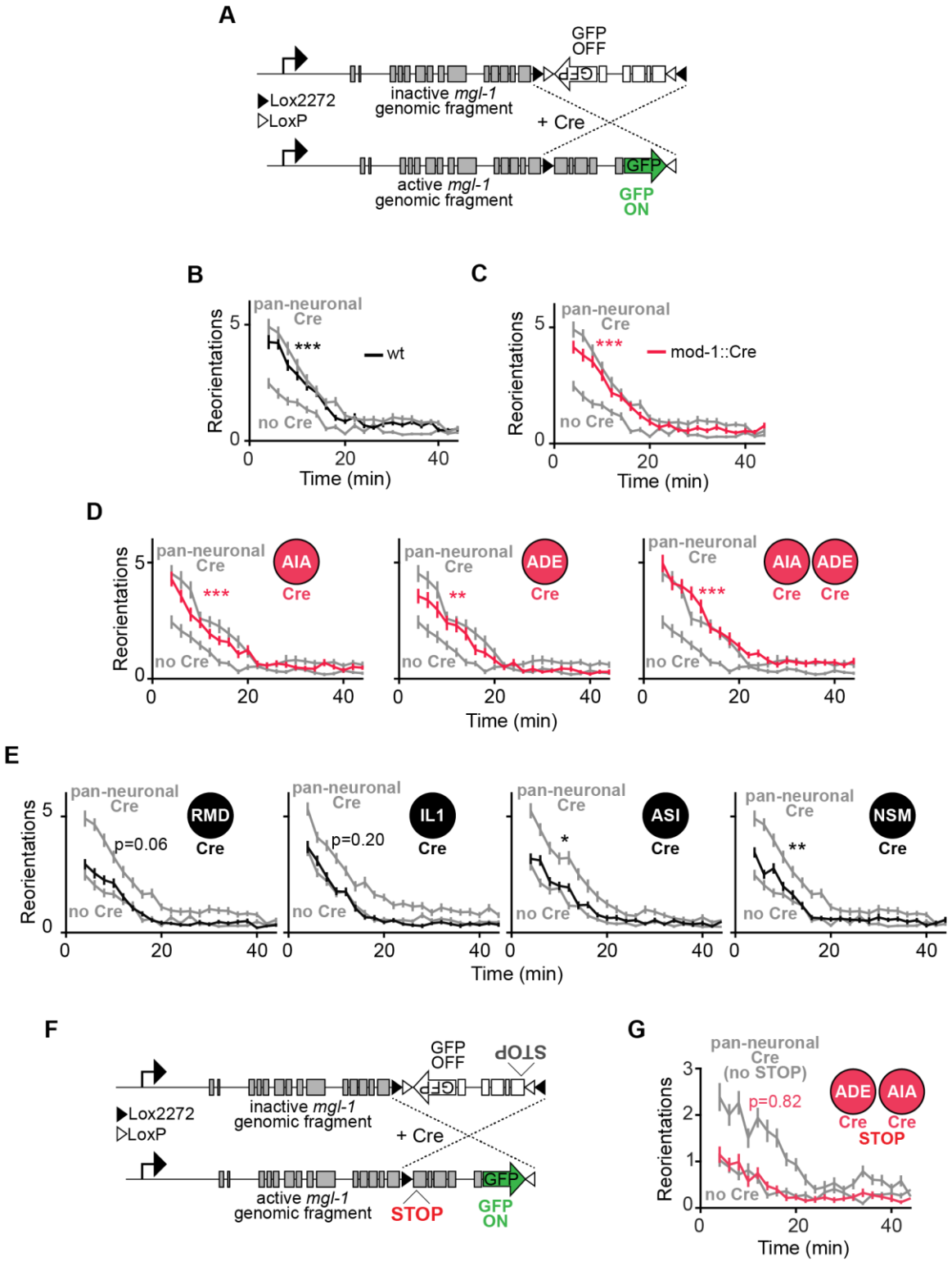
A
GFP
OFF
Lox2272
LoxP
inactive mgl-1
genomic fragment
+ Cre
active mgl-1
genomic fragment
GFP
ON
B
pan-neuronal
Cre
wt
no Cre
Reorientations
Time (min)
C
pan-neuronal
Cre
mod-1::Cre
no Cre
Reorientations
Time (min)
D
pan-neuronal
Cre
AIA
Cre
ADE
Cre
no Cre
Reorientations
Time (min)
E
pan-neuronal
Cre
RMD
Cre
p=0.06
IL1
p=0.20
ASI
*
NSM
**
no Cre
Reorientations
Time (min)
F
GFP
OFF
STOP
Lox2272
LoxP
inactive mgl-1
genomic fragment
+ Cre
active mgl-1
genomic fragment
STOP
GFP
ON
G
pan-neuronal
Cre
(no STOP)
p=0.82
ADE
Cre
AIA
Cre
STOP
no Cre
Reorientations
Time (min)

As *mgl-1* is predicted to be an inhibitory metabotropic receptor, animals that lack *mgl-1* may have defective local search because they fail to silence the AIA and ADE neurons. To test this possibility, we expressed tetanus toxin light chain in AIA, ADE, or both neurons in *mgl-1* mutant animals. Inhibiting neurotransmitter release from either AIA, ADE, or from both neurons with tetanus toxin rescued local search behavior in *mgl-1* (Fig. 3.4A-B). Tetanus toxin expression in another *mgl-1*-expressing neuron, NSM, did not rescue local search (Fig.3.4C), indicating rescue is specific to AIA and ADE.

Neurons expressing tetanus toxin lack synaptic vesicle release chronically throughout life. To silence AIA or ADE acutely during foraging behavior, we expressed the *Drosophila* histamine-gated chloride channel HisCl1 in either neuron (Pokala et al., 2014). *C. elegans* does not use histamine as an endogenous transmitter, so selective expression of HisCl1 permits rapid silencing of target neurons by adding histamine to the assay plate (Fig. 3.4D). Acutely silencing AIA off food partially rescued the local search defect in *mgl-1* mutants, albeit to a lesser extent than tetanus toxin (Fig. 3.4E). There are no ADE-specific promoters; acutely silencing ADE plus other dopaminergic neurons partly rescued local search and also increased reorientation frequencies at later time points after food removal, leading to altered global search (Fig. 3.4F).

Together these results indicate that when animals are removed from food, inhibition of AIA or ADE via MGL-1 generates local search. This interpretation in turn suggests that AIA and ADE normally suppress reorientations, and indeed an inhibitory effect of AIA on local search had been previously reported

(Wakabayashi et al., 2004). AIA and ADE each release multiple neurotransmitters and peptides that could mediate this behavioral effect. We unsuccessfully sought potential molecules mediating AIA and ADE action. ADE is a dopaminergic neuron but crossing *mgl-1* mutants into dopamine deficient *cat-2* mutants did not rescue the *mgl-1* foraging defect (Fig. 3.4G, left). AIA expresses *ins-1* which is known to modulate sensory neuron activity, but *mgl-1;ins-1* double mutants were indistinguishable from *mgl-1* (Fig. 3.4G, right). Identifying the relevant transmitters will require further screening.

Parallel, multimodal glutamatergic sensory pathways can redundantly generate foraging behavior

We next focused on the sources of glutamate that silence AIA and ADE through MGL-1 to generate local search. AIA and ADE do not express *eat-4*, the vesicular glutamate transporter that loads glutamate into synaptic vesicles for release (Serrano-Saiz et al., 2013), but they are postsynaptic to multiple glutamatergic neurons. The wiring diagram of *C. elegans* (White et al., 1986) and *eat-4* expression data (Serrano-Saiz et al., 2013) predict that AIA receives glutamatergic input from several chemosensory neurons that detect food-related volatile odors and soluble chemicals (Chalasani et al., 2007; Wakabayashi et al., 2009) (Fig. 3.5). ADE is predicted to receive glutamatergic input from mechanosensory neurons regulated by food texture (Albeg et al., 2011; Serrano-Saiz et al., 2013; White et al., 1986; Yemini et al., 2013) (Fig. 3.5).

Figure 3.4. *mgl-1* silences AIA and ADE to generate local search

(A) Rescue of *mgl-1(ky1037)* phenotype by expression of tetanus toxin light chain (TeTx) in AIA or ADE. (*mgl-1*, n=78; AIA::TeTx *mgl-1*, n = 63; ADE::TeTx *mgl-1*, n=82).

(B) Rescue of *mgl-1(ky1037)* phenotype by expression of tetanus toxin light chain (TeTx) in both AIA and ADE (*mgl-1*, n=72; AIA::TeTx+ ADE::TeTx *mgl-1*, n=69).

(C) No rescue of *mgl-1* mutant phenotype by expression of tetanus toxin light chain (TeTx) in NSM (*mgl-1*, n=94; NSM::TeTx *mgl-1*, n=93).

(D) Acute neuronal silencing by expressing cell-specific histamine-gated chloride channel and adding exogenous histamine to plates. Negative controls are *mgl-1(ky1037)* animals expressing the histamine gated chloride channel that were transferred to plates without histamine.

(E) Acutely silencing AIA off-food gives partial rescue of *mgl-1(ky1037)* phenotype (*mgl-1* AIA::HisCl -his, n=84; *mgl-1* AIA::HisCl +his, n=89).

(F) Acutely silencing ADE and other dopaminergic neurons (CEP, PDE) off-food gives partial rescue of local search and an altered pattern of global search behavior. (*mgl-1* ADE::HisCl -his, n=113; *mgl-1* ADE::HisCl +his, n=111). The dopaminergic neurons are known to affect locomotion speed and turning.

(G) *Left:* Off-food foraging for *mgl-1;cat-2* double mutants is indistinguishable from *mgl-1* single mutants, suggesting that *mgl-1* does not only act by decreasing dopamine release from ADE. *Right:* Off-food foraging for *mgl-1;ins-1* double mutants is indistinguishable from *mgl-1* single mutants, suggesting that *mgl-1* does not only act by decreasing *ins-1* release from AIA. (*mgl-1,* n=78; *mgl-1;cat-2*, n=80; *mgl-1;ins-1,* n=79).

All data presented as mean ± s.e.m. p-values calculated using Wilcoxon rank sum test with Bonferroni correction. *p<0.05 **p < 0.01 ***p < 0.001.

Figure 3.4

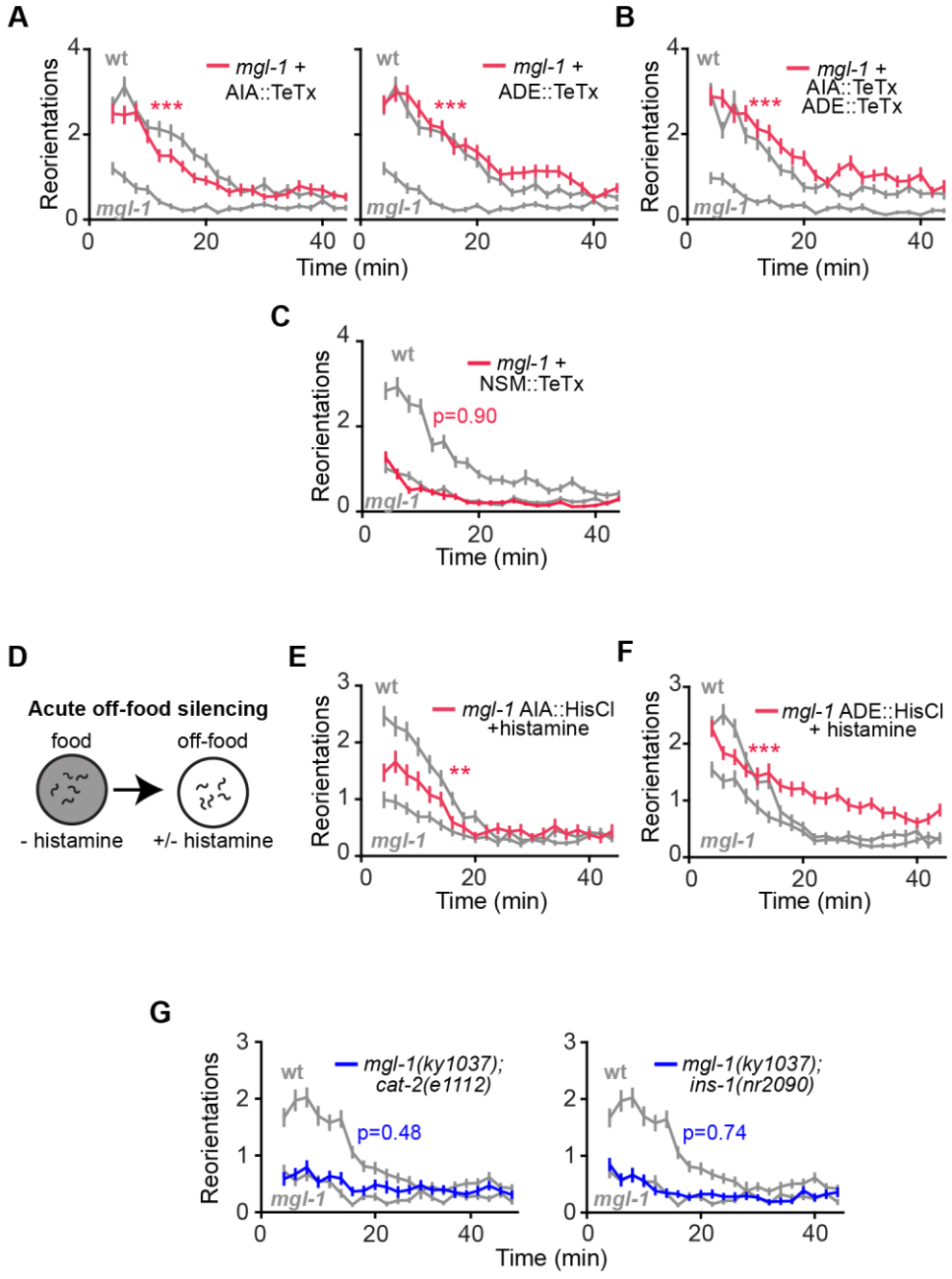
A
B
C
D
E
F
G
Reorientations
Time (min)
wt
mgl-1
mgl-1 + AIA::TeTx
mgl-1 + ADE::TeTx
mgl-1 + AIA::TeTx ADE::TeTx
mgl-1 + NSM::TeTx
p=0.90
***
**
Acute off-food silencing
food
off-food
- histamine
+/- histamine
mgl-1 AIA::HisCl +histamine
mgl-1 ADE::HisCl + histamine
mgl-1(ky1037); cat-2(e1112)
mgl-1(ky1037); ins-1(nr2090)
p=0.48
p=0.74

Figure 3.5. Circuit for local search behavior

Synaptic map of parallel glutamatergic modules for local search. Neurons whose activity may promote reversals are shown in blue; neurons whose activity inhibits reversals are shown in red. Arrows are weighted based on the number of chemical synapses from www.wormweb.org. The pathways consist of multimodal glutamatergic sensory neurons (blue) that converge on downstream mgl-1-expressing integrating neurons (red). There are no direct connections between the parallel pathways until the convergence on AIB and AVA neurons (blue), which have coupled activity that drives reversals and reorientations (coupled reorientation circuit).

The satiety state of the animal can gate the behavior parallel or downstream of the circuit modules (based on results at the end of this Chapter 3, and in the following Chapter 4).

Figure 3.5

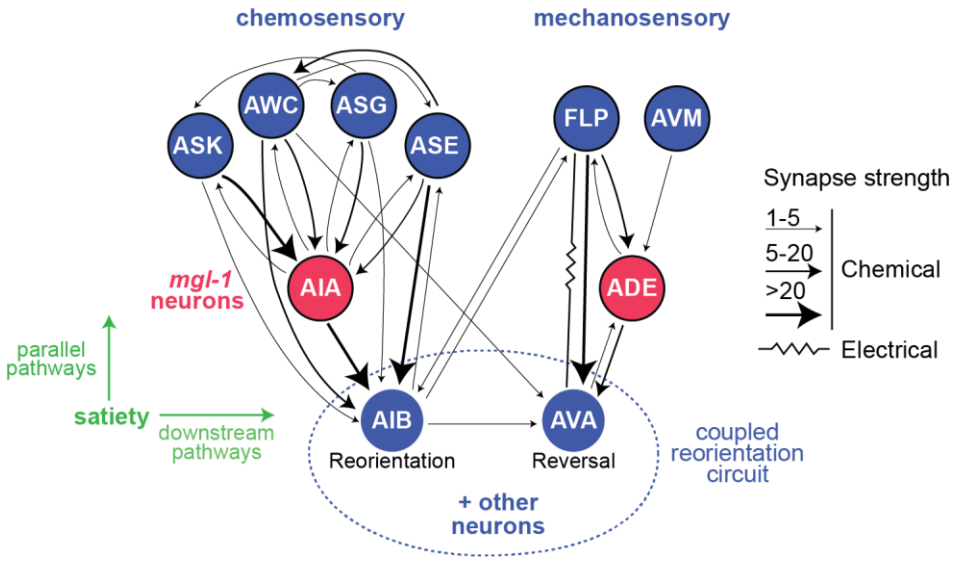
chemosensory
mechanosensory
AWC
ASG
ASK
ASE
FLP
AVM
Synapse strength
1-5
5-20
>20
Chemical
Electrical
mgl-1
neurons
AIA
ADE
parallel
pathways
satiety
downstream
pathways
AIB
AVA
Reorientation
Reversal
coupled
reorientation
circuit
+ other
neurons

To characterize the role of sensory glutamate inputs in local search behavior, we modified the endogenous *eat-4* (VGLUT1) locus of wild-type animals to permit cell-specific knockout of glutamate release. Two successive rounds of CRISPR/Cas9 editing were performed to insert an FRT before the start codon and *let-858*-3^{l}-UTR::FRT::mCherry after the stop codon of the endogenous *eat-4* coding region (Fig. 3.6A) (Schwartz and Jorgensen, 2016). In this edited *eat-4* strain, expression of a nuclear localized flippase (nFLP) under cell-specific promoters excised the *eat-4* coding region and resulted in the appearance of mCherry in the targeted cells (Fig. 3.6A). To validate this approach, we expressed nFLP under a pan-neuronal promoter (*tag-168::nFLP*); this resulted in a strong reorientation defect reminiscent of *eat-4* mutants (Hills et al., 2004) (Fig. 3.6B) and broad neuronal mCherry expression consistent with *eat-4* expression patterns (Fig. 3.6C-D).

We began to interrogate the sensory circuits by knocking out glutamate release from the individual chemosensory neurons AWC, ASK and ASG, which respond to the removal of chemosensory cues related to food (Chalasani et al., 2007; Wakabayashi et al., 2009). None of these single cell glutamate knockouts resulted in a striking behavioral defect (Fig. 3.7A-C). Next, we knocked out glutamate release more broadly: from all chemosensory glutamate neurons that synapse onto AIA, from all mechanosensory glutamate neurons that synapse onto ADE, or from both pathways simultaneously. Knocking out glutamate release from either sensory pathway individually had little effect on local search (Fig. 3.7D, left and middle panels). Only glutamate knockout from both the

chemosensory and mechanosensory pathways resulted in a local search defect, which was indistinguishable from that of *mgl-1* mutants (Fig. 3.7D, right panel). In control experiments, chemosensory and mechanosensory nFLP expression in wildtype animals did not affect local search (Fig. 3.7E)

To relate acute activity in these two sensory pathways to local search behavior, we transiently silenced the relevant glutamatergic sensory neurons of animals performing local search using optogenetics (Govorunova et al., 2015). We expressed the light-gated chloride channel *Gt*ACR2 in the glutamatergic chemosensory and mechanosensory neurons that synapse onto AIA and ADE by using an inverted Cre-Lox recombination strategy (See Experimental Procedures). Silencing the neurons for 30 sec with light led to a nearly two-fold decrease in reorientation probability, indicating that sensory activity is necessary to maintain a high reorientation state during local search (Fig. 3.7F).

The local search defect after chemosensory and mechanosensory glutamate knockout might be due to loss of glutamate necessary to inhibit AIA or ADE, or to loss of glutamate signaling to other neurons. To distinguish between these possibilities, we inhibited AIA or ADE with tetanus toxin in animals lacking glutamate in both sensory pathways. Tetanus toxin expression in either AIA or ADE fully restored local search behavior (Fig. 3.7G), supporting the importance of AIA and ADE as targets of sensory glutamate release.

Taken together, these results suggest that glutamatergic chemosensory and mechanosensory neurons can each independently drive full local search behavior by inhibiting either AIA or ADE.

Figure 3.6. Approach for cell-specific endogenous glutamate knockout

(A) Schematic of endogenous glutamate knockout strategy. Using CRISPR/Cas9, an FRT site was inserted immediately before the start codon of *eat-4* (VGLUT1), and *let-858* 3^{I}-UTR:: FRT::mCherry immediately after the stop codon of *eat-4*. *let-858* 3^{I}-UTR stops transcription so mCherry is not expressed. To knock out glutamate release in this edited strain, nls-flippase (nFLP) was expressed under cell-specific promoters, leading to excision of the *eat-4* ORF, confirmed by mCherry expression in the targeted cells.

(B) Validation of glutamate knockout strategy. Pan-neuronal glutamate knock out by expressing pan-neuronal nFLP (*tag-168::nls-FLP)* in the edited *eat-4* strain. Animals show phenotype reminiscent of *eat-4* mutants (control, n=65; pan-neuronal nFLP, n=56). ***p<0.001 using Wilcoxon rank sum

(C) Differential interference contrast (DIC) and mCherry fluorescence images of animals with edited endogenous *eat-4* (vGLUT1) locus. In the edited strain there is no mCherry expression, confirming that the *let-858*-3^{I}-UTR stops transcription.

(D) DIC and mCherry images for edited *eat-4* strain following pan-neuronal nFLP expression (*ptag-168:::nFLP*). mCherry is broadly expressed throughout the nervous system.

Figure 3.6

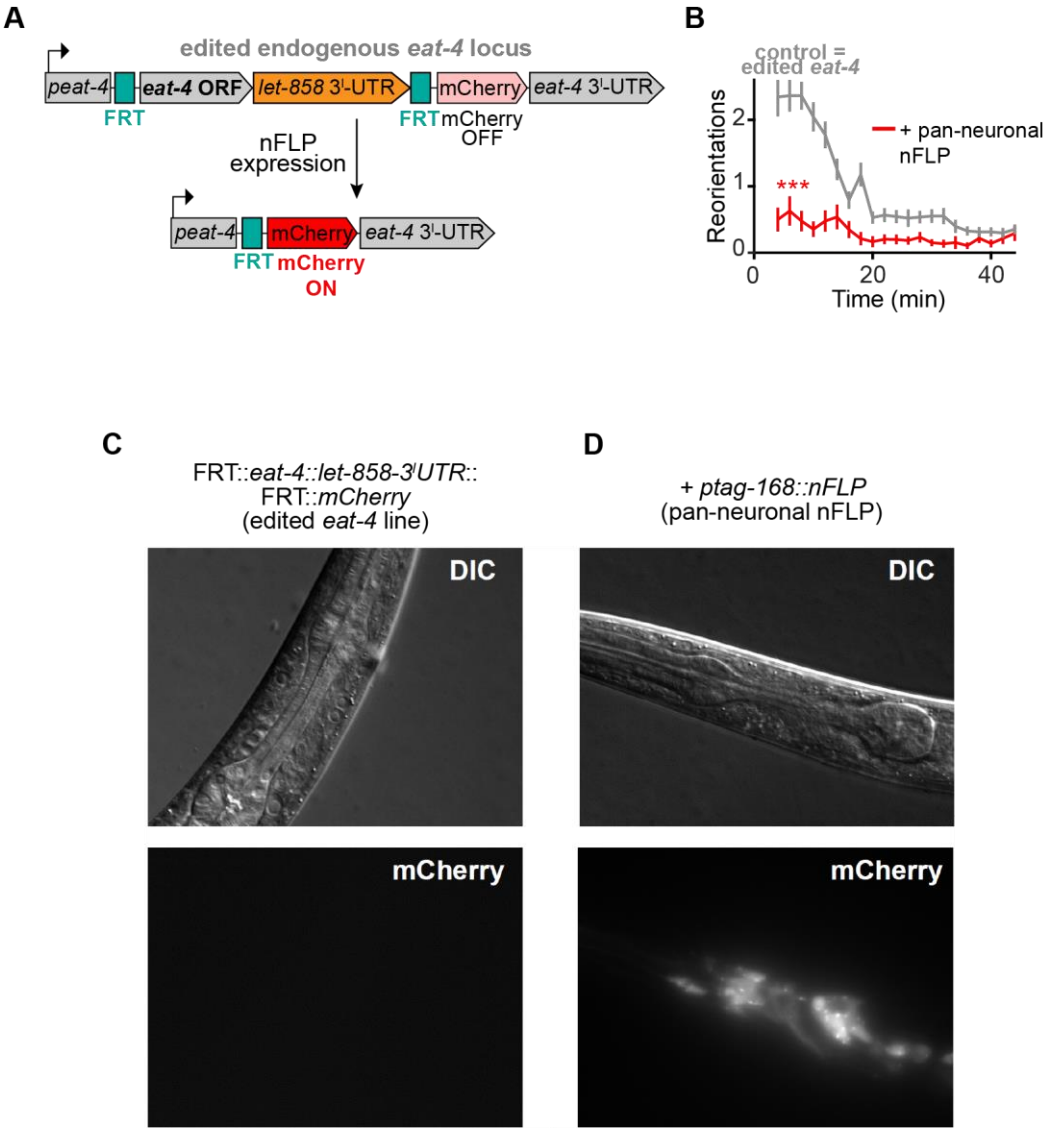
A
edited endogenous eat-4 locus
peat-4
eat-4 ORF
let-858 3'-UTR
mCherry
eat-4 3'-UTR
FRT
FRT mCherry OFF
nFLP expression
peat-4
mCherry
eat-4 3'-UTR
FRT mCherry ON
B
control = edited eat-4
+ pan-neuronal nFLP
***
Reorientations
0
1
2
0
20
40
Time (min)
C
FRT::eat-4::let-858-3'UTR::
FRT::mCherry
(edited eat-4 line)
DIC
mCherry
D
+ ptag-168::nFLP
(pan-neuronal nFLP)
DIC
mCherry

Figure 3.7. Parallel, multimodal glutamatergic sensory pathways redundantly generate local search.

(A-C) Off-food foraging after glutamate knockout from individual chemosensory neurons. (A) AWC glutamate knockout (control, n=55; AWC glut KO, n=57). (B) ASK glutamate knockout (control, n=108; ASK glut KO, n=92). (C) ASG glutamate knockout (control, n=60; ASK glut KO, n=58).

(D) Off-food foraging after glutamate knockout from all chemosensory neurons, all mechanosensory neurons, or both. (control, n=59; chemo glut KO, n=65; mechano glut KO, n=60; chemo+mechano glut KO, n=53).

(E) Control experiment for flippase expression. Off-food foraging of wildtype animals expressing nFLP in chemosensory and mechanosensory neurons is indistinguishable from wildtype controls. This suggests that the local search defect following chemosensory and mechanosensory glutamate knockout (D, right panel) is not caused by artifacts from flippase expression. (control, n=60; chemo+mechano nFLP in wt, n=63).

(F) Light-suppressed reorientations during local search in animals expressing the light-activated chloride channel, *Gt*ACR2 in glutamatergic chemosensory and mechanosensory neurons that synapse onto AIA and ADE (AWC, ASK, ASE, ASG, FLP, AVM). Controls express *Gt*ACR2 and are treated with light, but not pre-incubated with retinal. Data shows the instantaneous fraction of animals performing a reorientation. The mean fraction during stimulation is reported on the plot. Light stimulations were delivered during local search (2-14 min after food removal). (sensory *Gt*ACR2, n=151; controls, n=159).

(G) Off-food foraging for both mechano- and chemo- sensory glutamate knockout (glut KO), plus ADE (left) or AIA (right) inhibition with TeTx. (chemo+mechano glut KO, n=77; chemo+mechano glut KO + ADE::TeTx, n= 107; chemo+mechano glut KO + AIA::TeTx, n=77).

All data except (E) presented as mean ± s.e.m. p-values calculated using Wilcoxon rank sum test with Bonferroni correction. *$p<0.05$ ***$p < 0.001$.

Figure 3.7

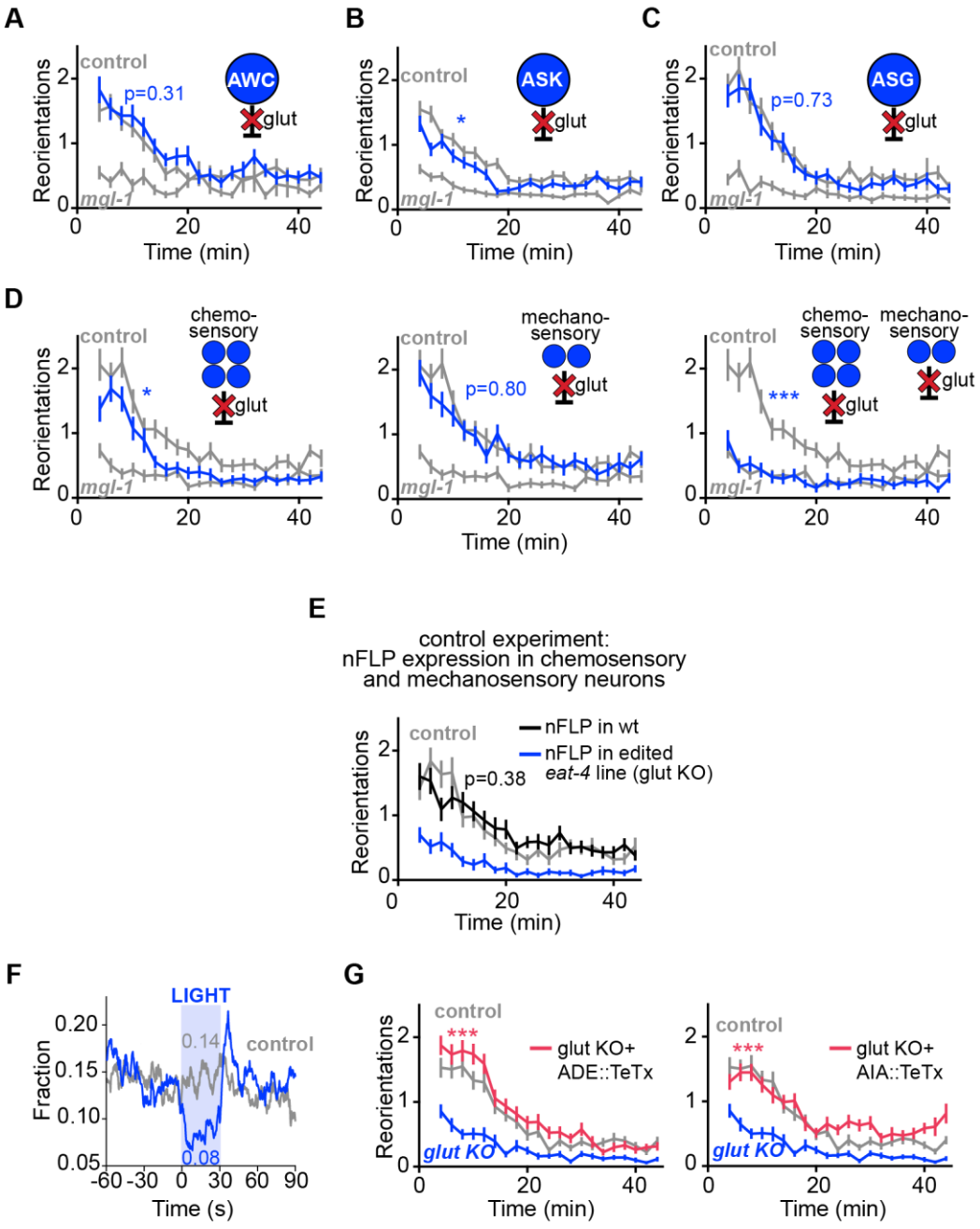
A
B
C
D
E
F
G
control
mgl-1
Reorientations
Time (min)
AWC
ASK
ASG
glut
p=0.31
p=0.73
p=0.80
p=0.38
*
***
chemo-sensory
mechano-sensory
control experiment:
nFLP expression in chemosensory
and mechanosensory neurons
nFLP in wt
nFLP in edited
eat-4 line (glut KO)
LIGHT
0.14
0.08
Fraction
Time (s)
glut KO+
ADE::TeTx
AIA::TeTx
glut KO

Internal satiety state is not encoded in the activity of AIA

In Chapter 2, we showed that the internal satiety state of animals can impact local search behavior, as inhibiting feeding for 45 min prior to food removal resulted in diminished local search (Fig. 2.6C). Our findings in this chapter show that local search is generated by silencing AIA or ADE through MGL-1. Therefore, it is possible that the internal satiety state of the animal interacts with MGL-1 and these neurons to gate local search. For example, a fasted internal state could lead to disinhibition of AIA which diminishes local search.

To test this idea, we asked if AIA inhibition is sufficient to rescue the local search defect after prolonged feeding inhibition. Using the optogenetic approach described in Chapter 2, we inhibited feeding for 45 min in animals expressing tetanus toxin in AIA. In contrast to its strong rescue of *mgl-1* mutants (Fig. 3.4A) and glutamate knockouts (Fig. 3.7G), silencing AIA with tetanus toxin did not rescue the foraging defect resulting from feeding inhibition (Fig. 3.8). This result indicates that the satiety state is not encoded purely in the activity of AIA.

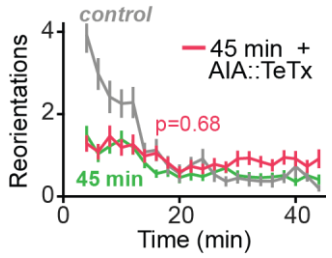

Figure 3.8 Satiety state is not encoded solely in the activity of AIA

Off-food foraging after 45 min of feeding inhibition prior to food removal + AIA silencing with tetanus toxin (TeTx) (45 min, n=47; 45 min + AIA::TeTx, n=45). Presented as mean ± s.e.m. p-value calculated using Wilcoxon rank sum test

DISCUSSION

Parallel sensory circuits generate multimodal control of local search

We characterized a circuit for local search behavior by finding a gene necessary for local search (MGL-1) and then identifying and characterizing the circuit in which MGL-1 acts.

The local search circuit is composed of two parallel modules: a set of glutamatergic chemosensory neurons that synapse onto the AIA interneurons, and a set of glutamatergic mechanosensory neurons that synapse onto the ADE sensory-inter neurons (Fig. 3.5). The chemosensory neurons detect food-related volatile odors (AWC) and amino acids (ASK), and are inhibited when these stimuli are present and active when stimulus are removed (Chalasani et al., 2007). The mechanosensory neurons detect touch and textures associated with food (Albeg et al., 2011; Sawin et al., 2000; Yemini et al., 2013). Each set of glutamatergic sensory neurons is predicted to inhibit AIA or ADE through the MGL-1 metabotropic glutamate receptor when animals are removed from food. Inhibition of AIA or ADE encodes a sensory food memory and allows the generation of local search. This circuit has several interesting features that shed light on multimodal sensory processing.

First, the chemosensory and mechanosensory modules that control local search are separate and parallel (Fig. 3.5). There are no direct connections between the identified chemosensory and mechanosensory neurons, no shared connections onto the AIA or ADE integrating neurons, and no connections

between AIA and ADE in the synaptic wiring diagram of *C. elegans* (White et al., 1986). AIA and ADE primarily synapse onto AIB and AVA interneurons, respectively. AIB and AVA are two members of a coupled neuronal group that are simultaneously activated during reversal behaviors (Fig. 3.5) (Gordus et al., 2015; Kato et al., 2015). The coupled circuit that links AIB and AVA is the first site of convergence between the chemosensory and mechanosensory modules. Modeling suggests that stochastic fluctuations between this reversal circuit and a mutually inhibitory forward circuit may be sufficient for occasional reversals in the absence of overt sensory cues (Roberts et al., 2016); our results suggest that local search represents a change in the balance between these antagonistic assemblies.

Second, the AIA and ADE modules are each sufficient to generate full local search behavior: they are not additive. Inhibiting the function of either AIA or ADE with MGL-1 or tetanus toxin permits local search (Fig. 3.3D, Fig. 3.4A). Similarly, glutamate release from either the chemosensory or the mechanosensory neurons can generate the full behavior (Fig 3.7D). This redundant circuit organization may allow a robust innate neuronal representation of food removal through multiple sensory modalities. Indeed, there may be other parallel sensory modules that can have the same effect. The sensory pathways described here were found by testing for *mgl-1* sufficiency. *mgl-1* is expressed broadly throughout the nervous system and we did not test for sufficiency in all *mgl-1*-expresing neurons, so it is possible that other redundant parallel pathways

exist. One good candidate is pathway that detects oxygen, a cue often associated with food in *C. elegans*.

Food and satiety cues are both diverse and critical to survival, features that would favor parallel processing and redundancy in their detection. In mammals, satiety is redundantly represented by mechanosensory input from gut distension (Baird et al., 2001; Sabbatini et al., 2004) and sensory inputs associated with feeding (Chen et al., 2015). Within the mammalian brain, hunger-generating AGRP neurons also act in parallel and redundant circuits: groups of non-connected AGRP neurons project separately to distinct forebrain regions and different projections have redundant capability to elicit feeding (Betley et al., 2013). Thus, a redundant organization may be a common feature of circuits involved in survival behaviors.

How do AIA and ADE mediate their behavioral effect?

The net effect of *mgl-1* is to inhibit its target neurons, AIA and ADE, to generate local search. Consistent with this, silencing AIA or ADE with tetanus toxin is sufficient for local search in animals lacking MGL-1. This in turn suggests that AIA and ADE normally inhibit reorientations, likely by silencing AIB and AVA, respectively. The nature of the AIA and ADE transmitters that normally inhibit reorientations is unknown.

AIA releases both acetylcholine and numerous neuropeptides. ADE releases dopamine and several peptides including the locomotion-stimulatory

peptide PDF-1. A previous area-restricted search assay identified a role for dopamine (Hills et al., 2004) that we did not recapitulate here with *cat-2* mutants, but we did identify the dopamine receptor *dop-2* in our mutant screen, suggesting that dopamine may contribute to the behavior along with other transmitters. Identifying the relevant transmitters will require crossing candidate mutants into *mgl-1* and looking for rescue of the *mgl-1* phenotype.

MGL-1 coordinates broader physiological response to food removal

In addition to generating local search, MGL-1 coordinates broader behavioral and physiological responses to food depletion. Upon food removal, *mgl-1* decreases pharyngeal pumping (feeding) (Dillon et al., 2015), promotes mobilization of fat stores downstream of TGF-β signaling (Greer et al., 2008), and modifies survival after starvation by regulating autophagy through action in AIY interneurons (Kang and Avery, 2009b). Its expression is regulated by AMPK and is dependent on satiety levels (Ahmadi and Roy, 2016). Therefore, by acting in different sites and tissues, MGL-1 may coordinate a broad response to food removal which includes behavioral, metabolic and physiological components. Identifying the cell type-specific readouts of MGL-1 action will provide a better understanding of conserved global responses to changes in food availability.

CHAPTER 4:

Neuronal dynamics associated with foraging behavior

INTRODUCTION

Neural circuits store information about recent sensory stimuli to generate sustained behavioral responses that outlast those stimuli. These short-term memories must be manifested in neuronal activity. In mammals, working memories are represented by changes in neuronal firing frequency. In the primate prefrontal cortex, neurons increase their firing rate in response to a salient visual or auditory cue and maintain that response for as long as the information is needed to perform a task, far longer than the duration of the cue (Fuster and Alexander, 1971; Romo et al., 1999). This sustained response is a neuronal manifestation of a short-term memory.

Local search is a short-term food memory that must have a neuronal manifestation. Acute food removal in *C. elegans* leads to a transient activation of multiple sensory neurons, including AWC and ASK, followed by a gradual return to a stable baseline (Chalasani et al., 2007; Wakabayashi et al., 2009). In both cases, the activation lasts between 20 sec and 3 min, far less that the duration of local search; thus, sensory activity alone cannot alone explain local search behavior. Spontaneous activity patterns, on the other hand, might encode information about recent food experience over time scales comparable to local search. Neurons in *C. elegans*, including ASK, show spontaneous activity in the absence of obvious external stimuli (Gordus et al., 2015; Skora et al., 2018). Here we look at spontaneous activity in the chemosensory module—in ASK and AIA—and find that these neurons encode information about the time since the last food encounter. We also characterize the role of glutamate within this circuit.

RESULTS

Spontaneous activity in ASK and AIA reports time after food removal

While animals are on food, glutamatergic sensory neurons like ASK and AWC have a low baseline calcium level and show limited spontaneous activity. Acute food removal leads to a transient activation of these glutamatergic sensory neurons, followed by a gradual return to baseline within seconds or a few minutes (Chalasani et al., 2007; Wakabayashi et al., 2009). To investigate the neuronal activity associated with longer-term food removal, we monitored the spontaneous calcium activity in neurons within the chemosensory module, ASK and AIA. To do this, we expressed the genetically encoded calcium indicator GCaMP5A in the ASK sensory neurons and in the AIA interneurons (Akerboom et al., 2012) (Fig. 4.1). Of the chemosensory neurons, ASK was selected because it was the only one to cause a significant, albeit mild, behavioral defect when *eat-4* was knocked out (Fig. 3.7B), and because it is directly activated by acute food removal (Calhoun et al., 2015; Wakabayashi et al., 2009).

Animals were removed from a standard bacterial food lawn and loaded into a microfluidic device (Chronis et al., 2007), where they were physically restrained but not paralyzed. The spontaneous activities of ASK and AIA were monitored either individually or simultaneously for 10 min immediately after food removal (0-10 min, corresponding to local search period) and again after 40 min (40-50 min, corresponding to global search period) (Fig. 4.1A).

Both ASK and AIA exhibited spontaneous activity in the absence of food or obvious external stimuli (Fig. 4.1B-C). ASK had a high baseline with spontaneous decreases in calcium levels, which we call negative transients (Fig. 4.1B, Fig. 4.1D left panel). Negative transients in ASK lasted between 4-80 sec (median=21.0 sec, Fig. 4.1D middle panel), with the longer transients corresponding to complex activity consisting of multiple events (arrowhead, Fig. 4.1B). Spontaneous neural activity consisting of sustained changes from a stable baseline has been described in interneurons in *C. elegans* (Gordus et al., 2015). However, unlike those interneurons which show a bimodal transient amplitude distribution corresponding to 'on' and 'off' states, ASK showed a continuous amplitude distribution (Fig. 4.1D, right panel).

AIA showed reciprocal activity patterns; a low baseline with spontaneous increases in calcium levels, which we call positive transients (Fig. 4.1C, Fig. 4.1E, left panel). AIA positive transients are shorter in duration than ASK transients, lasting between 3-20 sec (median=7.0 sec, Fig. 4.1E, middle panel), with the longer transients corresponding to complex activity. The amplitude of AIA transients also showed a continuous distribution (Fig. 4.1E, right panel).

To investigate the relationship between these neurons, we imaged their activity simultaneously (Fig. 4.2A). Strikingly, we found that spontaneous transients in ASK and AIA often occurred at the same time (Fig. 4.2A-B), with ASK negative transients on average coinciding with the start of AIA positive transient onsets (Fig. 4.2B). In agreement with this observation, the two neurons showed a strong negative correlation in activity (Fig. 4.2C).

Figure 4.1. Spontaneous activity patterns in the sensory neuron ASK and the interneuron AIA

(A) Experimental configuration for calcium imaging of ASK and AIA after food removal. GCaMP5A fluorescence levels were measured in the ASK cell body and in the AIA axon, either individually or simultaneously, 0-10 min after food removal and again 40-50 min after food removal. The animal is physically restrained within a custom-build microfluidic chamber that permits normal responses to chemosensory cues. Because the body is compressed in this environment, we did not attempt to record the activity of the mechanosensory circuit.

(B-C) Spontaneous off-food calcium activity in ASK or AIA neurons. Spontaneous calcium dynamics in a representative ASK neuron (B) or AIA neuron (C) expressing GCaMP5A, recorded 0-10 min and again 40-50 min after food removal.

(D) Average aligned traces, cumulative duration, and cumulative amplitude of ASK spontaneous negative transients in wildtype animals (n=18 animals, 327 transients). Data obtained from imaging ASK individually.

(E) Average aligned traces, cumulative duration, and cumulative amplitude of AIA spontaneous positive transients in wildtype animals (n=21 animals, 465 transients). Data obtained from imaging AIA individually.

Figure 4.1

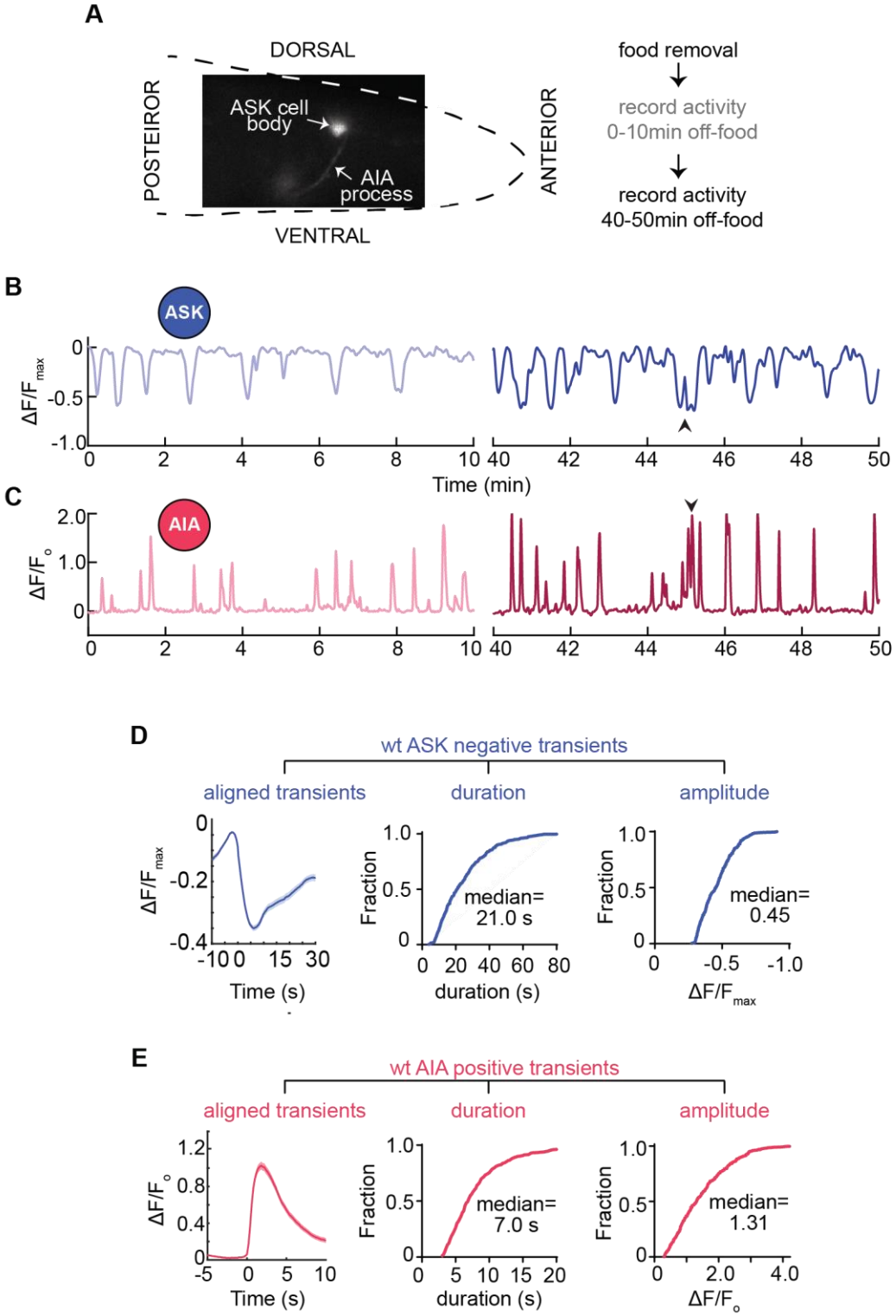
A
DORSAL
POSTEIROR
ANTERIOR
VENTRAL
ASK cell body
AIA process
food removal
record activity
0-10min off-food
record activity
40-50min off-food
B
ASK
ΔF/F max
Time (min)
C
AIA
ΔF/F o
D
wt ASK negative transients
aligned transients
duration
amplitude
Time (s)
Fraction
median= 21.0 s
duration (s)
median= 0.45
ΔF/F max
E
wt AIA positive transients
aligned transients
duration
amplitude
ΔF/F o
Time (s)
Fraction
median= 7.0 s
duration (s)
median= 1.31
ΔF/F o

Figure 4.2. ASK and AIA show anti-correlated activity

(A) Representative trace of single wildtype animal in buffer, showing spontaneous calcium dynamics in simultaneously recorded ASK and AIA neurons expressing GCaMP5A, 40-50 min after food removal.

(B) ASK traces aligned to the start of AIA transients in wildtype animals (n=19 animals, 248 transients). Data presented as mean + s.e.m (shaded region)

(C) Cross-correlation of ASK and corresponding lagged AIA traces 40-50 min after food removal in wildtype animals (n=19). We selected 40-50 min because all animals show at least some spontaneous activity changes during this period. Data presented as mean ± s.e.m. Individual traces shown as thin lines.

Figure 4.2

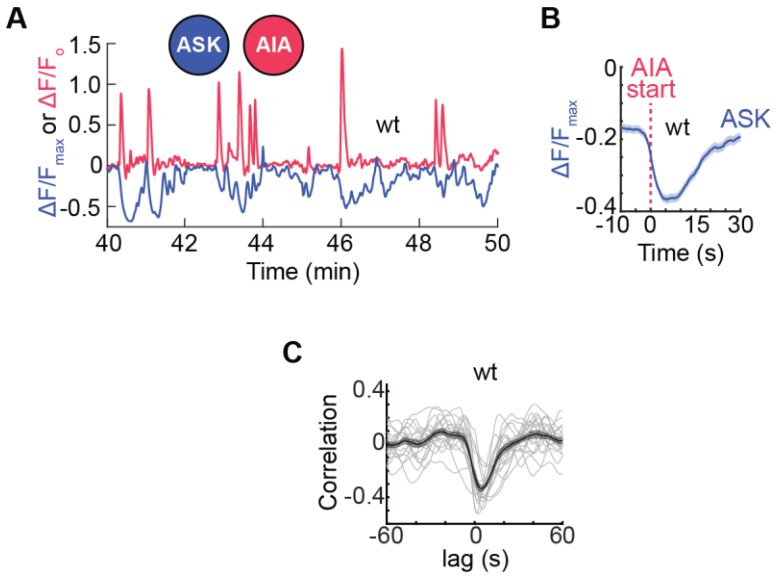
A
ASK
AIA
wt
ΔF/F_max or ΔF/F_o
1.5
1.0
0.5
0
-0.5
40
42
44
46
48
50
Time (min)
B
AIA
start
wt
ASK
ΔF/F_max
0
-0.2
-0.4
-10
0
15
30
Time (s)
C
wt
Correlation
0.4
0
-0.4
-60
0
60
lag (s)

The sensory neuron optogenetic silencing experiments in the previous chapter (result in Fig. 3.7F) suggest that ASK negative transients may correspond to a period of decreased reorientation probability (result in Fig. 3.7F). Thus, since the frequency of reorientations decreases over time since food removal, we might expect the number of ASK negative transients to increase over time. To test this prediction, we examined the activity of ASK at the early and late times after food removal associated with local and global search. As predicted, spontaneous negative transients in ASK became more frequent at later times after food removal (Fig 4.3A). This reduction in average ASK activity correlates with the decrease reorientation rates in global search. Thus, ASK shows activity patterns that correlate with the foraging behavior.

ASK reports time since last sensory food encounter, regardless of satiety

Internal satiety state can impact local search behavior (Chapter 2). Therefore, it is possible that internal satiety modifies the activity levels of ASK. To test this idea, we imaged the spontaneous activity of ASK for 0-10 min after removing animals from a plate of regular food, inedible food (as in Fig. 2.6D), or no food. Animals that had spent 45 min on inedible food showed a similar number of ASK negative transients as animals that had been on regular food, whereas animals that had spent 45 min on plates without food showed a higher number of transients (Fig. 4.3B). These results suggest that ASK activity reports the time since the last encounter with sensory features of food, regardless of the

internal satiety state. The internal state is therefore encoded in parallel or downstream from the circuits defined here.

AIA shows differences in frequency and amplitude at early vs. late times after food removal

We next examined the activity of AIA at early and late times after food removal. Like ASK, AIA had more positive transients at the later times after food removal (Fig.4.3C). In addition, the AIA transients at late time points were larger in amplitude than early transients (Fig. 4.3D). This was not the case for ASK transients (Fig. 4.3E).

Together, these results indicate that ASK and AIA activity states report information about the time since food removal, an essential component of local search behavior.

Figure 4.3. Activity in ASK and AIA depends on the time since the last food encounter

(A) Number of ASK negative transients in each animal early (0-10 min) vs. late (40-50 min) after food removal for wildtype (n=19). **p<0.01 by Wilcoxon signed rank test. Data obtained from imaging ASK individually.

(B) ASK calcium imaging immediately (0-10min) after spending 45 min on a plate containing inedible food (n=37), normal food (n=35), or no food (n=21). Number of ASK negative transients per animal. Data presented as median with 95% confidence intervals.

(C) Number of AIA positive transients in each animal early (0-10 min) vs. late (40-50 min) after food removal for wildtype. (n=21). **p<0.01 by Wilcoxon signed rank test.

(D) (left) Cumulative AIA positive transient amplitude early (0-10 min, n=210) vs. late (40-50 min, n=255) after food removal for wildtype animals. (right) Aligned AIA positive transients early (0-10 min, n=210) vs. late (40-50 min, n=255) after food removal for wildtype animals. ***p<0.001 for difference in amplitude by Kolmogorov-Smirnov test.

(E) Cumulative ASK negative transient amplitude early (0-10 min, n=111) vs. late (40-50 min, n=216) after food removal for wildtype animals. p-value calculated using Kolmogorov-Smirnov test.

Figure 4.3

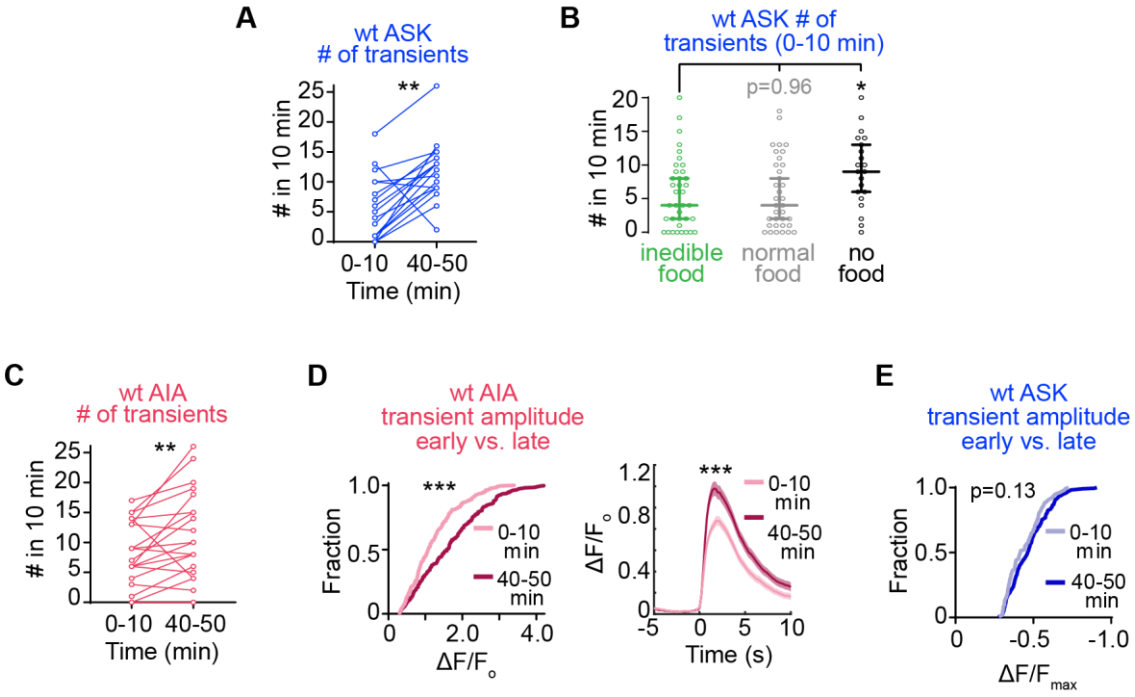
A
wt ASK
# of transients
in 10 min
25
20
15
10
5
0
**
0-10
40-50
Time (min)
B
wt ASK # of
transients (0-10 min)
p=0.96
*
in 10 min
20
15
10
5
0
inedible
food
normal
food
no
food
C
wt AIA
# of transients
in 10 min
25
20
15
10
5
0
**
0-10
40-50
Time (min)
D
wt AIA
transient amplitude
early vs. late
Fraction
1.0
0.5
0
***
0-10
min
40-50
min
0
2.0
4.0
ΔF/F
o
ΔF/F
o
1.2
0.8
0.4
0
***
0-10
min
40-50
min
-5
0
5
10
Time (s)
E
wt ASK
transient amplitude
early vs. late
Fraction
1.0
0.5
0
p=0.13
0-10
min
40-50
min
0
-0.5
-1.0
ΔF/F
max

Glutamate shapes activity patterns at multiple time scales

To investigate the role of *mgl-1* and glutamate in the observed spontaneous activity patterns, we imaged ASK and AIA simultaneously in *mgl-1* and *eat-4* mutants. Like wildtype animals, animals lacking *mgl-1* showed anticorrelated activity in ASK and AIA (Fig. 4.4A-B), and an increased number of AIA positive transients at later times (Fig. 4.4C). Thus *mgl-1* is not required for spontaneous AIA activity, for its entrainment by time off food, or for the fast coupling of ASK and AIA. Unlike wildtype, however, AIA transients in *mgl-1* animals had similar amplitudes at early and late time points after food removal (Fig. 4.4D). This result suggests that *mgl-1* may reduce the gain of the ASK-to-AIA synapse during local search.

Like *mgl-1* mutants, mutants in the glutamate transporter EAT-4 did not show a difference in AIA transient amplitude at early and late time points after food removal (Fig. 4.5A). In addition, *eat-4* animals lacking glutamate release showed decorrelation of ASK and AIA activity (Fig. 4.5B-C). The decreased correlation was not due to differences in the number, size, or duration of *eat-4* ASK transients, as those were indistinguishable from wildtype (Fig. 4.5D). Instead, this result suggests that additional glutamate receptors other than MGL-1, most likely glutamate-gated ion channels, mediate fast inhibitory synapses from ASK and AIA. The overall magnitude of AIA transients in *eat-4* mutants was also reduced, consistent with a wider role for glutamate signaling at AIA synapses (Fig. 4.5E). Together these results suggest that glutamate acts through multiple receptors including *mgl-1* to modulate AIA activity at multiple timescales.

Figure 4.4. *mgl-1* may affect the gain of ASK to AIA signaling, but not spontaneous activity dynamics.

(A) (Left) ASK traces aligned to the start of AIA transients in *mgl-1* mutants (n=12 animals, 89 transients). (Right) For comparison, aligned traces in wildtype animals are shown (same as Fig. 4.2B). Data presented as mean ± s.e.m (shaded region). Data obtained from imaging ASK and AIA simultaneously 40-50 min after food removal.

(B) Cross-correlation of ASK and corresponding lagged AIA traces 40-50 min after food removal *mgl-1* mutants (n=12) Data presented as mean ± s.e.m. Individual traces shown as thin lines. Data obtained from imaging ASK and AIA simultaneously.

(C) Number of AIA positive transients per animal early (0-10 min) vs. late (40-50 min) after food removal for *mgl-1* mutants (n=16). **p<0.01 by Wilcoxon signed rank test. Data obtained from imaging AIA individually.

(D) (Left) Cumulative AIA positive transient amplitude early (0-10 min, n=137) vs. late (40-50 min, n=240) after food removal for *mgl-1* animals. Data obtained from imaging AIA individually. (Middle) Aligned AIA positive transients early (0-10 min, n=137) vs. late (40-50 min, n=240) after food removal for *mgl-1* animals. Data obtained from imaging AIA individually. (Right) For comparison, aligned traces in wildtype animals are shown (same as Fig. 4.3D, right panel). p-values for difference in amplitude calculated using Kolmogorov-Smirnov test.

Figure 4.4

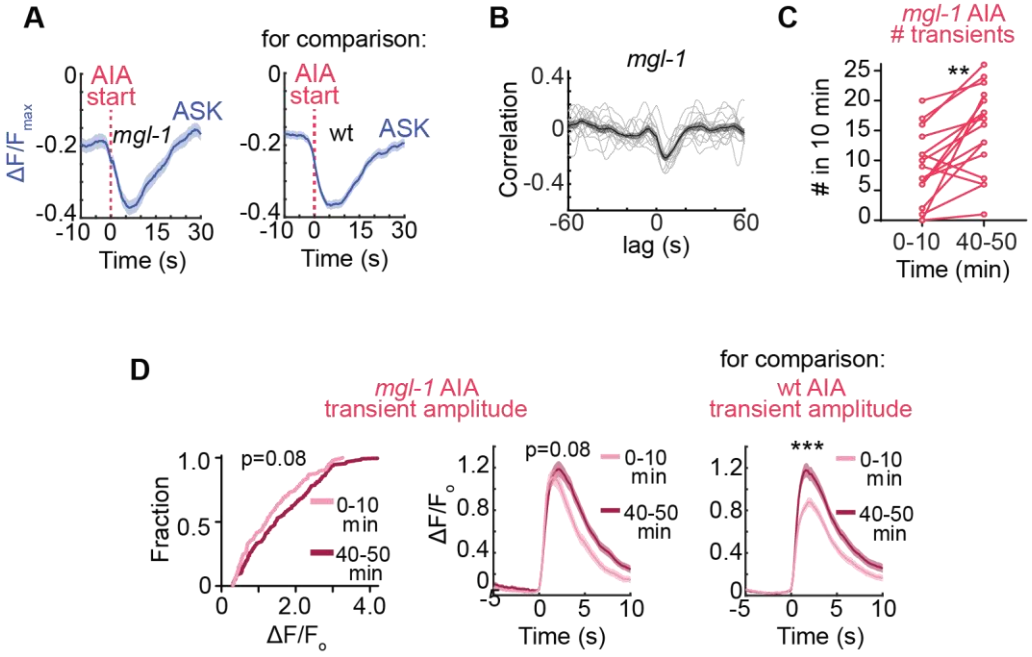
A
for comparison:
AIA start
ASK
mgl-1
wt
ΔF/F max
Time (s)
B
mgl-1
Correlation
lag (s)
C
mgl-1 AIA
transients
in 10 min
Time (min)
D
mgl-1 AIA
transient amplitude
wt AIA
transient amplitude
p=0.08
0-10 min
40-50 min
Fraction
ΔF/F o
Time (s)

Figure 4.5. Glutamate acts within the same circuit to modulate activity at different time scales

(A) Cumulative AIA positive transient amplitude early (0-10 min, n=179) vs. late (40-50 min, n=250) after food removal for *eat-4* mutants. p-value calculated using Kolmogorov-Smirnov test. Data obtained from imaging ASK and AIA simultaneously.

(B) (Left) ASK traces aligned to the start of AIA transients in *eat-4* mutants (n=21 animals, 410 transients). (Right) For comparison, aligned traces in wildtype animals are shown (same as Fig. 4.2B). Data presented as mean ± s.e.m (shaded region). Data obtained from imaging ASK and AIA simultaneously 40-50 min after food removal.

(C) Cross-correlation of ASK and corresponding lagged AIA traces 40-50 min after food removal in *eat-4* mutants (n=21). We selected 40-50 min because all animals show at least some spontaneous activity during this period. Data presented as mean ± s.e.m. Individual traces shown as thin lines. Data obtained from imaging ASK and AIA simultaneously

(D) Number (left), cumulative duration (middle), and cumulative amplitude (right) of ASK negative transients are similar in wildtype and *eat-4* mutants (data analyzed from 40-50 min period to match cross-correlations in panels B-D and aligned ASK transients in Fig. 5J). p-value on left panel calculated using Wilcoxon rank sum test. p-values on middle and right panels calculated using Kolmogorov-Smirnov test.

(E) Cumulative AIA positive transient amplitude for wildtype (n=248 transients) vs. *eat-4* mutants (n= 421 transients). ***p<0.001 by Kolmogorov-Smirnov test. All data obtained from imaging ASK and AIA simultaneously.

Figure 4.5

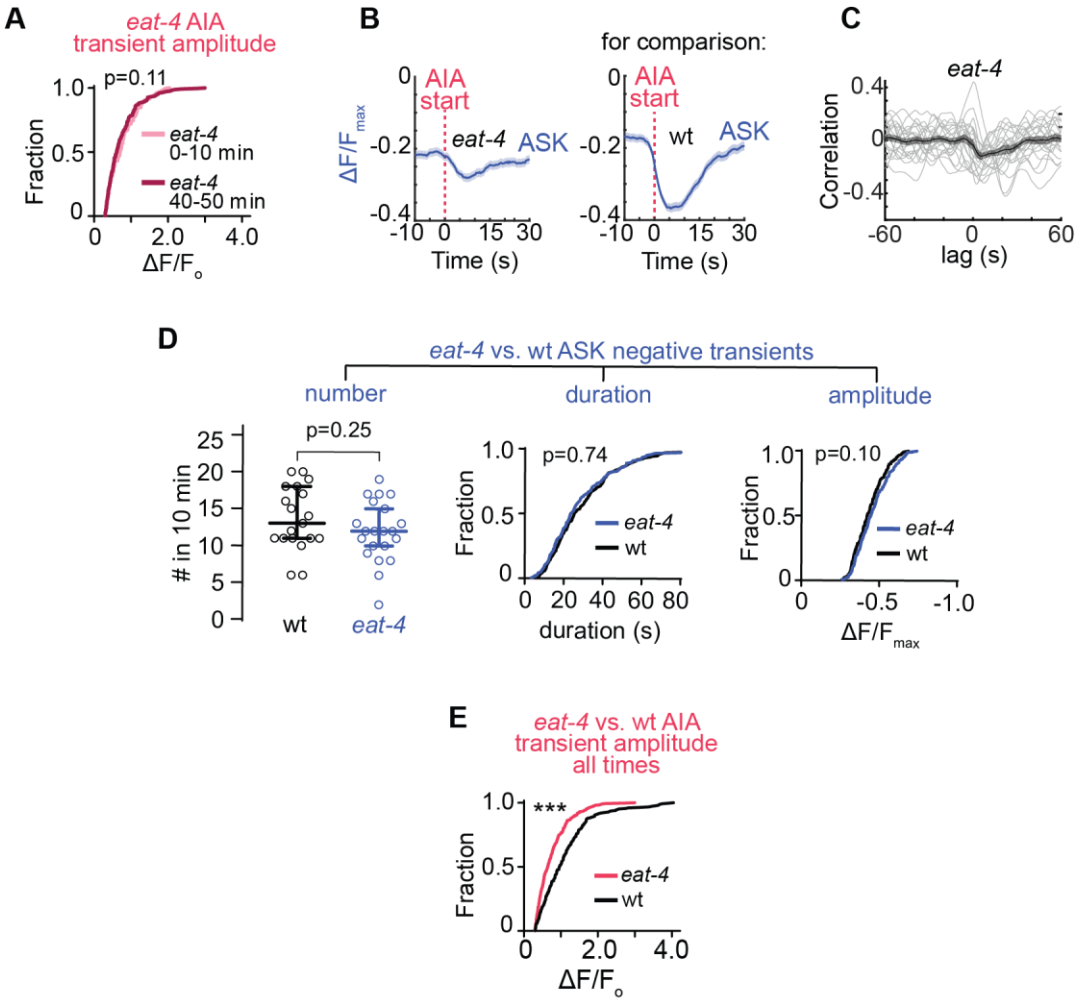
A
eat-4 AIA transient amplitude
p=0.11
Fraction
eat-4 0-10 min
eat-4 40-50 min
ΔF/F0
B
for comparison:
AIA start
eat-4
ASK
wt
ΔF/Fmax
Time (s)
C
eat-4
Correlation
lag (s)
D
eat-4 vs. wt ASK negative transients
number
duration
amplitude
p=0.25
# in 10 min
wt
eat-4
p=0.74
duration (s)
p=0.10
ΔF/Fmax
E
eat-4 vs. wt AIA transient amplitude all times
***
ΔF/F0

DISCUSSION

The role of glutamate in shaping neuronal activity

The reorientations associated with local search in *C. elegans* are present in different patterns in other behaviors such as chemotaxis (Pierce-Shimomura et al., 1999) and aerotaxis (Hums et al., 2016). Chemosensory neurons in the local search circuits such as ASK and AWC regulate acute reorientations during these behaviors by activating ionotropic glutamate receptors on downstream interneurons (Chalasani et al., 2007). Here, we found that the same sensory neurons regulate sustained local search behavior by signaling through an inhibitory metabotropic glutamate receptor, MGL-1.

Our imaging results suggest that glutamate acts at different timescales within the same circuit. Glutamate likely acts through an unknown inhibitory ionotropic glutamate receptor to synchronize fast activity between ASK and AIA (Fig. 4.5B), and simultaneously acts over longer timescales through *mgl-1* to suppress the amplitude of AIA calcium transients (Fig. 4.4D). Thus, the circuits that generate the fast motor components of local search may also generate the sustained search state by using different receptors.

The net effect of *mgl-1* is to inhibit its target neurons, AIA and ADE, but animals with and without *mgl-1* generate similar AIA calcium transients, suggesting that *mgl-1* does not eliminate neuronal excitability. *mgl-1* encodes a Group II metabotropic receptor (Dillon et al., 2006), whose mammalian homologs inhibit neurotransmitter release (Dong and Ennis, 2017; Hayashi et al., 1993);

therefore *mgl-1* may decrease the synaptic output of AIA and ADE. In agreement with this possibility, inhibition of AIA or ADE synaptic release with tetanus toxin can substitute for *mgl-1* action in local search behavior (Fig. 3D-E).

Preliminary experiments with a MGL-1::GFP fusion reporter show that MGL-1 is localized in puncta within neuronal processes. Determining whether these puncta correspond to pre-synaptic sites (by looking for co-localization with presynaptic markers) will give clues into how MGL-1 acts in AIA and ADE to generate local search behavior. This in turn can provide insight into the molecular mechanisms that generate short-term memories.

Spontaneous ASK activity holds information about time since food removal

Spontaneous activity patterns in both ASK and AIA change in the time frame from local to global search. ASK appears to hold information about the time since the last sensory encounter with food, and its spontaneous activity patterns correlate with the foraging behavior. ASK is a sensory neuron, but the activity occurs in the absence of any obvious external stimuli, suggesting an internal source for the activity. A recent study of *C. elegans* brain states at even longer times after food removal also reported changes in the endogenous activity in ASK, in agreement with our results (Skora et al., 2018). Identifying the internal sources that modify the activity of ASK over minutes, will provide insight into how recent experience is encoded neuronally to generate short term memories.

CHAPTER 5:

Conclusions and future directions

Foraging patterns incorporating local search are widely conserved and have been described in numerous animal species including insects, fish, birds, and mammals (Bell, 1985; Benedix, 1993; Dias et al., 2009; Eifler et al., 2012; Gray et al., 2005; Hills et al., 2013; Lihoreau et al., 2016; Nakamuta, 1985; Papastamatiou et al., 2012; Wakabayashi et al., 2004; Weimerskirch et al., 2007). In each case, the animal performs a time-limited exploration of the region where resources were last encountered, using a set of motor programs – reversals, turns, and changes in locomotion speed – that are undirected, apparently internally generated, and relatively nonspecific, as they appear in many other spontaneous and evoked behaviors. Here, we ask how the nervous system of *C. elegans* generates this ancient innate behavior.

A circuit mechanism for local search

We uncovered a circuit for local search behavior that consists of parallel chemosensory and mechanosensory circuit modules that each have the redundant ability to generate local search (Fig. 3.5). In each module, chemosensory or mechanosensory neurons that detect food related cues, silence the downstream AIA or ADE interneurons, respectively, through MGL-1 to generate local search. Silencing of AIA or ADE is sufficient for local search and thus encodes the food memory. A third gating signal, generated by the internal feeding state, controls local search in parallel or via downstream circuits.

Together with previous results, our results suggest the following model for sustained local search in *C. elegans* (Calhoun et al., 2015; Gray et al., 2005; Hills et al., 2004; Wakabayashi et al., 2004). Removal from food leads to the activation of multiple sensory neurons, which release glutamate onto targets including AIA and ADE, and inhibit them through MGL-1, a G protein-coupled glutamate receptor. MGL-1 decreases the gain of AIA and ADE signaling and neurotransmitter release for a 10 to 20-minute period corresponding to local search. The reduction of either AIA or ADE activity is sufficient to modify the balance between forward and reversal states to favor reversals. AIA and ADE synapse onto the reversal-promoting AIB and AVA neurons, respectively (Fig 3.5), consistent with the known antagonism between AIA (forward) and AIB (reversal) neurons and the more general antagonism between AVB (forward) and AVA (reversal) circuits (Roberts et al., 2016). After 10-20 minutes away from food, signaling from sensory neurons decreases, and the forward state is stabilized at the expense of the reversal state. After 45 minutes, a satiety signal from food is depleted or a food deprivation signal is generated to suppress local search regardless of sensory information.

Our findings reveal a circuit organization that allows for a robust generation of an innate behavior. Sensory neurons that detect two different sensory modalities, chemical or mechanical cues, have full capability of generating local search. This is achieved through a parallel sensory configuration that converges only on a downstream coupled circuit that can directly affect reorientations. This organization, in which different individual sensory modalities

are sufficient for local search, allows a reliable brain representation of food and may be a general feature of brain circuits involved in ancient survival behaviors. In addition, it highlights that nervous systems may have redundant features, and that there may be multiple solutions for encoding behaviors.

Though we have learned some principles about the mechanisms that generate local search, there are many open questions that may provide further insight into the basis of innate behaviors. Some of these questions and future experiments are discussed below.

How are the different sensory modalities used to generate local search?

The circuit we identified suggests that animals can use either chemosensory or mechanosensory cues to generate local search; this, however, has not been directly tested. One future direction is to characterize if and how sensory cues alone can elicit local search. To do this, animals can be exposed to either chemosensory cues such as bacteria-conditioned media, or mechanosensory cues such as Sephadex beads, and the subsequent local search behavior can be monitored. Since these sensory cues do not provide nutrition, animals will be exposed to these cues for only 20 min, as animals that haven't eaten for 45 min do not perform local search, regardless of sensory cues (Fig. 2.6C-D). An alternative approach is to enhance one of the sensory modalities by adding odor (chemosensory) or beads (mechanosensory) to the bacterial food and examining how that affects local search.

This line of experiments raises a second question: which individual cues in the chemosensory and mechanosensory food environment are being used to generate local search? Bacteria produce numerous chemosensory cues including volatile odors, amino acids, salt, and carbon dioxide. Are any of these components used more than others? Or is it only a combination them that can generate local search? Our glutamate knockout experiments (Fig. 3.7B) and previous ablation studies (Wakabayashi et al., 2004) suggest that ASK may be a particularly important sensory neuron for local search. ASK directly detects amino acids, so it is possible that this is the most significant chemosensory cue for sustained local search behavior. Mechanosensory cues are also diverse and vary depending on bacterial type, and conditions such as humidity. Do certain bacterial textures lead to more local search? Characterizing the nature of the sensory cues that generate local search will provide further insight into how animals represent their external world.

What dictates the duration of local search?

Theoretical models have demonstrated that local search is the most successful strategy when animals have information about food availability, such as a recent food encounter, and that a global search is most successful when animals need to locate random food sources with no prior information (Calhoun et al., 2014; Salvador et al., 2014). The circuits described here can encode the recent food encounter through sensory cues, and thereby drive an active local

search behavior that decays over time to a global search behavior. One open question that remains is the nature of the internal clock that sets the duration of local search. Our results limit but do not identify the nature of that clock

The timing of AIA and ADE inhibition by glutamate and MGL-1 represents sensory history, but it can be separated from the internal clock for local search duration. Tetanus toxin inhibits AIA and ADE synaptic release across life but does not affect the transition from local to global search (Fig. 3.4A-B). This result strongly argues that structured AIA and ADE activity alone do not define the duration of local search.

Nutritional cues act over slower timescales than the duration of local search. Inhibiting feeding for 10 min or 20 min before food removal did not affect the timing of local search, which is largely complete in 20 min after food removal (Fig. 2.6A-B). This suggest that a nutritional clock does not define the duration of local search. Consistent with this, individual well-fed animals show a large variation in the duration of local search (Fig. 2.3C), further arguing that local search isn't defined by a clock of the time since feeding.

Neuropeptides released from sensory neurons are attractive candidates to set the duration of local search. Local search is affected after laser ablation of either AWC or ASK sensory neurons (Gray et al., 2005), but our results show that glutamate release from either neuron can be eliminated with less effect (Fig. 3.7A-B). Co-transmitters such as neuropeptides could explain the difference between glutamate release and neuronal ablation, although other explanations

are also possible. Most of the sensory neurons in the local search circuit release FMRF neuropeptides, which are related to mammalian NPY peptides (Li and Kim, 2008), and several neuropeptides and G protein-coupled neuropeptide receptors affect local search (Campbell et al., 2016; Chalasani et al., 2010). In the rodent hypothalamus, NPY co-transmitter release converts transient GABA-dependent synaptic effects into sustained feeding behavior (Chen et al., 2016). By analogy, *C. elegans* sensory neuropeptide release could act with glutamate to generate sustained local search behaviors. Currently, we are identifying peptides that are highly expressed in sensory neurons in the local search circuit (Cao et al., 2017) and testing mutant animals lacking those peptides. By screening through various mutants, we hope to find molecules that contribute to dictating the duration of local search.

The temporal heterogeneity of fast glutamate receptors, slower MGL-1 and neuropeptide signaling, and nutritional input may store food memory in multiple clocks. Ultimately, this memory must be manifested in neuronal activity. One representation of food history that merits further study is the spontaneous activity of the ASK neuron, which changes over a time frame that matches the transition from local to global search. Identifying the sources of slowly-changing spontaneous activity in ASK may provide further understanding of how behavioral states are sustained and ultimately terminated.

How does internal metabolic state gate local search behavior?

Sensory evoked behaviors are often modulated by internal physiological states (Ezcurra et al., 2011; O'Donnell et al., 2018; Root et al., 2011; Yapici et al., 2016). Here, we found that sustained inhibition of feeding for 45 minutes eliminated all local search behavior (Fig. 2.6C-D), regardless of the sensory environment. Unlike *mgl-1* or glutamate knockout, the effect was not rescued by introducing tetanus toxin into AIA (Fig. 3.8). The all-or-none and delayed nature of this satiety effect suggests that metabolic cues from feeding regulate local search downstream of or in parallel to the sensory cues represented in the *mgl-1* glutamatergic circuit (Fig 3.5). In this formulation, internal satiety signals gate the ability of sensory information to generate local search behavior. The role of satiety in sensory food information may allow animals to represent food not only by its multiple sensory modalities, but also by its nutritional quality.

A future direction is to identify the mechanisms by which internal satiety states gate the ability of sensory signals to generate local search. In *Drosophila*, starvation modulates food search behavior by altering sensory responses at the first olfactory synapse, an effect mediated by the neuropeptide sNPF (Root et al., 2011). By analogy, peptides generated during starvation in *C. elegans* may affect the synaptic output of sensory neurons like ASK, even if ASK's spontaneous activity level is similar in well-fed vs. starved animals (Fig.4.3B). Identifying such peptides would require screening for mutants that perform local search even after a sustained 45 min feeding inhibition. A second possibility is that starvation acts on downstream neurons like RIM. RIM is an interneuron that is coupled to the

reorientation circuit of AIB and AVA, making it a good candidate to gate the ability of upstream sensory circuits to generate behaviors. Indeed, its activity has been shown to change the reliability of behavioral responses to odor stimuli (Gordus et al., 2015). Examining the activity of RIM early vs. late after food removal may shed light on this hypothesis. A final possibility is that satiety is sensed by a non-neuronal tissue, such as the gut, that signals to neurons and modulates their activity and thus the behavior. In *C. elegans* Rictor/TORC2 acts in the gut to regulate foraging behavior via neuropeptide signaling pathways (O'Donnell et al., 2018). Gut-to-brain signaling may change the ability of food sensory information to generate local search. Identifying how internal satiety states affect local search will provide insight into how external information is integrated with internal states to generate flexible adaptive behaviors.

EXPERIMENTAL PROCEDURES

Nematode Culture

Animals were grown at room temperature (21-22˚C, on the laboratory bench) on nematode growth media (NGM) plates seeded with 200 µL of an *E. coli* OP50 bacterial liquid culture (Brenner, 1974). This OP50 liquid culture was obtained by picking a single OP50 colony into 100 mL of sterile LB and growing it on the benchtop at room temperature for 48 hrs without shaking, and subsequently storing it at 4^{O}C for up to one month.

Wildtype animals were *C. elegans* Bristol strain N2. All mutant strains tested were backcrossed to wildtype animals to reduce unannotated background mutations. Mutants strains used for the candidate genetic screen are listed in Table 3.1. CRISPR-generated strains and transgenic strains are listed in Table 6.1. Mutant strains used in candidate screen were generated by other groups using random mutagenesis and selected by us based on the annotated mutations. Transgenic animals were generated by microinjection of a transgene derived from wildtype strain N2, a fluorescent co-injection marker (*myo-2::mCherry, myo-3:mCherry, elt-2::nls-GFP, elt-2::mCherry*), and empty pSM vector to reach a final DNA concentration of 100 ng/µL.

Transgenic and mutant strains were always compared to matched controls tested in an adjacent behavioral set-up. Each experiment included 12-18 animals. For the candidate genetic screen, each mutant strain was tested in six different experiments done on two different days. All other strains were tested in 4-8 experiments done on at least two different days.

Strains

CRISPR/Cas9-generated mutant strains

CX1030 *npr-9(ky1030)* X. *ky1030* is a CRISPR/Cas9 induced single nucleotide deletion in the second exon of *npr-9*. The resulting sequence is TGGTAATGCTCTGGTGGTGAT (deleted nucleotide is underlined). To generate the strain, we used a co-CRISPR protocol (Arribere et al., 2014). Young hermaphrodites were injected with a mix of plasmids encoding Cas9, a gRNA targeting *rol-6*, a gRNA targeting *npr-9*, and a ssDNA repair template that induces a dominant *rol-6(su1006)* mutation. F1 animals were isolated to individual plates based on their roller phenotype, allowed to lay eggs, and then screened for a target mutation by Sanger sequencing. F2 animals were isolated to find homozygotes for the target mutation. After inducing the target mutation, animals were backcrossed to wildtype twice.

CX1037 *mgl-1(ky1037)* X. *ky1037* is a CRISPR/Cas9 induced indel that results in a frameshift before the first transmembrane domain of *mgl-1*. Deletion is (G), insertion is (TTGTGTGGTTGTGTGGTTGTGGTTGTGTGTTGT). Resulting sequence is TGGAGCAACGTTGTGTGGTTGTGTGGTTGTGGTTGTGTGTTGTTGGTGGTTCT (insertion is underlined). We used the co-CRISPR protocol as described above (Arribere et al., 2014).

pJA42 was a gift from Andrew Fire (Addgene plasmid # 59930)

CRISPR/Cas9 editing of the endogenous *eat-4* (VGLUT1) locus

To generate a strain that would allow us to knock out endogenous glutamate release in a cell-specific manner, we performed two successive edits on the endogenous *eat-4* locus.

First, we used the co-CRISPR method described above (Arribere et al., 2014) to insert an FRT sequence (GAAGTTCCTATTCTCTAGAAAGTATAGGAACTTC) immediately before the start codon of *eat-4*. We injected the mix described above with an additional ssDNA repair template consisting of the FRT sequence with 35 bp homology arms on each side. The resulting edited genomic sequence is: *TCATCATCATTTTCAGAAACC*GAAGTTCCTATTCTCTAGAAAGTATAGGAACTTC***ATG***TCGTCATGGAACGAaGC (FRT insertion is underlined; *eat-4* locus is in italics; bolded ATG is the start codon of *eat-4*; lowercase *'a'* is a silent mutation induced to remove PAM site after successful homologous recombination).

Second, we used the CRISPR/Cas9 SapTrap method (Schwartz and Jorgensen, 2016) to insert *let-858 3^{I}-UTR::FRT::mCherry* immediately after the endogenous *eat-4* stop codon. SapTrap is a modular plasmid assembly approach that produces a single plasmid vector containing both a gRNA transcript and a repair template. We mutated some of the modular components used to assemble the repair template as follows: for pMLS279 (*FRT-let-858 3^{I}-UTR-FRT*) we deleted the 5^{I} FRT site (new plasmid is pALC01), and for pMLS291 (mCherry with syntron embedded inverted floxed *Cbr-unc-119*) we added a stop codon at the end of the mCherry coding region (new plasmid is pALC02). We cloned these

two edited plasmids along with 60 bp homology arms and the gRNA into the pMLS256 destination vector, producing a combined plasmid vector (pALC03). Young *unc-119(ed3)* hermaphrodites were injected with the combined plasmid vector, a Cas-9 expression vector, and fluorescent co-injection markers. F1 animals were picked 10 days after injection based on rescue of the *unc-119* phenotype, and the insertion was confirmed by PCR and Sanger sequencing. These edited animals were then injected with *peft-3::nCre* (pDD104) to excise the syntron embedded, inverted floxed *Cbr-unc-119*. F1 animals were selected based on the reappearance of the *unc-119* phenotype. This line was backcrossed once to wildtype animals to remove the *unc-119(ed3)* mutation, and an additional three times to remove any off-target CRISPR mutations. The resulting strain is CX17461.

Nuclear localized flippase (nFLP) was subcloned from pMLS262 (snt-1::2xNLS-FLP-D5) into pSM using Gibson assembly (New England Biolabs). A plasmid containing nFLP under cell specific promoters was injected into the *eat-4* edited strain (CX17461) by standard gonadal microinjection. Successful glutamate knockout in the target cells was confirmed by mCherry expression which was visualized using a Zeiss Axio Imager.Z1 Apotome microscope with a 40x objective.

For all glutamate knockout experiments, ‘control’ animals are the *eat-4* edited strain, and *‘mgl-1’* are *mgl-1(ky1037) eat-4* edited strain.

pMLS279 (Addgene plasmid # 73729), pMLS291 (Addgene plasmid # 73724), pMLS256 (Addgene plasmid # 73715), and pMLS262 (Addgene plasmid # 73718) were gifts from Erik Jorgensen.

Identification of *mgl-1(ky1060)* allele

We prepared genomic DNA from strain CX17083 using standard phenol/chloroform extraction protocols. Sequencing was conducted at the Rockefeller High-Throughput Sequencing Facility, where a DNA library was prepared using TruSeq Nano DNA kit (Illumina) and sequenced in an Illumina HiSeq 2500 System.

Deletions were identified using modifications to a previously described approach (McGrath et al., 2011). Candidate deletions were first identified using 'chimeric' reads as identified by bwa (i.e. reads that included the SA tag) where each alignment mapped to the same chromosome and strand (Li and Durbin, 2010). These reads were used to infer the breakpoints and insertion sequence of a candidate deletion. Candidate deletions that were also present in N2 sequenced controls were excluded as likely errors in the reference sequence. Each candidate deletion was then genotyped by collecting all the reads with primary alignments that fell within 10 bp of the candidate deletion and a mapping quality score greater than 10. These reads were realigned to both the reference and the candidate deletion sequence using a striped Smith Waterman Alignment implemented in the scikit-bio Python library (http://scikit-bio.org/). This analysis

identified a homozygous 225 bp deletion in the *mgl-1* gene that was verified using Sanger sequencing.

The identified *mgl-1(ky1060)* deletion is:

ATCTGCTCAACGACCAAGATTCATATCTCCCATCTCTCAGgtgagctccggtgacaa gccaacggaagtacactatttatagGTTGTCATGACTGCAATGCTAGCCGGAGTACAAT TGATCGGAAGTCTTATTTGGCTGTCAGTAGTGCCACCAGgtaaattggctatttatgaa gtgatgtctgagtaatttttagGTTGGAGACACCACTACCCCACCAGGGACCAGGTGGT TTTAACTTGTAATGTTCCTGACCATCACTTTTTGTATTC (deletion underlined, exons in uppercase, introns in lowercase)

Intersectional Cre/Lox *mgl-1* rescue

To rescue *mgl-1* in subsets of its endogenous expression pattern, we employed an intersectional transgene strategy. The inactive *mgl-1* genomic fragment plasmid was constructed using pSM-inv[sl2-GFP] as the backbone (Flavell et al., 2013). A portion of a *mgl-1* rescue genomic fragment sequence was cloned into pSM-inv[sl2-GFP] in its correct orientation (obtained using forward primer: 5′-GTAAGGTATGTTTTTATTTTCCAAC -3′ and reverse primer: 5′-TAGAACAGACAAACATATTTGAC -3′, and cloned in before the first Lox2272 and LoxP sites). The remaining *mgl-1* fragment sequence was cloned into pSM-inv[sl2-GFP] in an inverted orientation (obtained using forward primer: 5′-TCATAAGAAAGTATCGTGAGC -3′ and reverse primer: 5′-

CATTATGGCGTATGATGGG -3′, cloned in after the inverted sl2-GFP and before the inverted LoxP and Lox2272 sites). The cloning was done via Gibson assembly (New England Biolabs).

To rescue *mgl-1* in subsets of its endogenous expression pattern, we first injected the partially inverted plasmid described above into *mgl-1(ky1037)* animals using standard microinjection protocols. The resulting line is labelled ‘no Cre’. Subsequently, we injected plasmids expressing nls-Cre under cell specific promoters into this ‘noCre’ line. This led to Cre-mediated inversion and reconstitution of the *mgl-1* rescue fragment in subsets of cells, which was confirmed by GFP expression visualized using a Zeiss Axio Imager.Z1 Apotome microscope with a 40x objective.

All strains generated for this study are listed in Table 6.1.

Table 6.1. Strains generated for this study

Name	Strain	Genotype
npr-9 CRISPR	CX1030	*npr-9(ky1030) X*
mgl-1 CRISPR	CX1037	*mgl-1(ky1037) X*
CX17083	CX17083	*mgl-1(ky1060) npr-9(tm1652) X*
npr-9 transgene rescue	CX17094	*mgl-1(ky1060) npr-9(tm1652) X; kyEx5968[npr-9 fosmid, 5 ng μL^{-1}]*
mgl-1 transgene rescue	CX17218	*mgl-1(ky1060) npr-9(tm1652) X; kyEx6019[mgl-1 genomic PCR, 2.5 ng μL^{-1}]*
no Cre (inverted *mgl-1* genomic rescue)	CX17312	*mgl-1(ky1037) X; kyEx6056[mgl-1 first half::LOXinv(mgl-1 second half::sl2GFP), 25 ng μL^{-1}]*
pan-neuronal Cre	CX17345	*mgl-1(ky1037) X; kyEx6056; kyEx6062[tag-168::nCre, 20 ng μL^{-1}]*
mod-1::Cre	CX17347	*mgl-1(ky1037) X; kyEx6056; kyEx6064[mod-1::nCre, 20 ng μL^{-1}]*
AIA Cre	CX17354	*mgl-1(ky1037) X; kyEx6056; kyEx6072[gcy-28::nCre, 10 ng μL^{-1}]*
ADE Cre	CX17359	*mgl-1(ky1037) X; kyEx6056; kyEx6076[dat-1::nCre, 20 ng μL^{-1}]*
AIA Cre + ADE Cre	CX17362	*mgl-1(ky1037) X; kyEx6056; kyEx6079[gcy-28::nCre, 10 ng μL^{-1} ; dat-1::nCre, 20 ng μL^{-1}]*
RMD Cre	CX17349	*mgl-1(ky1037) X; kyEx6056; kyEx6066[glr-1::nCre, 15 ng μL^{-1}]*
NSM Cre	CX17350	*mgl-1(ky1037) X; kyEx6056; kyEx6067[tph-1::nCre, 30 ng μL^{-1}]*
ASI Cre	CX17356	*mgl-1(ky1037) X; kyEx6056; kyEx6073[str-3::nCre, 20 ng μL^{-1}]*
IL1 Cre	CX17358	*mgl-1(ky1037) X; kyEx6056; kyEx6075[odr-2b::nCre, 15 ng μL^{-1}]*
no Cre STOP	CX17393	*mgl-1(ky1037) X; kyEx6088[mgl-1 first half::inv(mgl-1 second half with nonsense::sl2GFP), 25 ng μL^{-1}]*
AIA Cre + ADE Cre STOP	CX17394	*mgl-1(ky1037) X; kyEx6088; kyEx6089[gcy-28::nCre, 10 ng μL^{-1} ; dat-1::nCre, 20 ng μL^{-1}]*
mgl-1 + AIA::TeTx	CX17419	*mgl-1(ky1037) X; kyEx6098[ttx-3(intron7)::TeTx::sl2GFP, 40 ng μL^{-1}]*
mgl-1 + ADE::TeTx	CX17422	*mgl-1(ky1037) X; kyEx6101[dat-1::TeTx::sl2GFP, 25 ng μL^{-1}]*
mgl-1 + AIA::TeTx ADE:TeTx	CX17457	*mgl-1(ky1037) X; kyEx6098; kyEx6101*
mgl-1 + NSM::TeTx	CX17441	*mgl-1(ky1037) X; kyEx6109[tph-1(short)::TeTx::sl2GFP, 15 ng μL^{-1}]*
mgl-1 AIA::HisCl	CX17418	*mgl-1(ky1037) X; kyIs698[ttx-3(intron7)::HisCl::sl2GFP, 30 ng μL^{-1}]*
mgl-1 ADE::HisCl	CX17415	*mgl-1(ky1037) X; kyEx6095[dat-1::HisCl::sl2GFP, 25 ng μL^{-1}]*
edited *eat-4*	CX17461	*kySi77[FRT before eat-4 start codon]; kySi76[let-858UTR::FRT::mCherry after eat-4 stop codon];*
pan-neuronal glut KO	CX17471	*kySi77; kySi76; kyEx6123[tag-168::nFLP, 20 ng μL^{-1}]*
mgl-1 (edited *eat-4)*	CX17505	*mgl-1(ky1037) X; kySi77; kySi76*
AWC glut KO	CX17524	*kySi77; kySi76; kyEx6142[odr-1::nFLP, 5 ng μL^{-1}]*
ASK glut KO	CX17539	*kySi77; kySi76; kyEx6150[sra-9::nFLP, 40 ng μL^{-1}]*
ASG glut KO	CX17551	*kySi77; kySi76; kyEx6169[gcy-15::nFLP, 25 ng μL^{-1}]*
chemosensory glut KO	CX17535	*kySi77; kySi76; kyEx6153[tax-4::nFLP, 40 ng μL^{-1}]*
mechanosensory glut KO	CX17556	*kySi77; kySi76; kyEx6174[mec-3::nFLP, 30 ng μL^{-1}]*
chemosensory + mechanosensory glut KO	CX17564	*kySi77 ;kySi76; kyEx6157[tax-4::nFLP, 40 ng μL^{-1} ; mec-3::nFLP, 30 ng μL^{-1}]*
chemosensory + mechanosensory nFLP in wt	CX 17667	*kyEx6157[tax-4::nFLP, 40 ng μL^{-1} ; mec-3::nFLP, 30 ng μL^{-1}]*
chemosensory + mechanosensory *Gt*ACR2	CX17603	*kyEx6203[tax-4::inv(GtACR2::sl2GFP), 50 ng μL^{-1} ; mec-3:inv(GtACR2::sl2GFP), 50 ng μL^{-1}] ; kyEx6202[eat-4::nCre, 10 ng μL^{-1}]*
glut KO + ADE::TeTx	CX17572	*kySi77; kySi76; kyEx6157; kyEx6101[dat-1::TeTx::sl2GFP 25, ng μL^{-1}]*
glut KO + AIA::TeTx	CX17571	*kySi77; kySi76; kyEx6157; kyEx6098[ttx-3(intron7)::TeTx::sl2GFP, 40 ng μL^{-1}]*
ASK::GCaMP5A	CX17590	*kyEx6191[sra-9::GCaMP5A 100 ng μL^{-1}]*
AIA::GCaMP5A	CX17449	*kyEx6115[gcy-28d:GCaMP5A 50 ng μL^{-1}]*
mgl-1 AIA::GCaMP5A	CX17455	*mgl-1(ky1037); kyEx6115[gcy-28d:GCaMP5A 50 ng μL^{-1}]*
ASK::GCaMP5A + AIA:GCaMP5A	CX17598	*kyEx6115[gcy-28d:GCaMP5A, 50 ng μL^{-1}]; kyEx6191[sra-9::GCaMP5A, 100 ng μL^{-1}]*
mgl-1 ASK::GCaMP5A + AIA:GCaMP5A	CX17614	*mgl-1(ky1037) X; kyEx6115[gcy-28d:GCaMP5A, 50 ng μL^{-1}]; kyEx6191[sra-9::GCaMP5A, 100 ng μL^{-1}]*
eat-4 ASK::GCaMP5A + AIA:GCaMP5A	CX17624	*eat-4(ky5) III; kyEx6115[gcy-28d:GCaMP5A, 50 ng μL^{-1}]; kyEx6191[sra-9::GCaMP5A, 100 ng μL^{-1}]*
feeding inhibition	CX16904	*kyIs703 [myo-2::ReaChR::sl2-GFP 1 ng μL^{-1}]*
feeding inhibiton + AIA::TeTx	CX17570	*kyIs703; kyEx6098[ttx-3(intron7)::TeTx::sl2GFP, 40 ng μL^{-1}]*

Foraging assay and quantification

Bacterial food lawns were made by seeding NGM plates with a thin uniform OP50 bacterial lawn (OD~0.5) 16 hours before the assay. The lawn covered the entire plate to eliminate effects of animals exploring the lawn edge (Calhoun et al., 2015), and contained a filter paper barrier soaked in 20 mM $CuCl_2$ that prevented the animals from leaving a 5 cm x 5 cm region on food. On the assay day, 15-20 adult hermaphrodites were first transferred for 45 min to this standard food lawn. To study off-food foraging, animals were transferred from the standard food plate to an unseeded NGM plate, allowed to crawl at least five body lengths to clean off excess food, and transferred to the assay plate which consisted of a large NGM plate with a circular filter paper barrier (~80 cm^2) soaked in 20 mM $CuCl_2$ to restrict animals to the recorded area. Up to 18 animals were observed on a single plate. Their behavior was recorded for 45 min, starting four minutes after the initial food removal, using a 15 MP PL-D7715 CMOS video camera (Pixelink). Frames were acquired at 3 fps using Streampix software (Norpix). Individual worm trajectories were analyzed using custom Matlab (Mathworks) software, as previously described (Pokala et al., 2014). We were able to track the behavior of some individuals for the entire 45 min of food. When collisions occurred, however, the data points around the collision were excluded (to ignore reorientations associated with collisions) and sometimes we were unable to link tracks after the collision, resulting in separate tracks before and after collisions. These track fragments were included in average quantifications.

To quantify reorientation frequencies, we counted the number of reorientations that each animal performed in 2-minute time windows and divided it by the number of animals tracked in that time window. We only counted animals that we were able to track in the entire 2-min time window. The plots show the mean number of reorientations in 2-min time windows. For analysis of local search, we quantified the number of time-dependent reorientations only.

To calculate Mean Square Displacement (MSD), we used the centroid x-y position of each animal. MSD was the square of the distance travelled in one minute. For each animal, we first we calculated the MSD for each frame by measuring the squared of the distance travelled from 30 sec before the frame to 30 sec after the frame. We then calculated the average MSD in two-minute time windows for each animal (the average MSD in 360 frames = 2 min).

For the food concentration experiment, the usual OP50 culture (OD~0.5) was diluted 10x or 100x in LB before seeding on NGM plates and growing for 16 hours overnight. The off-food experiment was the same as described above.

Histamine silencing experiments (Pokala et al., 2014)

Neurons expressing histamine-gated chloride channels (HisCl1) were silenced by adding histamine to NGM assay plates. 1 M histamine-dihydrochloride (Sigma-Aldrich) in deionized water was filtered and stored at -20^{o}C. NGM histamine plates were made by adding 1M histamine to NGM solution (50-55^{o}C) to a final concentration of 10 mM histamine. Plates were stored at 4^{o}C and used within a

week. Controls included: (1) animals expressing the HisCl1 tested on normal plates and (2) animals with no transgene tested on histamine NGM plates.

Calcium imaging

Transgenic animals expressing GCaMP5A (Akerboom et al., 2012) in ASK (*sra-9::GCaMP5A*), in AIA (*gcy-28d::GCaMP5A*), or in both neurons (crossing the two single neuron GCaMP5A lines), were generated in a wildtype background and crossed into *mgl-1 or eat-4* if indicated. Adult animals were first transferred to a standard food lawn for 45 min prior to imaging. Animals were then removed from the lawn, washed in NGM buffer to remove any food, and loaded into a custom PDMS microfluidic chamber in NGM buffer, where they were restrained but not paralyzed (Chronis et al., 2007). Animals received a constant flow of NGM buffer through the experiment. Imaging began 6 min after removal from food (time=0 min). Animals were imaged for 10 min initially (0-10 min), left in the device for 30 min with the light off, and imaged again for another 10 min (40-50 min). Calcium fluorescence signals were acquired at 5 frames per second through a 40x objective on an upright Axioskop 2 microscope (Zeiss) with an iXon3 DU-897 EMCCD camera (Andor), using Metamorph Software (Molecular Devices). Custom Image J and MATLAB software were used to track, quantify, and analyze neuronal activity. ASK imaging data was bleach-corrected. AIA did not show significant bleaching.

For ASK, the maximum baseline fluorescence in 1-minute intervals, F_{max} (95th percentile value), was used to calculate the change in fluorescence for each frame in the interval ($\Delta F = F-F_{max}$), and subsequently normalized to F_{max} ($\Delta F/F_{max}$). Changes in fluorescence observed were spontaneous decreases from the ASK baseline fluorescence (negative transients). To characterize negative transients, we wrote custom MATLAB software where we defined parameters to identify transients (start/end of transients = $-0.1\Delta F/F_{max}$, minimum transient amplitude = $-0.3\Delta F/F_{max}$, minimum transient duration = 3 sec). Additionally, we used the MATLAB function *findpeaks* to identify complex transients which consist of multiple local minima within one transient. Parameters were optimized to match manually assigned negative transients. For transient number and amplitude quantifications we measured all local minima within a complex transient. For transient duration quantifications we calculated the duration of the entire complex transient. For *eat-4* analysis, we used the same parameters used in wildtype data.

For AIA, the minimum baseline fluorescence, F_0, was calculated using the MATLAB function *statelevels* which divides the data into two histograms and computes the mode of the lower histogram. F_0 was used to calculate the change in fluorescence for each frame ($\Delta F = F- F_0$), and subsequently normalized to F_0 ($\Delta F/ F_0$). AIA shows a low baseline fluorescence with spontaneous positive transients. To characterize positive transients, we used the same procedure described above (parameters: start/end of transients = $0.1\Delta F/F_0$, minimum transient amplitude = $0.3\Delta F/F_o$, minimum transient duration = 2 sec). Parameters

were optimized to match manually assigned transients. For transient number and amplitude quantifications we measured all local maxima within a complex transient. For transient duration quantifications we calculated the duration of the entire complex transient. For *mgl-1* and *eat-4* analysis, we used parameters used in wildtype data.

To align ASK traces to AIA positive transient onset in the simultaneous imaging experiments, we first identified the start time of each AIA transient, and then extracted ASK frames from 10 sec (50 frames) before the start time until 30 s after the start time. We then averaged all extracted ASK frames.

To calculate correlations, we first z-scored each trace and then computed the autocorrelation, or the cross-correlation between ASK and matching lagged AIA traces, using the MATLAB function *xcorr*.

Optogenetic neuronal manipulations

To silence neurons optogenetically we expressed the light-gated anion channel, *Guillardia theta* anion channel rhodopsin 2 (*Gt*ACR2). A codon-optimized *Gt*ACR2 was synthesized based on the *Gt*ACR2 ORF (Govorunova et al., 2015) and cloned into the pSM vector backbone via Gibson Assembly (New England Biolabs).

To express *Gt*ACR2 selectively in glutamatergic sensory neurons that synapse onto AIA and ADE (the same neurons in which glutamate knockout leads to a

local search defect), we employed an inverted Cre-Lox recombination strategy. A floxed *Gt*ACR2 cDNA was placed in an inverted orientation under the *tax-4* (chemosensory subset) and *mec-3* promoters (mechanosensory subset), and subsequently activated in the relevant cells by Cre expression under the *eat-4* promoter (glutamate specific).

16 hours before the experiment, L4 animals expressing *Gt*ACR2 were picked to NGM plates seeded with OP50 containing 12.5 µM all-trans retinal (Sigma). Control animals, which also expressed *Gt*ACR2, were transferred to NGM plates seeded with OP50 but no retinal. On the experimental day, 15-20 animals were first transferred to a standard food lawn (with or without retinal) for 45 min, and then transferred to the large off-food assay plate (~80 cm^2) where their behavior was recorded as described above. During video recording, green light (~45 $\mu W/mm^2$) was delivered at 10 Hz (50% duty cycle) using a Solis High Power LED (ThorLabs) controlled with custom MATLAB software.

For the sensory silencing experiments, we delivered four 30 s light pulses with 2 min in between each pulse. The pulses began 2 min after initiating recording. To analyze the effect of the neuronal manipulation, we calculated the fraction of animals reorienting in each frame. We aligned all pulses and averaged the behavior for ten experiments (40 light pulses).

Pumping inhibition experiments

16 hours before the experiment, L4 animals expressing *myo-2::ReaChR* were picked to NGM plates seeded with OP50 containing 50 µM all-trans retinal (Sigma). Controls animals, which also expressed *myo-2::ReaChR*, were transferred to NGM plates seeded with OP50 but not retinal. On the experimental day, 15-20 animals were transferred to a standard food lawn (without retinal) for 45 min, and green light was delivered (10 Hz, ~45 µW/mm^2) for different amounts of time (10, 20, 45 min) prior to food removal. Animals were recorded on food to monitor their speed. Successful feeding inhibition was confirmed by a sustained increase in locomotion speed on food (increased roaming). The off-food experiment was the same as described above.

Inedible bacteria experiments

Inedible bacteria were generated using a modified protocol developed by Gruninger et. al 2008. In this method, bacteria were treated with a low concentration of aztreonam, which prevents septal closure during division, resulting in long chains of undivided bacteria. It has been shown that these inedible bacteria have similar sensory properties to regular bacteria, but that they cannot be ingested by *C. elegans* (Gruninger et al., 2008).

To make these inedible bacteria, OP50 cultures were grown overnight in LB at 37°C. The next day this culture was diluted 5x in LB with aztreonam (Sigma) at final concentration of 10 µg/ml, and grown overnight at 37°C. The next day, 16

hours before the assay, this culture was seeded on NGM plates with 10 µg/mL aztreonam. Control lawns were made the same way, but without adding aztreonam. Lawns were thin and uniform as described above, and covered the entire plate. Aztreonam and control plates were made fresh for every experiment.

Statistical Methods

Differences in local search behavior between groups was assessed by counting the number of reorientations that each animal in each group performed 2-12 min after food removal. Statistical significance was assessed using a Wilcoxon rank sum test with Bonferroni correction. The Wilcoxon signed rank test was used to compare matched data (imaging experiments, same animal early vs late). The Kolmogorov-Smirnov test was used for comparing cumulative probability distributions.

REFERENCES

Ahmadi, M., and Roy, R. (2016). AMPK acts as a molecular trigger to coordinate glutamatergic signals and adaptive behaviours during acute starvation. eLife;5:e16349.

Akerboom, J., Chen, T.W., Wardill, T.J., Tian, L., Marvin, J.S., Mutlu, S., Calderon, N.C., Esposti, F., Borghuis, B.G., Sun, X.R., et al. (2012). Optimization of a GCaMP calcium indicator for neural activity imaging. J Neurosci 32, 13819-13840.

Albeg, A., Smith, C.J., Chatzigeorgiou, M., Feitelson, D.G., Hall, D.H., Schafer, W.R., Miller, D.M., 3rd, and Treinin, M. (2011). *C. elegans* multi-dendritic sensory neurons: morphology and function. Mol Cell Neurosci 46, 308-317.

Arribere, J.A., Bell, R.T., Fu, B.X., Artiles, K.L., Hartman, P.S., and Fire, A.Z. (2014). Efficient marker-free recovery of custom genetic modifications with CRISPR/Cas9 in *Caenorhabditis elegans*. Genetics 198, 837-846.

Baird, J.P., Travers, J.B., and Travers, S.P. (2001). Parametric analysis of gastric distension responses in the parabrachial nucleus. Am J Physiol Regul Integr Comp Physiol 281, R1568-1580.

Bargmann, C.I. (2006). Chemosensation in *C. elegans*. (October 25, 2006), WormBook, doi/10.1895/wormbook.1.123.1, http://www.wormbook.org. In WormBook, T.C.e.R. Community, ed. (WormBook).

Bargmann, C.I., and Horvitz, H.R. (1991). Chemosensory neurons with overlapping functions direct chemotaxis to multiple chemicals in *C. elegans*. Neuron 7, 729-742.

Bartumeus, F., Campos, D., Ryu, W.S., Lloret-Cabot, R., Mendez, V., and Catalan, J. (2016). Foraging success under uncertainty: search tradeoffs and optimal space use. Ecol Lett 19, 1299-1313.

Bartumeus, F., and Catalan, J. (2009). Optimal search behavior and classic foraging theory. Journal of Physics A: Mathematical and Theoretical 42, 434002.

Bell, W.J. (1985). Sources of information controlling motor patterns in arthropod local search orientation. Journal of Insect Physiology 31, 837-847.

Bell, W.J., Cathy, T., Roggero, R.J., Kipp, L.R., and Tobin, T.R. (1985). Sucrose-stimulated searching behaviour of *Drosophila melanogaster* in a uniform habitat: modulation by period of deprivation. Animal Behaviour 33, 436-448.

Ben Arous, J., Laffont, S., and Chatenay, D. (2009). Molecular and sensory basis of a food related two-state behavior in *C. elegans*. PLoS ONE 4(10): e7584. https://doi.org/10.1371/journal.pone.0007584

Bendena, W.G., Boudreau, J.R., Papanicolaou, T., Maltby, M., Tobe, S.S., and Chin-Sang, I.D. (2008). A *Caenorhabditis elegans* allatostatin/galanin-like receptor NPR-9 inhibits local search behavior in response to feeding cues. Proc Natl Acad Sci U S A 105, 1339-1342.

Bendesky, A., Tsunozaki, M., Rockman, M.V., Kruglyak, L., and Bargmann, C.I. (2011). Catecholamine receptor polymorphisms affect decision-making in *C. elegans*. Nature 472, 313-318.

Benedix, J.J.H. (1993). Area-restricted search by the plains pocket gopher (*Geomys bursarius*) in tallgrass prairie habitat. Behavioral Ecology 4, 318-324.

Betley, J.N., Cao, Z.F., Ritola, K.D., and Sternson, S.M. (2013). Parallel, redundant circuit organization for homeostatic control of feeding behavior. Cell 155, 1337-1350.

Brenner, S. (1974). The genetics of *Caenorhabditis elegans*. Genetics 77, 71-94.

Calhoun, A.J., Chalasani, S.H., and Sharpee, T.O. (2014). Maximally informative foraging by *Caenorhabditis elegans*. eLife 2014;*3*:e04220.

Calhoun, A.J., Tong, A., Pokala, N., Fitzpatrick, J.A., Sharpee, T.O., and Chalasani, S.H. (2015). Neural Mechanisms for Evaluating Environmental Variability in *Caenorhabditis elegans*. Neuron 86, 428-441.

Campbell, J.C., Polan-Couillard, L.F., Chin-Sang, I.D., and Bendena, W.G. (2016). NPR-9, a galanin-like G-protein coupled receptor, and GLR-1 regulate interneuronal circuitry underlying multisensory integration of environmental cues in *Caenorhabditis elegans*. PLoS Genet 12(5): e1006050. https://doi.org/10.1371/journal.pgen.1006050.

Cao, J., Packer, J.S., Ramani, V., Cusanovich, D.A., Huynh, C., Daza, R., Qiu, X., Lee, C., Furlan, S.N., Steemers, F.J., et al. (2017). Comprehensive single-cell transcriptional profiling of a multicellular organism. Science 357, 661-667.

Cassini, M.H., Kacelnik, A., and Segura, E.T. (1990). The tale of the screaming hairy armadillo, the guinea pig and the marginal value theorem. Animal Behaviour 39, 1030-1050.

Chalasani, S.H., Chronis, N., Tsunozaki, M., Gray, J.M., Ramot, D., Goodman, M.B., and Bargmann, C.I. (2007). Dissecting a circuit for olfactory behaviour in *Caenorhabditis elegans*. Nature 450, 63-70.

Chalasani, S.H., Kato, S., Albrecht, D.R., Nakagawa, T., Abbott, L.F., and Bargmann, C.I. (2010). Neuropeptide feedback modifies odor-evoked dynamics in *Caenorhabditis elegans* olfactory neurons. Nat Neurosci 13, 615-621.

Charnov, E.L. (1976). Optimal foraging, the marginal value theorem. Theor Popul Biol 9, 129-136.

Chen, Y., Lin, Y.C., Kuo, T.W., and Knight, Z.A. (2015). Sensory detection of food rapidly modulates arcuate feeding circuits. Cell 160, 829-841.

Chen, Y., Lin, Y.C., Zimmerman, C.A., Essner, R.A., and Knight, Z.A. (2016). Hunger neurons drive feeding through a sustained, positive reinforcement signal. eLife 2016;*5*:e18640.

Choi, S., Chatzigeorgiou, M., Taylor, Kelsey P., Schafer, William R., and Kaplan, Joshua M. (2013). Analysis of NPR-1 reveals a circuit mechanism for behavioral quiescence in *C. elegans*. Neuron 78, 869-880.

Chronis, N., Zimmer, M., and Bargmann, C.I. (2007). Microfluidics for in vivo imaging of neuronal and behavioral activity in *Caenorhabditis elegans*. Nat Methods 4, 727-731.

Cowie, R.J. (1977). Optimal foraging in great tits (*Parus major*). Nature 268, 137-139.

Culotti, J.G., and Russell, R.L. (1978). Osmotic avoidance defective mutants of the nematode *Caenorhabditis elegans*. Genetics 90, 243-256.

Dall, S.R.X., Giraldeau, L.-A., Olsson, O., McNamara, J.M., and Stephens, D.W. (2005). Information and its use by animals in evolutionary ecology. Trends in Ecology & Evolution 20, 187-193.

de Bono, M., and Maricq, A.V. (2005). Neuronal substrates of complex behaviors in *C. elegans.* Annu Rev Neurosci 28, 451-501.

Dias, M.P., Granadeiro, J.P., and Palmeirim, J.M. (2009). Searching behaviour of foraging waders: does feeding success influence their walking? Animal Behaviour 77, 1203-1209.

Dillon, J., Franks, C.J., Murray, C., Edwards, R.J., Calahorro, F., Ishihara, T., Katsura, I., Holden-Dye, L., and O'Connor, V. (2015). Metabotropic glutamate receptors: Modulator of context-dependent feeding behaviour in *C. elegans*. J Biol Chem 290, 15052-15065.

Dillon, J., Hopper, N.A., Holden-Dye, L., and O'Connor, V. (2006). Molecular characterization of the metabotropic glutamate receptor family in Caenorhabditis elegans. Biochem Soc Trans 34, 942-948.

Dong H-W and Ennis M (2018) Activation of group II metabotropic glutamate receptors suppresses excitability of mouse main olfactory bulb external tufted and mitral cells. Front. Cell. Neurosci. 11:436. doi: 10.3389/fncel.2017.00436.

Eifler, D.A., Baipidi, K., Eifler, M.A., Dittmer, D., and Nguluka, L. (2012). Influence of prey encounter and prey identity on area-restricted searching in the lizard *Pedioplanis namaquensis*. J Ethol 30, 197-200.

Elner, R.W., and Hughes, R.N. (1978). Energy Maximization in the Diet of the Shore Crab, *Carcinus maenas*. Journal of Animal Ecology 47, 103-116.

Ezcurra, M., Tanizawa, Y., Swoboda, P., and Schafer, W.R. (2011). Food sensitizes *C. elegans* avoidance behaviours through acute dopamine signalling. EMBO J 30, 1110-1122.

Flavell, S.W., Pokala, N., Macosko, E.Z., Albrecht, D.R., Larsch, J., and Bargmann, C.I. (2013). Serotonin and the neuropeptide PDF initiate and extend opposing behavioral states in *C. elegans*. Cell 154, 1023-1035.

Fujiwara, M., Sengupta, P., and McIntire, S.L. (2002). Regulation of body size and behavioral state of *C. elegans* by sensory perception and the EGL-4 cGMP-dependent protein kinase. Neuron 36, 1091-1102.

Fuster, J.M., and Alexander, G.E. (1971). Neuron activity related to short-term memory. Science 173, 652-654.

Gjorgjieva, J., Biron, D., and Haspel, G. (2014). Neurobiology of *Caenorhabditis elegans* locomotion: where do we stand? Bioscience 64, 476-486.

Gloria-Soria, A., and Azevedo, R.B.R. (2008). *npr-1* regulates foraging and dispersal strategies in *Caenorhabditis elegans*. Current Biology 18, 1694-1699.

Gordus, A., Pokala, N., Levy, S., Flavell, S.W., and Bargmann, C.I. (2015). Feedback from network states generates variability in a probabilistic olfactory circuit. Cell 161, 215-227.

Govorunova, E.G., Sineshchekov, O.A., Janz, R., Liu, X., and Spudich, J.L. (2015). Natural light-gated anion channels: A family of microbial rhodopsins for advanced optogenetics. Science 349, 647-650.

Gray, J.M., Hill, J.J., and Bargmann, C.I. (2005). A circuit for navigation in *Caenorhabditis elegans*. Proc Natl Acad Sci U S A 102, 3184-3191.

Gray, J.M., Karow, D.S., Lu, H., Chang, A.J., Chang, J.S., Ellis, R.E., Marletta, M.A., and Bargmann, C.I. (2004). Oxygen sensation and social feeding mediated by a *C. elegans* guanylate cyclase homologue. Nature 430, 317-322.

Greer, E.R., Perez, C.L., Van Gilst, M.R., Lee, B.H., and Ashrafi, K. (2008). Neural and molecular dissection of a *C. elegans* sensory circuit that regulates fat and feeding. Cell Metab 8, 118-131.

Grünbaum, D. (1998). Using Spatially Explicit Models to Characterize Foraging Performance in Heterogeneous Landscapes. The American Naturalist 151, 97-113.

Grünbaum, D. (2000). Advection-Diffusion Equations for Internal State-Mediated Random Walks. SIAM Journal on Applied Mathematics 61, 43-73.

Gruninger, T.R., Gualberto, D.G., and Garcia, L.R. (2008). Sensory perception of food and insulin-like signals influence seizure susceptibility. PLoS Genet 4(7): e1000117. https://doi.org/10.1371/journal.pgen.1000117.

Hayashi, Y., Momiyama, A., Takahashi, T., Ohishi, H., Ogawa-Meguro, R., Shigemoto, R., Mizuno, N., and Nakanishi, S. (1993). Role of a metabotropic glutamate receptor in synaptic modulation in the accessory olfactory bulb. Nature 366, 687-690.

Hilliard, M.A., Bergamasco, C., Arbucci, S., Plasterk, R.H., and Bazzicalupo, P. (2004). Worms taste bitter: ASH neurons, QUI-1, GPA-3 and ODR-3 mediate quinine avoidance in *Caenorhabditis elegans*. EMBO J 23, 1101-1111.

Hills, T., Brockie, P.J., and Maricq, A.V. (2004). Dopamine and glutamate control area-restricted search behavior in *Caenorhabditis elegans*. J Neurosci 24, 1217-1225.

Hills, T.T., Kalff, C., and Wiener, J.M. (2013). Adaptive Levy processes and area-restricted search in human foraging. PLoS One 8, e60488.

Humphries, N.E., Queiroz, N., Dyer, J.R., Pade, N.G., Musyl, M.K., Schaefer, K.M., Fuller, D.W., Brunnschweiler, J.M., Doyle, T.K., Houghton, J.D., et al. (2010). Environmental context explains Levy and Brownian movement patterns of marine predators. Nature 465, 1066-1069.

Iino, Y., and Yoshida, K. (2009). Parallel use of two behavioral mechanisms for chemotaxis in *Caenorhabditis elegans*. The Journal of Neuroscience 29, 5370-5380.

Kang, C., and Avery, L. (2009a). Systemic regulation of autophagy in *Caenorhabditis elegans*. Autophagy 5, 565-566.

Kang, C., and Avery, L. (2009b). Systemic regulation of starvation response in *Caenorhabditis elegans*. Genes Dev 23, 12-17.

Kareiva, P., and Odell, G. (1987). Swarms of predators exhibit "preytaxis" if individual predators use area-restricted search. The American Naturalist 130, 233-270.

Kato, S., Kaplan, H.S., Schrodel, T., Skora, S., Lindsay, T.H., Yemini, E., Lockery, S., and Zimmer, M. (2015). Global brain dynamics embed the motor command sequence of *Caenorhabditis elegans*. Cell 163, 656-669.

Klein, M., Krivov, S.V., Ferrer, A.J., Luo, L., Samuel, A.D., and Karplus, M. (2017). Exploratory search during directed navigation in *C. elega*ns and *Drosophila* larva eLife 2017;*6*:e30503.

Kramer, D.L. (2001). Foraging Behavior. In Evolutionary Ecology: Concepts and Case Studies, C.W. Fox, D.A. Roff, and D.J. Fairbairn, eds. (Oxford University Press), p. 232-238.

Kramer, D.L., and McLaughlin, R.L. (2001). The behavioral ecology of intermittent locomotion. American Zoologist 41, 137-153.

Larsch, J., Flavell, S.W., Liu, Q., Gordus, A., Albrecht, D.R., and Bargmann, C.I. (2015). A circuit for gradient climbing in *C. elegans* chemotaxis. Cell Rep 12, 1748-1760.

Lee, K.S., Iwanir, S., Kopito, R.B., Scholz, M., Calarco, J.A., Biron, D., and Levine, E. (2017). Serotonin-dependent kinetics of feeding bursts underlie a

graded response to food availability in *C. elegans*. Nat. Commun. 8, 14221 doi: 10.1038/ncomms14221.

Li, H., and Durbin, R. (2010). Fast and accurate long-read alignment with Burrows-Wheeler transform. Bioinformatics 26, 589-595.

Lihoreau, M., Ings, T.C., Chittka, L., and Reynolds, A.M. (2016). Signatures of a globally optimal searching strategy in the three-dimensional foraging flights of bumblebees. Sci Rep 6, 30401.

Lin, J.Y., Knutsen, P.M., Muller, A., Kleinfeld, D., and Tsien, R.Y. (2013). ReaChR: a red-shifted variant of channelrhodopsin enables deep transcranial optogenetic excitation. Nat Neurosci 16, 1499-1508.

Macosko, E.Z., Pokala, N., Feinberg, E.H., Chalasani, S.H., Butcher, R.A., Clardy, J., and Bargmann, C.I. (2009). A hub-and-spoke circuit drives pheromone attraction and social behaviour in *C. elegans*. Nature 458, 1171-1175.

Maricq, A.V., Peckol, E., Driscoll, M., and Bargmann, C.I. (1995). Mechanosensory signalling in *C. elegans* mediated by the GLR-1 glutamate receptor. Nature 378, 78-81.

McFarland, D.J. (1977). Decision making in animals. Nature 269, 15-21.

McGrath, P.T., Xu, Y., Ailion, M., Garrison, J.L., Butcher, R.A., and Bargmann, C.I. (2011). Parallel evolution of domesticated *Caenorhabditis species* targets pheromone receptor genes. Nature 477, 321-325.

Meire, P.M., and Ervynck, A. (1986). Are oystercatchers (*Haematopus ostralegus*) selecting the most profitable mussels (*Mytilus edulis*)? Animal Behaviour 34, 1427-1435.

Murata, S., Brockmann, A., and Tanimura, T. (2017). Pharyngeal stimulation with sugar triggers local searching behavior in *Drosophila*. J Exp Biol 220, 3231-3237.

Nakamuta, K. (1985). Mechanism of the switchover from extensive to area-concentrated search behaviour of the ladybird beetle, *Coccinella septempunctata bruckii*. Journal of Insect Physiology 31, 849-856.

O'Donnell, M.P., Chao, P.H., Kammenga, J.E., and Sengupta, P. (2018). Rictor/TORC2 mediates gut-to-brain signaling in the regulation of phenotypic plasticity in *C. elegans*. PLOS Genetics 14(2): e1007213. https://doi.org/10.1371/journal.pgen.1007213

Paiva Vitor, H., Geraldes, P., Ramírez, I., Garthe, S., and Ramos Jaime, A. (2010). How area restricted search of a pelagic seabird changes while performing a dual foraging strategy. Oikos 119, 1423-1434.

Papastamatiou, Y., DeSalles, P.A., and McCauley, D.J. (2012). Area-restricted searching by manta rays and their response to spatial scale in lagoon habitats, Vol 456. 233-244.

Pereira, L., Kratsios, P., Serrano-Saiz, E., Sheftel, H., Mayo, A.E., Hall, D.H., White, J.G., LeBoeuf, B., Garcia, L.R., Alon, U., et al. (2015). A cellular and regulatory map of the cholinergic nervous system of *C. elegans*. eLife 2015;4:e12432.

Pierce-Shimomura, J.T., Morse, T.M., and Lockery, S.R. (1999). The fundamental role of pirouettes in *Caenorhabditis elegans* chemotaxis. The Journal of Neuroscience 19, 9557-9569.

Pierce, G.J., and Ollason, J.G. (1987). Eight reasons why optimal foraging theory is a complete waste of time. Oikos 49, 111-118.

Pokala, N., Liu, Q., Gordus, A., and Bargmann, C.I. (2014). Inducible and titratable silencing of *Caenorhabditis elegans* neurons in vivo with histamine-gated chloride channels. Proc Natl Acad Sci U S A 111, 2770-2775.

Pyke, G.H., Pulliam, H.R., and Charnov, E.L. (1977). Optimal foraging: A selective review of theory and tests. The Quarterly Review of Biology 52, 137-154.

Richardson, H., and Nicolaas, A.M.V. (1986). Diet selection and optimization by northwestern crows feeding on japanese littleneck clams. Ecology 67, 1219-1226.

Roberts, W.M., Augustine, S.B., Lawton, K.J., Lindsay, T.H., Thiele, T.R., Izquierdo, E.J., Faumont, S., Lindsay, R.A., Britton, M.C., Pokala, N., et al. (2016). A stochastic neuronal model predicts random search behaviors at multiple spatial scales in *C. elegans*. eLife 2016;5:e12572.

Romo, R., Brody, C.D., Hernandez, A., and Lemus, L. (1999). Neuronal correlates of parametric working memory in the prefrontal cortex. Nature 399, 470-473.

Root, C.M., Ko, K.I., Jafari, A., and Wang, J.W. (2011). Presynaptic facilitation by neuropeptide signaling mediates odor-driven food search. Cell 145, 133-144.

Sabbatini, M., Molinari, C., Grossini, E., Mary, D.A., Vacca, G., and Cannas, M. (2004). The pattern of c-Fos immunoreactivity in the hindbrain of the rat following stomach distension. Exp Brain Res 157, 315-323.

Salvador, L.C., Bartumeus, F., Levin, S.A., and Ryu, W.S. (2014). Mechanistic analysis of the search behaviour of *Caenorhabditis elegans*. J. R. Soc. Interface 2014 11 20131092; DOI: 10.1098/rsif.2013.1092. Published 15 January 2014.

Sawin, E.R., Ranganathan, R., and Horvitz, H.R. (2000). *C. elegans* locomotory rate is modulated by the environment through a dopaminergic pathway and by experience through a serotonergic pathway. Neuron 26, 619-631.

Schal, C., Tobin, T.R., Surber, J.L., Vogel, G., Tourtellot, M.K., Leban, R.A., Sizemore, R., and Bell, W.J. (1983). Search strategy of sex pheromone-stimulated male German cockroaches. Journal of Insect Physiology 29, 575-579.

Schoener, T.W. (1987). A Brief History of Optimal Foraging Ecology. In Foraging Behavior, K. A.C., K. J.R., and P. H.R., eds. (Boston, MA: Springer).

Schwartz, M.L., and Jorgensen, E.M. (2016). SapTrap, a toolkit for high-throughput CRISPR/Cas9 gene modification in *Caenorhabditis elegans*. Genetics 202, 1277-1288.

Serrano-Saiz, E., Poole, R.J., Felton, T., Zhang, F., De La Cruz, E.D., and Hobert, O. (2013). Modular control of glutamatergic neuronal identity in *C. elegans* by distinct homeodomain proteins. Cell 155, 659-673.

Shtonda, B.B., and Avery, L. (2006). Dietary choice behavior in *Caenorhabditis elegans*. Journal of Experimental Biology 209, 89-102.

Sims, D.W., Southall, E.J., Humphries, N.E., Hays, G.C., Bradshaw, C.J.A., Pitchford, J.W., James, A., Ahmed, M.Z., Brierley, A.S., Hindell, M.A., et al. (2008). Scaling laws of marine predator search behaviour. Nature 451, 1098-1102.

Skora, S., Mende, F., and Zimmer, M. (2018). Energy scarcity promotes a brain-wide sleep state modulated by insulin signaling in *C. elegans*. Cell Rep 22, 953-966.

Stern, S., Kirst, C., and Bargmann, C.I. (2017). Neuromodulatory Control of Long-Term Behavioral Patterns and Individuality across Development. Cell 171, 1649-1662 e1610.

Strand, M.R., and Vinson, S.B. (1982). Behavioral response of the parasitoid *Cardiochiles nigriceps* to a kairomone. Entomologia Experimentalis et Applicata 31, 308-315.

Takayanagi-Kiya, S., Zhou, K., and Jin, Y. (2016). Release-dependent feedback inhibition by a presynaptically localized ligand-gated anion channel. eLife 2016;5:e21734.

Viswanathan, G.M., Buldyrev, S.V., Havlin, S., da Luz, M.G.E., Raposo, E.P., and Stanley, H.E. (1999). Optimizing the success of random searches. Nature 401, 911-914.

Wakabayashi, T., Kimura, Y., Ohba, Y., Adachi, R., Satoh, Y., and Shingai, R. (2009). In vivo calcium imaging of OFF-responding ASK chemosensory neurons in *C. elegans*. Biochim Biophys Acta 1790, 765-769.

Wakabayashi, T., Kitagawa, I., and Shingai, R. (2004). Neurons regulating the duration of forward locomotion in *Caenorhabditis elegans*. Neurosci Res 50, 103-111.

Weimerskirch, H., Pinaud, Pawlowski, F., and Bost (2007). Does prey capture induce area-restricted search? A fine-scale study using GPS in a marine predator, the wandering albatross, The American Naturalist 2007 170:5, 734-743

White, J., Tobin, T.R., and Bell, W.J. (1984). Local search in the housefly *Musca domestica* after feeding on sucrose. Journal of Insect Physiology 30, 477-487.

White, J.G., Southgate, E., Thomson, J.N., and Brenner, S. (1986). The structure of the nervous system of the nematode *Caenorhabditis elegans*. Philos Trans R Soc Lond B Biol Sci 314, 1-340.

Yapici, N., Cohn, R., Schusterreiter, C., Ruta, V., and Vosshall, L.B. (2016). A Taste Circuit that Regulates Ingestion by Integrating Food and Hunger Signals. Cell 165, 715-729.

Yemini, E., Jucikas, T., Grundy, L.J., Brown, A.E., and Schafer, W.R. (2013). A database of *Caenorhabditis elegans* behavioral phenotypes. Nat Methods 10, 877-879.

Zhao, B., Khare, P., Feldman, L., and Dent, J.A. (2003). Reversal frequency in *Caenorhabditis elegans* represents an integrated response to the state of the animal and its environment. J Neurosci 23, 5319-5328.